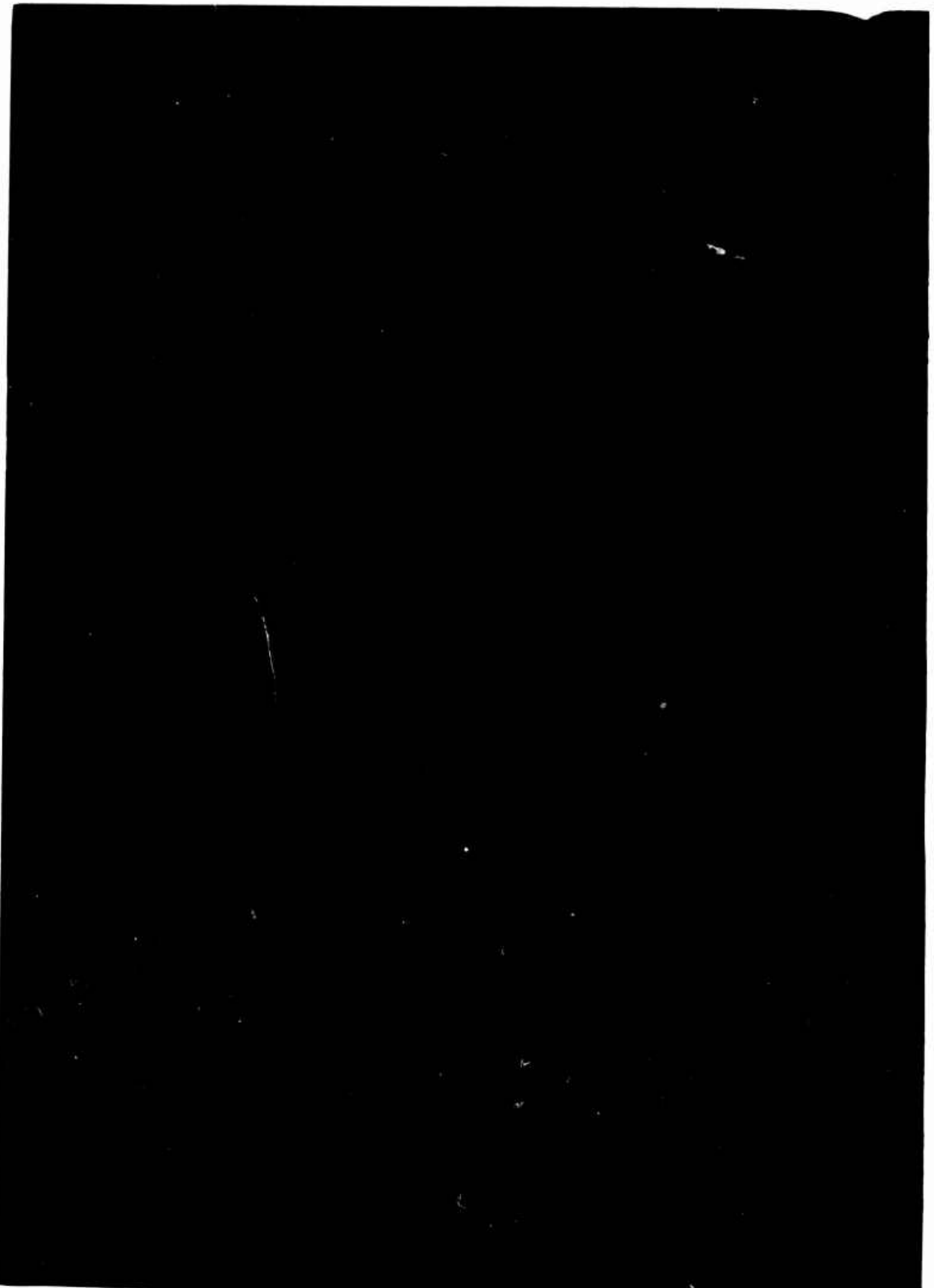


CONFIDENTIAL REPORT NO. 205

SCIENCE STERILIZATION

TECHNICAL INFORMATION AND METHODS

Reproduced by the
CLEARINGHOUSE
for Federal Scientific & Technical
Information, Springfield, Va. 22151



Soil Stabilization

Phase Report No. 6

**COMPRESSIBILITY-PERMEABILITY BEHAVIOR
OF UNTREATED AND CEMENT STABILIZED
CLAYEY SILT**

by

Anwar E.Z. Wissa
Randolph P. Monti

Sponsored by

U.S. Army Materiel Command
DA Project No. I-T-O-1451-B-52-A30

Conducted for

U.S. Army Engineer Waterways Experiment Station
Vicksburg, Mississippi

under

Contract No. DA-22-079-eng-465

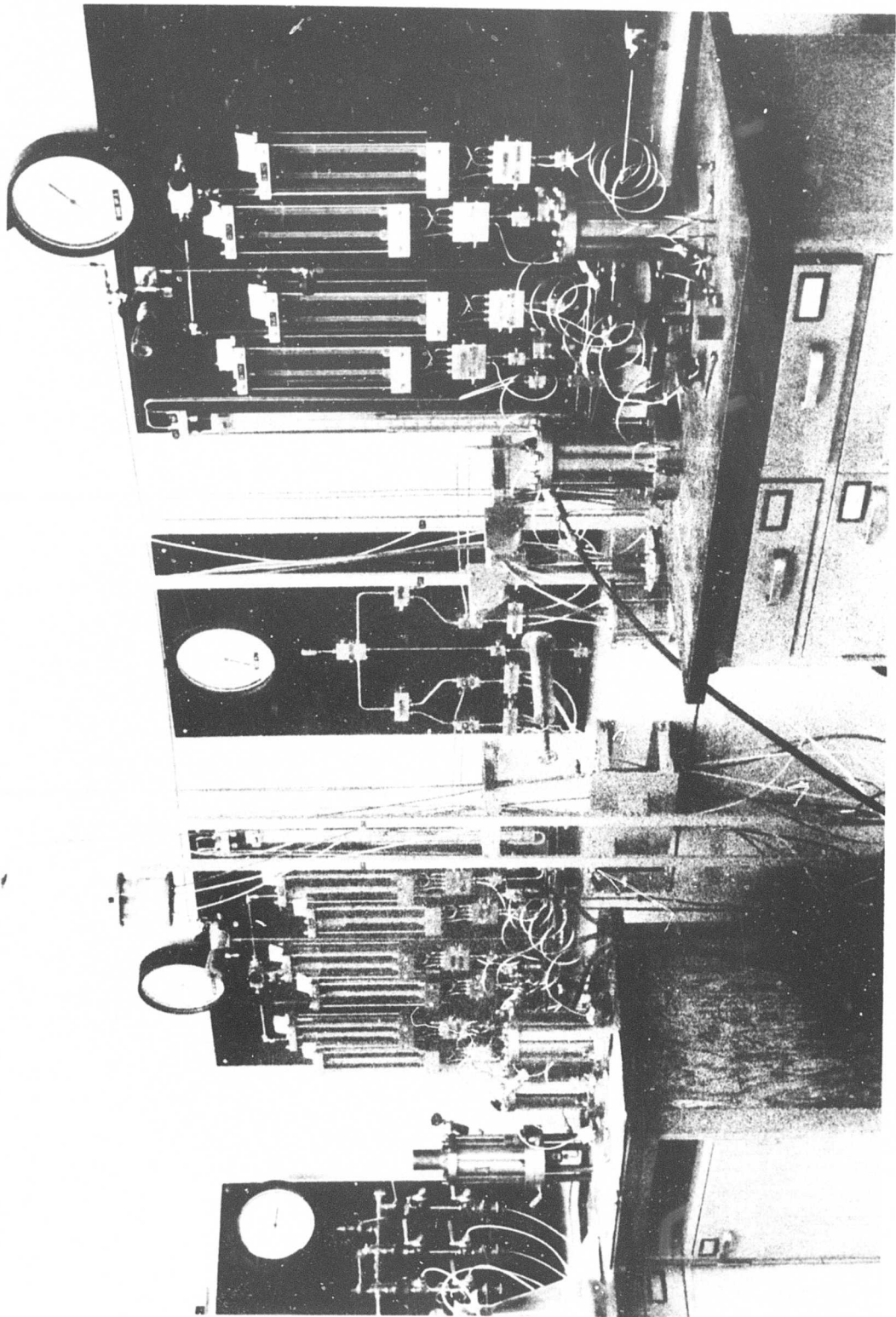


Research Report R68-94
Soil Mechanics Division
Department of Civil Engineering
Massachusetts Institute of Technology

December 1968

Soils Publication No. 227

FRONTISPICE - OVERALL VIEW OF CONSOLIDATION-PERMEABILITY EQUIPMENT AT M.I.T.



ABSTRACT

High pressure triaxial-permeability equipment has been developed to study the compressibility and permeability behavior of compacted untreated and stabilized soils at confining pressures up to 70 kg/cm^2 under back pressures up to 15 kg/cm^2 . Permeabilities down to 10^{-10} cm/sec. can be measured using cylindrical test specimens 3 cm long and 10 cm^2 cross-sectional area.

This equipment has been used to study the influence of cement stabilization, molding water content, and type of compaction on the compressibility and permeability behavior of Massachusetts clayey silt (M-21). The results of this investigation show:

- (1) Both molding water content and type of compaction influence the degree of cracking that occurs during unsealed hot curing of M-21 plus 5% cement.
- (2) Sealing during curing eliminates cracking.
- (3) Cracking causes an increase in the permeability and compressibility of the stabilized soil at consolidation pressures up to 50 kg/cm^2 .
- (4) Provided cracking during curing is prevented, the stabilized soil shows a much larger decrease in permeability with increasing molding water

content than does the untreated soil. Further, kneading compaction results in a lower permeability than static compaction at molding water contents around optimum for the stabilized soil.

- (5) The permeability of the stabilized soil decreases with increasing curing time and increasing time of permeation.

PREFACE

This report is the sixth in a series of reports on soil stabilization issued by the Massachusetts Institute of Technology for the U.S. Army Material Command. The work was conducted during fiscal years 1968 and 1969 under Contract No. DA-22-079-eng-465 between the U.S. Army Engineer Waterways Experiment Station, Vicksburg, Mississippi, and the Soils Research Laboratory of the Department of Civil Engineering at the Massachusetts Institute of Technology.

The work covered by this report was conducted by Mr. Randolph P. Monti, Research Assistant, and Mr. Albert S. Lucks, Research Engineer, in Soils under direct supervision of Dr. Anwar E.Z. Wissa, Assistant Professor of Civil Engineering. Dr. Wissa and Mr. Monti prepared this report.

The contract was monitored by Mr. G.R. Kozan, formerly Chief, Stabilization Section, Expedient Surfaces Branch, under the general supervision of Messrs. W.J. Turnbull, Chief (retired) and A.A. Maxwell, Acting Chief, Soils Division, Waterways Experiment Station. Contracting Officers were COL John R. Oswalt, Jr., CE, and COL Levi A. Brown, CE.

LIST OF SOIL STABILIZATION
PHASE REPORTS

1. "Engineering Behavior of Partially Saturated Soils,"
May, 1963.
2. "Triaxial Equipment and Computer Program for Measuring
the Strength Behavior of Stabilized Soils,"
September, 1963.
3. "Effective Stress-strength Behavior of Compacted
Stabilized Soils," July, 1964.
4. "Chemical Stabilization of Selected Tropical Soils,
[From Puerto Rico and Panama]," October, 1964.
5. "Shear Strength Generation in Stabilized Soils,"
June, 1965.
6. "Compressibility-Permeability Behavior of Untreated
and Cement Stabilized Clayey Silt," December, 1968.

TABLE OF CONTENTS

	<u>Page</u>
Abstract	1
Preface	3
List of Previous Reports .	4
Table of Contents	5
List of Tables	9
List of Figures	10
Chapter I. INTRODUCTION	16
1.1 Background	16
1.2 Scope of the Report	18
Chapter II. MATERIALS, EQUIPMENT, AND TESTING PROCEDURES	20
2.1 Materials	20
2.1.1 Soils	20
2.1.2 Stabilizers	21
2.2 Preparation of Test Specimens	21
2.2.1 Mixing Procedures	21
2.2.2 Compaction	22
2.2.2.1 Kneading Compaction	22
2.2.2.2 Static Compaction	23
2.2.2.3 Trimming of Samples	23
2.3 Curing	24
2.3.1 Standard Curing	24
2.3.2 Special Curing	25
2.4 Consolidation-permeability Equipment	26
2.4.1 Permeability Cells	26
2.4.2 Confining Pressure System	27

	<u>Page</u>
2.4.3 Back Pressure System	28
2.4.4 Volume Change and Flow Measurement	28
2.5 Testing Procedure	29
2.5.1 Setting up of Test Specimens	29
2.5.2 Initial Consolidation and Saturation	30
2.5.3 Consolidation	30
2.5.4 Permeation	31
2.5.5 Unloading and Dismantling	31
Chapter III. EXPERIMENTAL RESULTS: MAJOR TESTING PROGRAM	38
3.1 Introduction	38
3.2 Behavior During Standard Curing	39
3.2.1 Weight Changes During Curing	39
3.2.2 Volume Changes During Curing	40
3.2.3 Volume Change During Room Temperature Cure	42
3.2.4 Effect of Soaking	42
3.3 Behavior During Consolidation and Permeation	43
3.3.1 Untreated M-21	43
3.3.1.1 Void Ratio versus Consolidation Pressure	43
3.3.1.2 Permeability versus Molding Water Content	45
3.3.1.3 Permeability as a Function of Void Ratio	45
3.3.1.4 Permeability and Compaction Method	46
3.3.2 M-21 With 5% Portland Cement	46
3.3.2.1 Consolidation to 5 kg/cm ²	46

3.3.2.2	Void Ratio and Consolidation Pressure	47
3.3.2.3	Permeability versus Molding Water Content	48
3.3.2.4	Permeability as a Function of Void Ratio	49
3.3.2.5	Permeability and Compaction Method	49
Chapter IV.	DISCUSSION OF TEST RESULTS FROM THE MAJOR TESTING PROGRAM	85
4.1	Introduction	85
4.2	Behavior During Standard Curing	85
4.3	Void Ratio Versus Consolidation Pressure	88
4.3.1	Untreated Soil	88
4.3.2	Stabilized Soil	89
4.4	Permeability Behavior	90
4.4.1	Untreated Soil	90
4.4.2	Stabilized Soil	94
Chapter V.	CLARIFICATION TESTS: RESULTS AND DISCUSSION	106
5.1	Objectives	106
5.2	Testing Program	106
5.3	Curing Behavior	107
5.3.1	Sealed Versus Unsealed Test Specimens	107
5.3.2	Room Temperature Versus Hot Cure	108
5.4	Compressibility Behavior	109
5.4.1	Sealed Versus Unsealed Test Specimens	109
5.4.2	Influence of Molding Water Content and Type of Compaction	110
5.4.3	Influence of Curing Conditions	112

5.5 Permeability	113
5.5.1 Sealed Test Specimens	113
5.5.2 Influence of Curing and Permeation Time	115
5.5.3 Influence of Curing Conditions	116
5.5.4 Influence of Molding Conditions	118
Chapter VI. SUMMARY AND CONCLUSIONS	139
6.1 Objectives of the Investigation	139
6.2 Compressibility Behavior	140
6.2.1 Untreated M-21	140
6.2.2 M-21 + 5% Cement	141
6.3 Permeability Behavior	142
6.3.1 Untreated M-21	142
6.3.2 M-21 + 5% Cement	143
6.4 Conclusions	146
List of References	150
Appendix A. DISCUSSION OF TESTING COMPUTATIONS	152

LIST OF TABLES

Table No.	Title	Page
2.1	Properties of Untreated and 5% Cement-Stabilized M-21	33
3.1	Weights and Lengths of Stabilized Test Specimens as a Function of Curing Time During Standard Cure	50
3.2	Summary Sheet: Void Ratio and Permeability Characteristics of Untreated Massachusetts Clayey Silt	51
3.3	Summary Sheet: Void Ratio and Permeability Characteristics of M-21 + 5% Portland Cement	52
3.4	Summary of Compressibility Charac- teristics of Untreated M-21 Test Specimens	53
5.1	Summary of Clarification Test Results for M-21 + 5% Cement	122
A.1	Justification for Figure A.1	157

LIST OF FIGURES

Figure	Title	Page
Frontis-piece	Overall View of Consolidation-Permeability Equipment at M.I.T.	
2.1	Grain-Size Distribution of Untreated Massachusetts Clayey Silt	34
2.2	Moisture-Density Relationships for Treated and Untreated M-21	35
2.3	High Pressure Consolidation-Permeability Cell	36
2.4	Consolidation-Permeability Setup Showing Volume Change, Back Pressure, and Confining Pressure Systems for Three Tests	37
3.1	Moisture-Density Relations of Untreated and Cement-Stabilized Samples Used in the Major Testing Program	54
3.2	Weight Changes During Cure versus Time for Static Stabilized Samples	55
3.3	Weight Changes During Cure versus Time for Kneading Stabilized Samples	56
3.4	Volume Change During Cure for Static Stabilized Samples	57
3.5	Volume Change During Cure for Kneading Stabilized Samples	58
3.6	Change Overall Void Ratio versus Curing Time for Kneading Stabilized Samples	59
3.7	Change in Overall Void Ratio versus Curing Time for Static Stabilized Samples	60

Figure	Title	Page
3.8	Influence of Type of Compaction on Overall Void Ratio Change During Curing for Stabilized Samples Compacted Dry and Wet of Optimum	61
3.9	Influence of Type of Compaction on Overall Void Ratio Change During Curing for Stabilized Samples Compacted Very Dry and Very Wet of Optimum	62
3.10	Influence of Type of Compaction on Overall Void Ratio Change During Curing for Stabilized Samples Compacted at Optimum	63
3.11a	Void Ratio versus Consolidation Pressure for Untreated M-21 Compacted Dry of Optimum [$W_m = 9\%$]	64
3.11b	Void Ratio versus Consolidation Pressure for Untreated M-21 Compacted at Optimum [$W_m = 11\%$]	65
3.11c	Void Ratio versus Consolidation Pressure for Untreated M-21 Compacted Slightly Wet of Optimum [$W_m = 13\%$]	66
3.11d	Void Ratio versus Consolidation Pressure for Untreated M-21 Compacted Wet of Optimum [$W_m = 15\%$]	67
3.11e	Void Ratio versus Consolidation Pressure for Untreated M-21 Compacted Very Wet of Optimum [$W_m = 17\%$]	68
3.12	Permeability versus Molding Water Content for Kneading Compaction Untreated M-21 Specimens	69
3.13	Permeability versus Molding Water Content for Static Compaction Untreated M-21 Specimens	70
3.14	Influence of Void Ratio on the Permeability of Kneading Compacted M-21	71

Figure	Title	Page
3.15	Influence of Void Ration on the Permeability of Statically Compacted M-21	72
3.16a	Influence of Type of Compaction on the Permeability of Untreated M-21	73
3.16b	Influence of Type of Compaction on the Permeability of Untreated M-21[continued]	74
3.17a	Void Ratio versus Consolidation Pressure for M-21 + 5% Cement Compacted Very Dry of Optimum [$W_m = 9\%$]	75
3.17b	Void Ratio versus Consolidation Pressure for M-21 + 5% Cement Compacted Dry of Optimum [$W_m = 11\%$]	76
3.17c	Void Ratio versus Consolidation Pressure for M-21 + 5% Cement Compacted at Optimum [$W_m = 13\%$]	77
3.17d	Void Ratio versus Consolidation Pressure for M-21 + 5% Cement Compacted Wet of Optimum [$W_m = 15\%$]	78
3.17e	Void Ratio versus Consolidation Pressure for M-21 + 5% Cement Compacted very Wet of Optimum [$W_m = 17\%$]	79
3.18	Ratio of Void Ratio Change During Initial Consolidation to Void Ratio Chage During Consolidation to 50 kg/cm^2 versus Molding Water Content	80
3.19	Permeability versus Molding Water Content for Static Compaction Stabilized Samples	81
3.20	Permeability versus Molding Water Content for Kneading Compaction Stabilized Samples	82
3.21	Permeability versus Void Ratio for Static Compaction Stabilized Samples	83
3.22	Permeability versus Void Ratio for Kneading Compaction Stabilized Samples	84

Figure	Title	Page
4.1	Influence of Molding Water Content and Type of Compaction on the Behavior of the Stabilized Samples during Unsealed Hot Curing	99
4.2	Compressibility of the Untreated Soil as a Function of Molding Water Content and Type of Compaction	100
4.3	Compressibility of the Stabilized Soil as a Function of Molding Water Content and Type of Compaction	101
4.4	Influence of Molding Water Content and Type of Compaction on the Permeability of Untreated M-21 at a Void Ratio of 0.350	102
4.5	Influence of Molding Water Content and Type of Compaction on the Permeability of Untreated M-21 as a Function of Consolidation Pressure	103
4.6	Influence of Molding Water Content and Type of Compaction on the Permeability of M-21 + 5% Cement at a Void Ratio of 0.470	104
4.7	Influence of Molding Water Content and Type of Compaction on the Permeability of M-21 + 5% Cement as a Function of Consolidation Pressure	105
5.1	Molding Conditions of Clarification Test Specimens	123
5.2	Influence of Sealing Test Specimens on Weight and Length Changes During Hot Curing	124
5.3	Unsealed and Sealed Test Specimens After Hot Curing Showing Cracking and Overall Expansion of Unsealed Samples	125

Figure	Title	Page
5.4	Influence of Curing Conditions on Overall Void Ratio Change During Curing and Initial Consolidation of M-21 + 5% Cement Compacted at Optimum	126
5.5	Influence of Curing Conditions on the Compressibility of M-21 + 5% Cement Compacted at Optimum and Hot Cured	127
5.6	Influence of Molding Conditions on the Compressibility of Sealed M-21 + 5% Cement Test Specimen	128
5.7	Influence of Curing Temperature on the Compressibility of M-21 + 5% Cement	129
5.8	Influence of Curing Conditions on the Compressibility of M-21 + 5% Cement Compacted Near Optimum Water Content Using Kneading Compaction	130
5.9	Influence of Molding Conditions on The Permeability Behavior of Sealed Specimens of M-21 + 5% Cement	131
5.10	Influence of Curing Time and Permeation Time on the Permeability of M-21 + 5% Cement	132
5.11	Influence of Curing Time on the Initial Permeability of M-21 + 5% Cement	133
5.12	Influence of Curing Conditions on the Permeability-Void Ratio Relations of M-21 + 5% Cement Compacted at Optimum	134
5.13	Influence of Sealing During Hot Cure on Permeability Behavior of M-21 + 5% Cement Compacted Dry of Optimum	135
5.14	Influence of Curing Temperature on the Permeability of Unsealed M-21 + 5% Cement Specimens Compacted Wet of Optimum	136
5.15	Moisture-Density-Permeability Behavior of Untreated M-21 Used in 1964 and 1967-1968	137

Figure	Title	Page
5.16	Moisture-Density-Permeability Behavior of M-21 + 5% Cement Using Unsealed Curing at Room Temperature and 70°C	138
6.1	Compressibility Behavior of Untreated M-21 as a Function of Molding Water Content and Type of Compaction	147
6.2	Influence of Cement Stabilization on the Permeability of Static Compacted M-21	148
6.3	Influence of Cement Stabilization on the Permeability of Kneading Compacted M-21	149
A.1	Dial Gage Used to Measure Length Changes of Test Specimens	158
A.2	Assumed Volume versus Length Change During Hot Curing of Unsealed Stabilized Samples	159

Chapter I

INTRODUCTION

1.1 Background

Improvement in the engineering properties of soils by the addition of a small quantity of a cementing agent is called soil stabilization. Use of this technique has grown markedly in recent years, especially in underdeveloped areas where the need for inexpensive techniques for upgrading soils with marginal engineering properties is a matter of critical economic importance.

In spite of the increased interest in and use of stabilized soils in recent years, criteria by which their engineering properties are evaluated are still in relative infancy. The two most common methods for evaluating stabilized soils are the California Bearing Ratio (CBR) and the unconfined compression test. Wissa and Ladd (1965)* discuss the severe limitations of these tests, and propose a method of evaluation for stabilized soils employing effective stress-strength parameters, similar to that commonly used for natural soils.

Thus, from 1960, stabilization at M.I.T. shifted

* Author names followed by dates shown in parentheses refer to entries arranged alphabetically in the List of References located at the end of this report.

away from research directed toward development of new chemical stabilizers and methods for improving the effectiveness of conventional stabilizers, and toward a study of the mechanisms of shear strength generation.

The most significant of the engineering properties of stabilized soil, the effective stress-strength behavior, has been studied at M.I.T. employing primarily undrained triaxial compression tests on fully saturated stabilized soil systems (Wissa and Ladd, 1964 and 1965). These studies have shown that for fine-grained soils the addition of portland cement, or hydrated lime, can increase the effective angle of internal friction as well as the effective cohesion.

The purpose of this research has not only been to determine the influence of artificial cementation on the effective stress-strength parameters of soils, but also to study the mechanisms responsible for the improved behavior. From this research has come the conclusion that chemically stabilized clays derive their added strength from two phenomena: (1) a clustering or aggregation of the clay in locations of high cement concentrations which causes an increase in the effective angle of internal friction, and (2) a general weaker cementation between the aggregations which causes an increase in the effective cohesion intercept. Feferbaum (1966) has shown

that molding conditions (molding water content and dry density) primarily influence the effective cohesion intercept.

Effective stress-strength behavior is, however, only one of three main engineering properties that concern the soil mechanician, the other two being permeability and compressibility. In stabilized soils as in natural soils, permeability is of interest not only in its own right, but in addition because it is a useful means by which changes in fabric of a fine-grained soil can be examined (Lambe 1955 and 1958).

The volume change behavior of stabilized soils during curing and consolidation can also assist in obtaining an insight into the mechanisms of soil stabilization. While some work has been done in this area for compacted clays, a quite limited amount of work on shrinkage during cure (the majority of it by George, 1968) and an even smaller amount on consolidation behavior of stabilized soils has been performed.

1.2 Scope of the Report

This report presents the results of a series of permeability tests on a cement-stabilized, low-plasticity silty clay (referred to as M-21 soil) employed for a considerable portion of the stabilization work at M.I.T.

The permeability measurements were obtained utilizing a specially designed triaxial-permeability setup that allowed the use of high back pressure (up to 15 kg/cm²) to ensure saturation during permeation, and could apply confining pressures up to 70 kg/cm².

For both the natural and cement-treated soil (stabilized with 5% portland cement), two sets of test specimens were prepared utilizing two methods of compaction (kneading and static) that correspond to the extremes of common field compaction conditions. For each type of compaction, five samples of the cement-treated and the untreated soil were prepared at different molding water contents. The influences of molding water content, type of compaction, and confining pressure on the permeability and compressibility behavior of the untreated and cement-stabilized soil were determined. The volume change behavior during humid cure and soaking was also established as a function of molding conditions.

A supplementary testing program was also conducted to determine the influence of curing conditions on the permeability behavior of the stabilized soil.

Chapter II

MATERIALS, EQUIPMENT, AND TESTING PROCEDURES

2.1 Materials

2.1.1 Soil

The fine-grained soil used for this investigation is the minus No. 40 sieve size fraction of a glacial till locally called Massachusetts clayey silt (M-21). This soil is obtained from a drumlin in East Boston that overlooks Logan Airport. The soil has a liquid limit of 20.5% and a plasticity index of 5.8 and classifies as a CL-ML soil according to the Unified system. The textural composition, physical properties, and mineralogical composition of the soil are given in Table 2.1. The grain-size distribution of the minus No. 40 sieve size fraction is shown in Fig. 2.1.

To obtain the minus No. 40 sieve size fraction, the natural soil containing gravel size particles was air-dried and passed through a No. 4 size sieve to remove coarse particles. The material passing this sieve size was then mechanically ground to break up any dry soil aggregates before sieving through a No. 40 size sieve. All material retained on this sieve was discarded and

only the finer material was used.

2.1.2 Stabilizer

The stabilizing agent used for this investigation was commerical grade Type I portland cement. Five per cent, based on air-dried weight of soil, was used for all stabilized test specimens. The influence of 5% cement on the Atterberg Limits of M-21 is given in Table 2.1.

2.2 Preparation of Test Specimens

2.2.1 Mixing Procedures

For stabilized samples, the cement was first mixed with air-dried soil until homogeneous mixtures were obtained. The water was added slowly with a squeeze bottle, while mixing the sample with a spoon. After all the water had been added (total time approximately two minutes), additional hand mixing was performed until a consistant mixture was obtained. This additional mixing took on the order of about two minutes. Only one sample was prepared at a time. For the untreated soil samples, the same procedure was used except that the addition and mixing in of cement was omitted.

The soil was compacted immediately after the addition of water (and cement, if stabilized). Two water

content determinations were taken for each sample, one before and one immediately after compaction. The time between first mixing in of the water and final compaction took no longer than fifteen minutes for the kneading samples and no longer than twenty-five minutes for the static ones.

2.2.2 Compaction

Two methods of compaction were used in the investigation. Both methods employed stainless steel molds having the following dimensions:

Length : 3.150 inches
diameter : 1.405 inches
Volume : 80 cc

2.2.2.1 Kneading Compaction

A Harvard miniature compaction tamper, spring loaded to forty pounds, was used for kneading compaction. The soil was compacted in five layers with 32 blows/layer. The surface of each compacted layer was well scarified with a blunt knife to improve bonding between layers. A forty-pound hammer was chosen to duplicate the compaction effort applied in previous studies on stabilized soils. Kneading compaction, because of its shearing effect upon soil, is somewhat analogous to field compaction, using a sheep'sfoot roller. Fig. 2.2 shows the

moisture-density relationship for untreated and stabilized M-21 compacted using the kneading tamper described above.

2.2.2.2 Static Compaction

The static compaction samples were prepared by forcing the soil mixture into the mold using a piston having a diameter equal to the internal diameter of the mold. The samples were compacted in five layers to minimize density variations due to side friction. The same amount of soil and same load on the piston was used for each layer. The surface of each layer was scarified after compaction to improve bonding between layers. The desired load on the piston was applied with a hydraulic jack and measured with a proving ring. It was maintained for one minute on each layer. The compaction load for each test specimen was varied in order to duplicate the dry densities obtained with the corresponding kneading compaction specimen molded at the same water content.

2.2.2.3 Trimming of Samples

Excess soil was added to the mold initially so that the ends of the sample could be trimmed after compaction but before extrusion. A sharp, straight-edged knife was used to trim the samples and to straighten the

ends. All samples were weighed in the molds before extrusion in order to compute the as-molded dry density. Following extrusion from the mold, the samples were reweighed and the length measured.

2.3 Curing

2.3.1 Standard Curing

For the major testing program, an accelerated curing process was employed with the stabilized soil samples. Immediately after compaction, the stabilized samples were placed on perforated plates in air-tight jars which had water in the base below the plate. Moistened filter paper was placed along the sides of the jars to increase the relative humidity of the air. The jars were then placed in a 70°C water bath. The bath was a styrofoam-insulated waterproof plywood box and was heated by an immersion-type heater controlled by an adjustable power source. A small stirrer was employed continuously during the cure to ensure a constant temperature throughout the water bath. Temperature of the water was monitored daily and was found to vary by $\pm 2^{\circ}\text{C}$ during the curing period. This procedure will be referred to as "standard curing."

The full hot-curing period was fourteen days, during which time weight and length change data were periodically

recorded as functions of curing time. At the end of hot cure, each humid jar was removed and placed at room temperature until the time of test.

Before being placed in the permeability cells for testing, each sample was weighed and measured for length change, completely immersed in water for at least twenty-four hours, and then weighed and measured again immediately before being set up in the permeability cells.

2.3.2 Special Curing

In addition to the standard curing procedure, there were several stabilized samples compacted towards the end of the investigation which were wrapped in a thin polyvinylidene chloride film and sealed in micro-crystalline (nonshrinking) wax before hot curing in the standard manner. This will be referred to as "sealed curing."

A few samples were also cured at room temperature. The procedure was essentially the same as that used for standard curing except that the jars were not placed in the hot temperature bath. This will be called "room temperature curing".

2.4 Consolidation - Permeability Equipment

2.4.1 Permeability Cells

Five high pressure consolidation-permeability cells were constructed for this research. The cells were essentially similar to high pressure triaxial cells with the axial loading ram (piston) omitted. The cell chamber had a stainless steel wall and was designed to withstand a confining pressure of 100 kg/cm². Two ports were located in the top plate of the cell chamber. One was used for filling the cell and applying the confining pressure and had a Whitey needle valve mounted in it. The other port was used for venting the chamber during filling, and an O-ring seal was used to close it off once the cell chamber was filled with de-aired water. The cell base was made of a single piece of stainless steel and had a 1.405-inch-diameter sample pedestal 1.25 inches high. The surface of the pedestal was highly polished to ensure good sealing of the membrane. Three ports were located in the cell base. One port was used for draining the cell chamber and a Circle Seal valve located in it. The second port connected directly to the center of the sample pedestal and was used for bottom drainage. The third port was for top drainage and connected to the drainage line from the top cap. The top and bottom drainage ports used

Geomeasurements no-volume change on-off valves for controlling drainage. The stainless steel top cap was 1.405 inches in diameter and had a highly polished surface. The top drainage line connecting the top cap to the top drainage port in the cell base consisted of spiraled 1/8-inch-diameter soft copper tubing. Geomeasurements copper tube O-ring connectors were used at both ends of the top drainage line, thus permitting the top drainage line to be easily disconnected. A closeup photograph of the permeability cell is shown in Fig. 2.3.

2.4.2 Confining Pressure System

The confining pressure system for high pressures was an improved version of the system developed for the high pressure triaxial tests and described in Phase Report No. 2 (M.I.T., 1963). The main improvements were:

- (1) Use of a very accurate metering valve (Nupro Model S) to give a constant small bleed of nitrogen through the pressure regulators. This eliminated binding of the regulators and made it possible to maintain the confining pressure to ± 2 psi.
- (2) The volume of nitrogen-water interchange was increased to 1000 cc, and 60 ft. of tubing was placed between the interchange and the

cell, thus reducing the risk of nitrogen diffusion into the cell chamber.

For confining pressures below 15 kg/cm^2 , self-compensating mercury control apparatuses were used. These systems were based on the system described by Bishop and Henkel (1962) but were designed for pressures up to 16 kg/cm^2 . Geomeasurements supplied the mercury pots for these systems.

2.4.3 Back Pressure System

Geomeasurements self-compensating mercury control systems were used for back pressuring during consolidation and saturation and for applying the hydraulic gradient during permeation. Pressures up to 16 kg/cm^2 could be obtained and maintained constant to $\pm 0.005 \text{ kg/cm}^2$. Independent systems were connected to the top and bottom drainage lines of the cells, and the difference in the pressure between the two systems was determined with a differential pressure mercury manometer in order to obtain an accurate measure of the applied hydraulic gradient.

2.4.4 Volume Change and Flow Measurements

Volume changes during saturation and consolidation were measured with twin burette paraffin-type volume

change apparatuses supplied by Geomeasurements. Low viscosity Silicon Oil was used in these burettes; the capacity of each burette was 5 cc; and volume changes could be determined to \pm 0.01 cc. By use of a reverse flow, no-volume change valve, volume changes in excess of 5 cc could be measured without interrupting flow. Two twin burettes were used with each permeability cell, one connected to the top drainage line and the other to the bottom drainage line. During saturation and consolidation, the back pressure applied to both twin burettes was 14 kg/cm^2 . When measuring permeability the back pressure was increased to one of the twin burettes, and was decreased by an equal amount to the other twin burette to produce the desired hydraulic gradient through the test specimen. The hydraulic gradients were adjusted to give at least 0.05 cc of flow per day in the lowest permeability test specimens.

Fig. 2.4 is a photograph of the complete permeability setup and shows the volume change equipment, back pressure system, and the confining pressure system for three tests.

2.5 Testing Procedure

2.5.1 Setting up of Test Specimens

After the stabilized samples had been soaked for at

least twenty-four hours, or immediately after compaction in the case of the untreated samples, they were weighed, measured, and mounted in the permeability cells. Porous stones, which had been saturated by boiling under water for at least twenty minutes, were placed on both ends of each sample. The samples with their stones were placed on the cell pedestals and the top drainage caps placed on top of them. Single Latex sheaths, 0.024 inches thick, were used to enclose the samples. The membranes were sealed to the base pedestals and top drainage caps by means of neoprene O-rings. The cells and nitrogen-water interchanges were then filled with deaired water.

2.5.2 Initial Consolidation and Saturation

Once the cells and nitrogen-water interchanges were filled, a confining pressure of 5 kg/cm^2 was first applied and then gradually increased during application of a back pressure of 14 kg/cm^2 to achieve the desired initial effective consolidation pressure of 5 kg/cm^2 .

2.5.3 Consolidation

Most of the samples were consolidated and permeated at effective pressures of 5, 10, 25, and 50 kg/cm^2 . The initial consolidation to 5 kg/cm^2 was in addition, a saturation process, and therefore no time-rate data were

kept. For the higher increments of stress, time-rate of consolidation data were recorded. Consolidation of a sample at any increment was generally continued until all flow had ceased from the sample. The time for consolidation varied for each sample, but generally the drainage lines to all samples were kept open until the last had finished consolidation. During consolidation the back pressure to the top and bottom drainage lines was maintained equal at 14 kg/cm².

2.5.4 Permeation

Following consolidation, the samples were permeated by reducing the top back pressure and increasing the bottom back pressure by equal amounts. Permeation was continued until the rates of flow equalized into and out of the samples. Once again, this equalization took different times for the different samples, but generally all samples in a set were permeated until the last one had equalized.

2.5.5 Unloading and Dismantling

In order to reduce the tendency to suck in water, the samples were rebounded to 2 kg/cm² before dismantling. The volume change during the rebound was measured. After the rebound was complete, the cells were taken apart, and the samples removed. Length, circumference, and weight

**data were recorded. The water content of the total sample
was then determined.**

Table 2.1

PROPERTIES OF UNTREATED AND 5% CEMENT-STABILIZED M-21

Textural Composition % by wt.

Sand	2 mm to 0.06 mm	42
Silt	0.06 mm to 0.002 mm	42
Clay	<0.002 mm	16

Physical Properties.

	Untreated:	Treated:
Liquid Limit %	20.5	21.2 (1)
Plastic Limit %	14.7	17.6 (1)
Plasticity Index %	5.8	3.6 (1)
Specific Gravity	2.75	2.78
Max. Dry Density (2) lb/ft ³	123.0	120.6
Optimum Water content (2) %	11.50	13.0

Classification.

Unified	CL-ML
AASHO	A-4 (0)

Chemical Properties.

Organic Matter, % by wt.	0.2
Cation exchange capacity meq/100 gm	10
Glycol Retention mg/gm	22

Mineralogical Composition

Clay Composition % by wgt	30
Illite: montmorillonoid	1:0
Free Iron oxide, % FeO	2.9

(1) determined immediately after mixing

(2) kneading compaction, 40-pound hammer

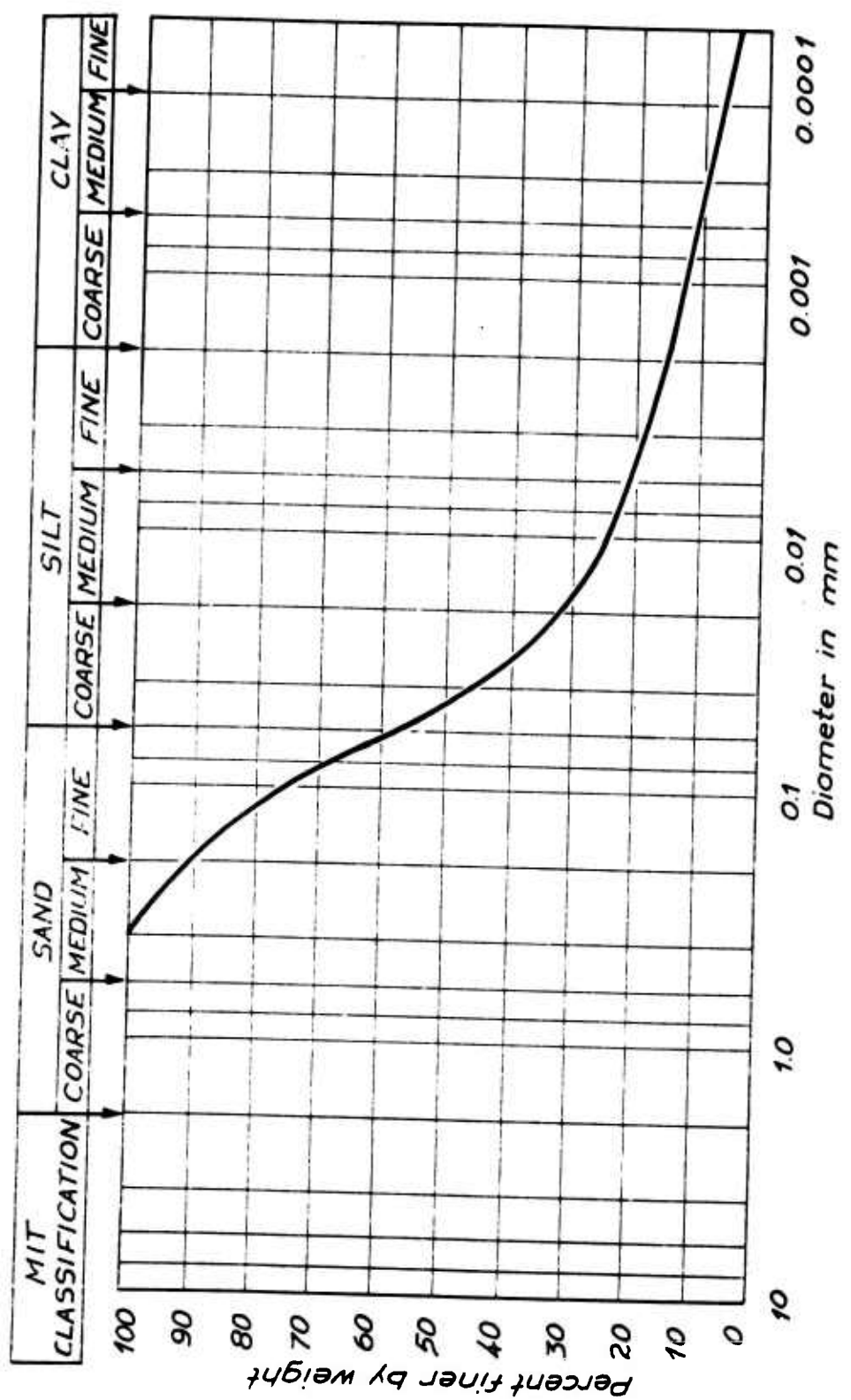


FIG. 2.1 GRAIN-SIZE DISTRIBUTION OF UNTREATED MASSACHUSETTS CLAYEY SILT

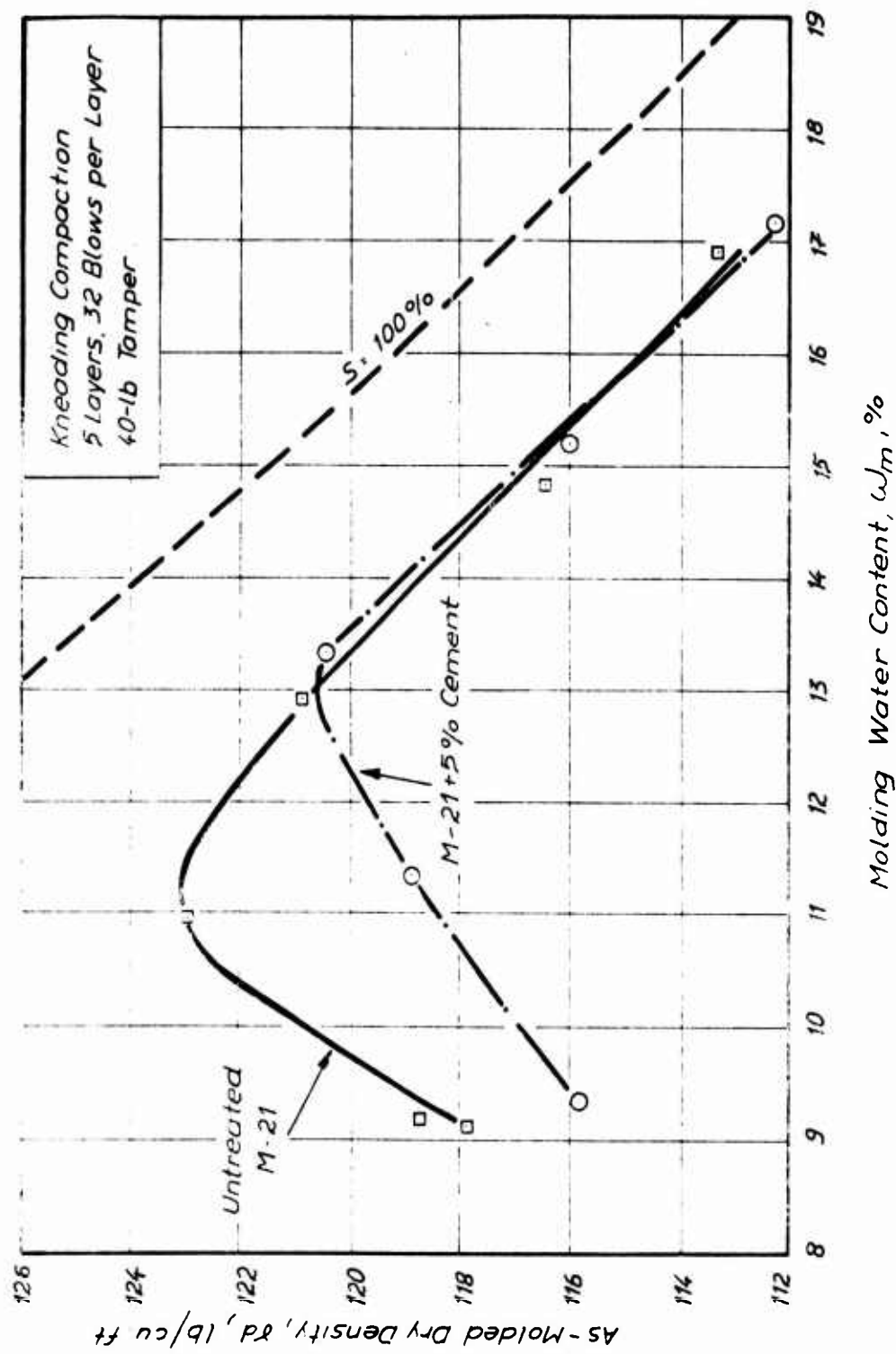
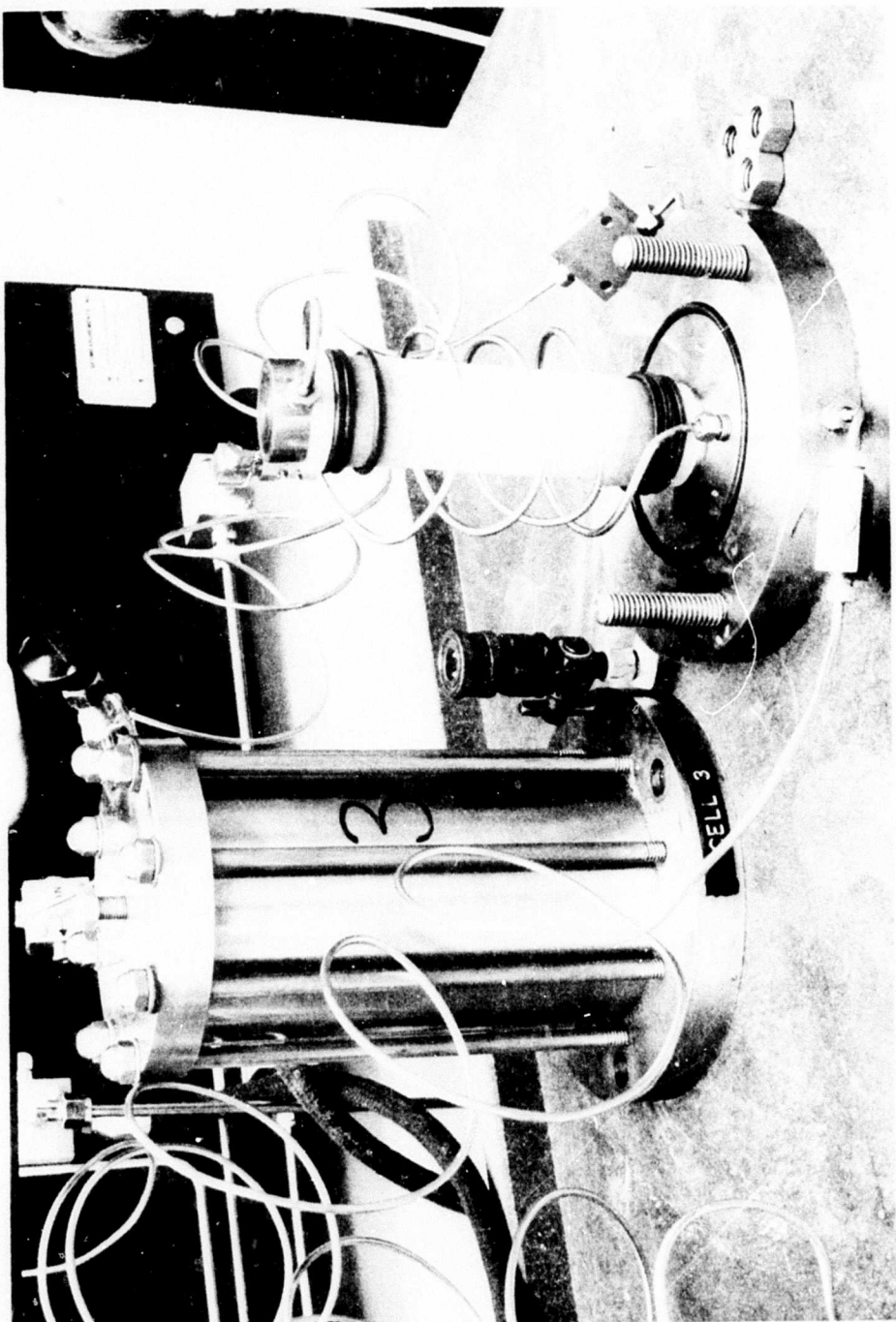


FIG. 2.2 MOISTURE-DENSITY RELATIONSHIPS FOR
TREATED AND UNTREATED M-21

FIG. 2.3 A HIGH PRESSURE CONSOLIDATION - PERMEABILITY CELL



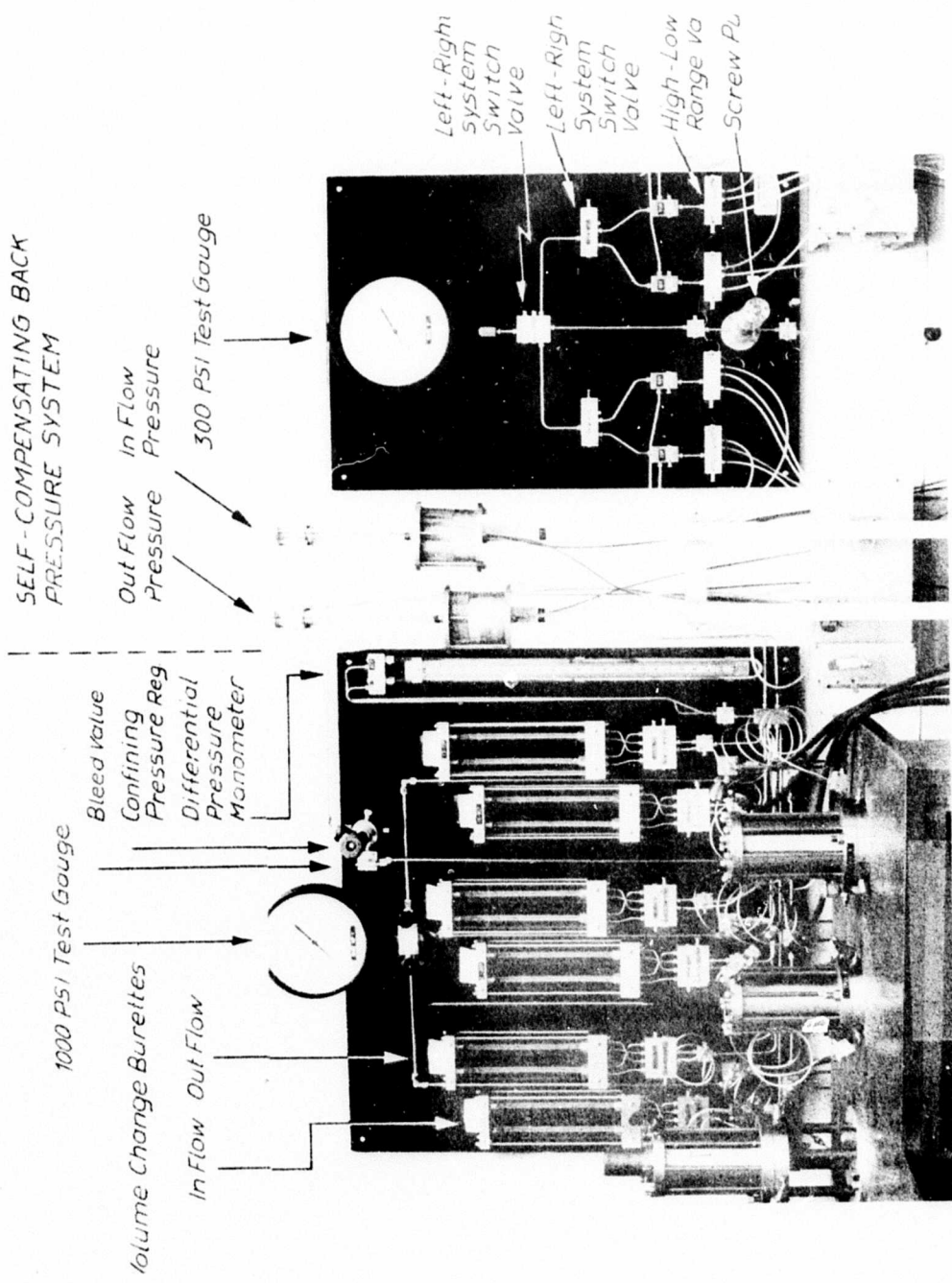


FIG. 2.4 CONSOLIDATION - PERMEABILITY SETUP SHOWING VOLUME CHANGE BACK PRESSURE AND CONFINING PRESSURE SYSTEMS FOR THREE TESTS

Chapter III

EXPERIMENTAL RESULTS

Major Testing Program

3.1 Introduction

The objective of the major testing program was to determine the influence of molding water content and type of compaction on the permeability behavior of stabilized soils. The moisture-density relations of the stabilized samples used for this investigation are shown in Fig. 3.1. The kneading compaction test specimens were prepared using a constant compactive effort as described in Art. 2.2.2.1 while the compaction effort for the statically compacted samples was varied to give approximately the same as-molded dry density as the corresponding kneading compaction samples at the same molding water content (see Art. 2.2.2.2).

In addition, for comparison purposes, a series of untreated M-21 samples were prepared using both kneading and static compaction. The moisture-density relations of these samples are also shown in Fig. 3.1. Note that, for the same kneading compaction effort, the untreated samples had higher as-molding dry densities than the corresponding treated samples compacted dry of optimum; while on the wet

side of optimum, the as-molded moisture-density relations were about the same for the treated and untreated test specimens.

The standard curing procedure described in Art. 2.3.1 was used for the stabilized samples in this program. The untreated samples were tested immediately after compaction.

3.2 Behavior During Standard Curing

3.2.1 Weight Changes During Curing

Even though the stabilized samples were cured at 70°C in sealed containers with free water in their bases and moistened filter paper around their sides, the samples tended to lose weight during the curing period.

Table 3.1 is a summary of weights and lengths of the stabilized samples as a function of time. It will be noted from this table, and from Fig. 3.2 and 3.3, that all samples lost weight during the first week of curing. This initial weight loss is greatest for those samples compacted dry of optimum. Type of compaction influenced the weight change for samples wet of optimum, but not dry of optimum.

The percentage fluid weight loss during hot cure for the driest samples (9% water content) using both compaction

methods is about 27% and for the samples with an initial molding water content, w_m , of 11% is 24%. With increasing water contents, however, the difference in water loss between the two compaction methods becomes significant. For samples close to optimum (13%), the water loss for the kneading sample is 11.6%; while for the static sample, it is much lower, 3%. For samples at 15%, the weight loss is 8% versus 3%, and for $w_m = 17\%$, 6% versus 3%, respectively. The weight loss of the static samples is relatively small and constant (about 1 gram) for the three samples on the wet side of optimum.

3.2.2 Volume Changes During Curing

From the length changes recorded during the curing period, volume changes were computed, and thereby, data on void ratio change was obtained. For the purpose of these computations, the change in lateral dimensions was assumed to be proportional to the measured change in axial length (for a complete discussion on the validity of this assumption, as well as an explanation of the meaning of "overall void ratio" used in Figs. 3.6 through 3.10, see Appendix A).

There is a tendency during cure for the samples to increase in volume. This tendency increases with increasing molding water content until the wettest sample (17%), where

a decrease is noted (Figs. 3.4 and 3.5). The driest samples have little volume change: the kneading samples decrease in volume by about 1-1/2%, while the static sample remain about constant. For both types of compaction, increasing the molding water content resulted in an increase in the expansion during curing except for the samples at the highest water content where the expansion was slightly less than for the wet samples closer to optimum.

An inspection of Figures 3.4 and 3.5 reveals that for static and kneading samples at any given molding water content, the kneading samples always yield a greater absolute volume change. The difference is small at low molding water contents (-2% volume change for $w_m = 9\%$ for kneading, versus 0.3% for the static sample) and relatively large at the point of maximum volume change ($w_m = 15\%$) (10% versus 4% respectively). Essentially, all of this volume change occurs in the first week of curing. For a given test specimen, the rate of void ratio change thus agrees, at least qualitatively, with the weight loss during curing, i.e. the largest volume increases occur when the water losses are greatest. In addition, the kneading samples which experienced greater volume changes than the static samples also lost larger quantities of water. But it should be noted that while the quantity of water lost (in both compaction methods) is greatest in the dry ($w_m = 9\%, 11\%$) samples,

volume change is smallest for these samples, and largest in those with molding water contents of 13, 15, and 17% where the weight loss is smallest.

3.2.3 Volume Change During Room Temperature Cure

Figures 3.6 and 3.7 show overall void ratio versus time prior to test and up to the first increment of consolidation pressure, for the statically and kneading compacted stabilized samples. Figures 3.8 through 3.10 show the difference in curing behavior for identical molding conditions but different compaction methods. As can be seen from these plots, there is essentially no void ratio change and no loss in water (Table 3.1) in the period between the end of hot cure and beginning of the twenty-four-hour soaking period. The length of this period was different for the two sets of samples, being nineteen days for the static samples and only one day for the kneading samples.

3.2.4 Effect of Soaking

During the soaking period only minor changes in sample length were measured, and these may have been due to inaccuracies in the measurements.

There are fairly large weight increases in the samples during soaking (Figures 3.2 and 3.3). These weight changes are largest in the driest samples, being about 86% (weight

of water absorbed divided by initial weight of molding water) for both static and kneading samples at a molding water content of 9%, and 48% for a molding water content of 11%. With increasing molding water, the weight gain decreases sharply to 10.5, 8.5 and 6.5% for static samples and 29, 18, and 12.8% for kneading samples at molding water contents of 13%, 15% and 17% respectively.

3.3 Behavior During Consolidation and Permeation

The stabilized samples after curing were consolidated to and then permeated at effective stresses of 5, 10, 25 and 50 kg/cm². A set of static and a set of kneading untreated M-21 samples at the same initial molding water contents as the stabilized samples were also tested in a similar manner. Tables 3.2 and 3.3 are complet summaries of the void ratio-permeability data obtained for the untreated and the stabilized test specimens respectively.

3.3.1 Untreated M-21

3.3.1.1 Void Ratio Versus Consolidation Pressure

Figures 3.11a through 3.11e are plots of void ratio versus consolidation pressure comparing static and kneading compaction for the unstabilized M-21 soil at the same molding water content and dry density. Table 3.4 summarizes the compressibility characteristics of these test specimens.

From the figures it can be seen that, at any given consolidation pressure, void ratios for the kneading samples are smaller than those for the static samples. The initial compression during saturation and consolidation to 5 kg/cm² was always greater for the kneading compaction samples than for the corresponding static compaction samples. However, the compression index between consolidation pressures of 25 kg/cm² and 50 kg/cm² was greatest for the static compaction samples (Table 3.4). Initial compaction is dependent on both molding water content and as-molded dry density: the higher the as-molded dry density, the lower the initial compression and the smaller the compression index; and in addition, the higher the molding water content, the higher the initial compression and the lower the compression index at high consolidation pressures.

All kneading samples exhibit an almost straight-line behavior between void ratio and log confining stress, except for the driest sample (9%), which exhibits a flat over-consolidated portion for confining stress between 5 and 10 kg/cm². The static samples, on the other hand, exhibit a far more pronounced over-consolidated portion, being greatest in the three driest samples, beyond which the consolidation behavior becomes similar to that obtained with the kneading samples (i.e., a straight-line relationship between void ratio and log consolidation stress over the entire range of consolidation stresses investigated).

When rebounded from 50 kg/cm² to 2 kg/cm², the static samples tend to experience a larger increase in volume than the kneading samples.

3.3.1.2 Permeability versus Molding Water Content

Figures 3.12 and 3.13 are plots of permeability versus initial molding water content for the kneading and the static compacted specimens, respectively, at the four consolidation pressures investigated. From these plots, it can be seen that permeability is greatest in the driest samples and decreases with increasing water content, reaching a minimum wet of optimum beyond which it only increases slightly with further increase in molding water content. At the higher consolidation pressures, the influence of molding water content on permeability is less significant than at low consolidation pressures (i.e., curves in Figures 3.12 and 3.13 become flatter with increasing consolidation pressure).

3.3.1.3 Permeability as a Function of Void Ratio

Figures 3.14 and 3.15 show the relationship between void ratio and log permeability for the kneading and static compaction samples of untreated M-21, respectively. There is a linear relationship between the two quantities for each sample, but the relation is a function of molding conditions.

3.3.1.4 Permeability and Compaction Method

Figures 3.16a and 3.16b show the influence of type of compaction on the void ratio (e) - log permeability (k) relations of the untreated samples having the same as-molded dry density and molding water content. For the samples very dry or very wet of optimum, the e -log k relation is independent of type of compaction. However, for molding water contents around optimum, the kneading compaction samples have a lower permeability than the corresponding static compaction sample at the same void ratio.

3.3.2 M-21 with 5% Portland Cement

3.3.2.1 Consolidation to 5 kg/cm²

Consolidation from zero effective stress (since the samples were soaked) to 5 kg/cm² causes a void ratio decrease in all stabilized samples regardless of compaction method. In most cases the volume decrease during consolidation to 5 kg/cm² is greater than the volume increase that occurs during the curing period as can be seen from Figs. 3.6 and 3.7. In other words, the void ratio after consolidation is lower than the as-molded void ratio even though the overall volume of the samples increases during the curing period.

The void ratio decrease during this initial consolidation

is related to the overall void ratio change during curing: the larger the overall void ratio increase during curing, the larger the void ratio decrease during initial consolidation.

From Figures 3.17a through 3.17e, which give the $e - \log \bar{\sigma}_c$ relations for the stabilized samples, it is also seen that in most cases the void ratios after consolidation to 5 kg/cm^2 are lower than the as-molded void ratios.

3.3.2.2 Void Ratio and Consolidation Pressure

Figures 3.17a through 3.17e show the relations between void ratio and log consolidation pressure for the stabilized samples. As can be seen, the amount of volume decrease occurring from 5 kg/cm^2 to 25 kg/cm^2 consolidation pressures is less than that occurring from 25 kg/cm^2 to 50 kg/cm^2 , especially for samples compacted wet of optimum. The compressibility of the stabilized samples in the range of 25 kg/cm^2 to 50 kg/cm^2 increases with increasing molding water content. At the same molding water content and dry density, the kneading compaction samples are more compressible at high consolidation pressures than the static compaction samples.

From Figure 3.18 (a plot of void ratio change from 0 to 5 kg/cm^2 consolidation pressure divided by the change from 5 to 50 kg/cm^2), it is seen that up to optimum, this

ratio is approximately the same for kneading and static samples and it increases with increasing molding water. Beyond optimum the ratio decreases and is larger for the kneading samples than for the static samples.

3.3.2.3 Permeability versus Molding Water Content

Figures 3.19 and 3.20 are plots of log permeability as a function of molding water content for the cement-stabilized samples. These plots show general similarities to those observed with the untreated samples, i.e., a high permeability for the dry samples decreasing very rapidly to a minimum at either 11% (static) or 13% (kneading) molding water content. As like the untreated soil, permeability is more a function of molding water content when the soil is compacted dry than when it is wet of optimum. The vertical distance between the top and bottom curves in Figures 3.19 and 3.20 represents the change in permeability occurring in consolidation from 5 to 50 kg/cm². It can be seen that the smallest change in permeability occurs at a molding water content of 11%. On either side of this point, the change in permeability with change in consolidation pressure increases. It reaches a maximum for the wettest samples, where the change in permeability for the static samples is about 1-1/2 orders of magnitude and for kneading samples about one order of magnitude. For the samples at 9% molding water, the permeability change is about one order of magnitude for static compaction, and

about 2/3 an order of magnitude for the kneading compaction.

3.3.2.4 Permeability as a Function of Void Ratio

Figures 3.21 and 3.22 are plots of log permeability versus void ratio. Log permeability is not always a linear function of log void ratio as it was in the untreated samples. From these figures, it can be seen that for samples wet of optimum, an approximately linear relation does exist between the two quantities, but that for drier samples, the permeability decreases more slowly with decreasing void ratio at the higher consolidation pressures. As for the untreated soil, the permeability of the stabilized soil is not only a function of void ratio but also depends on the molding water content.

3.3.2.5 Permeability and Compaction Method.

By comparing Figures 3.21 and 3.22, it is seen that type of compaction has very little effect on the permeability-void ratio relations of the stabilized soil compacted wet of optimum. Dry of optimum the kneading samples have higher permeabilities than the corresponding static samples (at the same molding water content) at the same void ratio.

Table 3.1

WEIGHTS AND LENGTHS OF STABILIZED TEST SPECIMENS
AS A FUNCTION OF CURING TIME DURING STANDARD CURE

Sample No.	KNEADING		COMPACTION		TEST		SPECIMENS			
	PT 6		PT 7		PT 8		PT 9		PT 10	
As-Molded Dry Density, lb/cu ft.	115.8		118.0		120.4		115.9		112.1	
Molding Water Content, %	9.35		11.35		13.33		15.20		17.15	
DATE	Wgt. gms.	lgth. ins.								
7/20/67 (1)	162.60	3.131	169.50	3.135	175.21	3.151	171.20	3.137	168.65	3.126
7/27/67	159.00	3.133	164.80	3.135	172.50	3.236	169.10	3.250	166.80	3.188
8/1/67	158.80	3.132	164.69	3.135	172.35	3.240	169.25	3.253	166.40	3.184
8/3/67 (2)	158.70	3.124	164.69	3.136	172.33	3.234	---	---	---	---
8/4/67 (3)	158.80	3.122	164.70	3.133	172.25	3.236	169.15	3.253	166.50	3.181
8/5/67 (4)	171.13	3.131	173.46	3.134	178.99	3.237	173.89	3.251	170.18	3.185

Sample No.	STATIC COMPACTION TEST SPECIMENS									
	PT 16		PT 17		PT 18		PT 19		PT 20	
As-Molded Dry Density, lb/cu ft.	116.4		118.0		120.7		116.8		112.3	
Molding Water Content, %	9.28		11.18		13.20		15.42		17.34	
DATE	Wgt. gms.	lgth. ins.	Wgt. gms.	lgth. ins.	Wgt. gms.	lgth. ins.	Wgt. gms.	lgth. ins.	Wgt. gms.	lgth. ins.
8/30/67 (1)	162.91	3.148	169.47	3.151	175.0	3.152	171.02	3.139	168.91	3.122
9/5/67	158.84	3.145	164.85	3.151	174.3	3.198	170.20	3.183	167.90	3.168
9/11/67	158.70	3.151	165.02	3.155	174.5	3.189	170.30	3.201	167.90	3.182
9/13/67 (2)	158.60	3.147	165.00	3.153	174.40	3.185	170.15	3.184	167.75	3.170
10/2/67 (3)	---	3.148	---	3.158	175.1	3.183	170.20	3.184	168.15	3.170
10/3/67 (4)	171.50	3.135	173.92	3.154	177.54	3.186	172.42	3.185	170.10	3.167

- Notes:
- (1) Start of 70°C curing.
 - (2) End of 70°C curing.
 - (3) Beginning of 24-hour soaking period.
 - (4) End of soaking period.

Table 3.2
Void Ratio and Permeability Characteristics
of Untreated Massaghi Silt

Sample No.	γ_d' , p.c.f.	STATIC			COMPACTION			KNEADING			COMPACTION		
		w_m , %	$\bar{\sigma}_c$, kg/cm ²	k , cm/sec	e	Sample No.	γ_d' , p.c.f.	w_m , %	$\bar{\sigma}_c$, kg/cm ²	e	Sample lost in test	k , cm/sec	
PU-11	118.7	9.0	5	0.4071	1.6×10^{-7}	PU-1	118.7	9.2	5	0.3797	8.3×10^{-8}		
		10	0.4021	1.5×10^{-7}				10	25	0.3768	7.3×10^{-8}		
		25	0.3627	---					35	---	0.3431	2.8×10^{-8}	
		35	0.3421	3.1×10^{-8}					50	0.3103	1.3×10^{-8}	---	
PU-12	122.8	11.1	5	0.3720	5.5×10^{-8}	PU-2	122.9	11.0	5	0.3602	3.0×10^{-8}		
		10	0.3675	5.5×10^{-8}				10	25	0.3458	2.1×10^{-8}		
		25	0.3518	---					35	---	0.3219	1.2×10^{-8}	
		35	0.3387	2.2×10^{-8}					50	0.2969	6.9×10^{-9}	---	
PU-13	120.4	13.2	5	0.3695	2.8×10^{-8}	PU-3	120.9	13.0	5	0.3320	1.0×10^{-8}		
		10	0.3650	2.9×10^{-8}				10	25	0.3191	8.6×10^{-9}		
		25	0.3417	1.9×10^{-8}					50	0.2921	6.2×10^{-9}		
		50	0.3086	1.0×10^{-8}						0.2691	3.5×10^{-9}		
PU-14	116.2	15.2	5	0.3876	2.7×10^{-8}	PU-4	---	---	---	---	Sample lost in test		
		10	0.3653	1.8×10^{-8}									
		25	0.3323	1.1×10^{-8}									
		50	0.3029	5.9×10^{-9}									
PU-15	113.4	17.3	5	0.3769	2.3×10^{-8}	PU-5	113.3	16.9	5	0.3512	1.6×10^{-8}		
		10	0.3531	1.7×10^{-8}				10	25	0.3328	1.2×10^{-8}		
		25	0.3218	1.0×10^{-8}					50	0.3039	7.2×10^{-9}		
		50	0.2921	6.4×10^{-9}						0.2769	3.8×10^{-9}		

Table 3.3 SUMMARY SHEET: VOID RATIO AND PERMEATION CHARACTERISTICS
OF M-21 + 58 PORTLAND CEMENT

Sample No.	d' p.c.f.	STATIC COMPACTION				Sample No.	KINFADING COMPACTATION			
		w _{m'} %	σ _c kg/cm ²	e	k, cm/sec		d' p.c.f.	w _{m'} %	σ _c kg/cm ²	e
PT-16	116.3	9.3	5	0.472	2.3 × 10 ⁻⁶	PT-6	116.1	9.4	5	0.466
	10	0.471	1.2 × 10 ⁻⁶	0.467	4.9 × 10 ⁻⁷		10	10	10	0.465
	25	0.467	4.9 × 10 ⁻⁷	0.462	3.5 × 10 ⁻⁷		25	25	10	0.463
PT-17	118.9	11.2	5	0.453	2.9 × 10 ⁻⁷	PT-7	118.9	11.4	5	0.433
	10	0.453	1.9 × 10 ⁻⁷	0.448	2.2 × 10 ⁻⁷		10	10	10	0.432
	25	0.448	2.2 × 10 ⁻⁷	0.442	1.6 × 10 ⁻⁷		25	25	10	0.430
PT-18	120.6	13.2	5	0.449	7.5 × 10 ⁻⁷	PT-8	120.7	13.3	5	0.434
	10	0.448	6.6 × 10 ⁻⁷	0.446	3.1 × 10 ⁻⁷		10	10	10	0.433
	25	0.446	3.1 × 10 ⁻⁷	0.438	6.1 × 10 ⁻⁸		25	25	10	0.432
PT-19	115.7	15.4	5	0.507	8.0 × 10 ⁻⁷	PT-9	115.9	15.2	5	0.496
	10	0.506	7.0 × 10 ⁻⁷	0.499	4.5 × 10 ⁻⁷		10	10	10	0.496
	25	0.499	4.5 × 10 ⁻⁷	0.478	3.5 × 10 ⁻⁸		25	25	10	0.490
PT-20	112.3	17.3	5	0.539	5.2 × 10 ⁻⁷	PT-10	112.4	17.2	5	0.533
	10	0.539	4.6 × 10 ⁻⁷	0.529	2.4 × 10 ⁻⁷		10	10	10	0.533
	25	0.529	2.4 × 10 ⁻⁷	0.504	1.4 × 10 ⁻⁸		25	25	10	0.530
	50	0.504	1.4 × 10 ⁻⁸				50	50	10	0.500

Table 3.4 SUMMARY OF COMPRRESSIBILITY CHARACTERISTICS
OF UNTREATED M-21 TEST SPECIMENS

Sample No.	Molding Water Content %	As-Molded Dry Density lb/cu. ft.	Molding Void Ratio	Void Ratio at 5 kg/cm ²	KNEADING COMPACTION		Compress. Index (2)	Void Ratio Change (3)
					Change in Void Ratio (1)	Compres- sion Index (2)		
KNEADING COMPACTION								
PU-1	9.2	118.7	0.446	0.380	0.066	0.107	0.029	
PU-2	11.0	122.9	0.396	0.360	0.036	0.082	0.025	
PU-3	13.2	120.4	0.425	0.332	0.093	0.080	0.025	
PU-4	--	--	--	--	--	--	--	
PU-5	16.9	113.3	0.515	0.352	0.163	0.090	0.024	
STATIC COMPACTION								
PU-11	9.0	118.7	0.446	0.407	0.039	0.126	0.039	
PU-12	11.1	122.8	0.397	0.372	0.025	0.108	0.037	
PU-13	13.0	120.9	0.419	0.369	0.050	0.114	0.030	
PU-14	15.2	116.2	0.477	0.388	0.089	0.099	0.029	
PU-15	17.3	113.4	0.513	0.377	0.136	0.095	0.026	

NOTES

- (1) Decrease in void ratio during saturation and consolidation to 5 kg/cm².
- (2) Compression index between consolidation pressures of 25 kg/cm² and 50 kg/cm².
- (3) Increase in void ratio during rebound from 50 kg/cm² to 2 kg/cm².

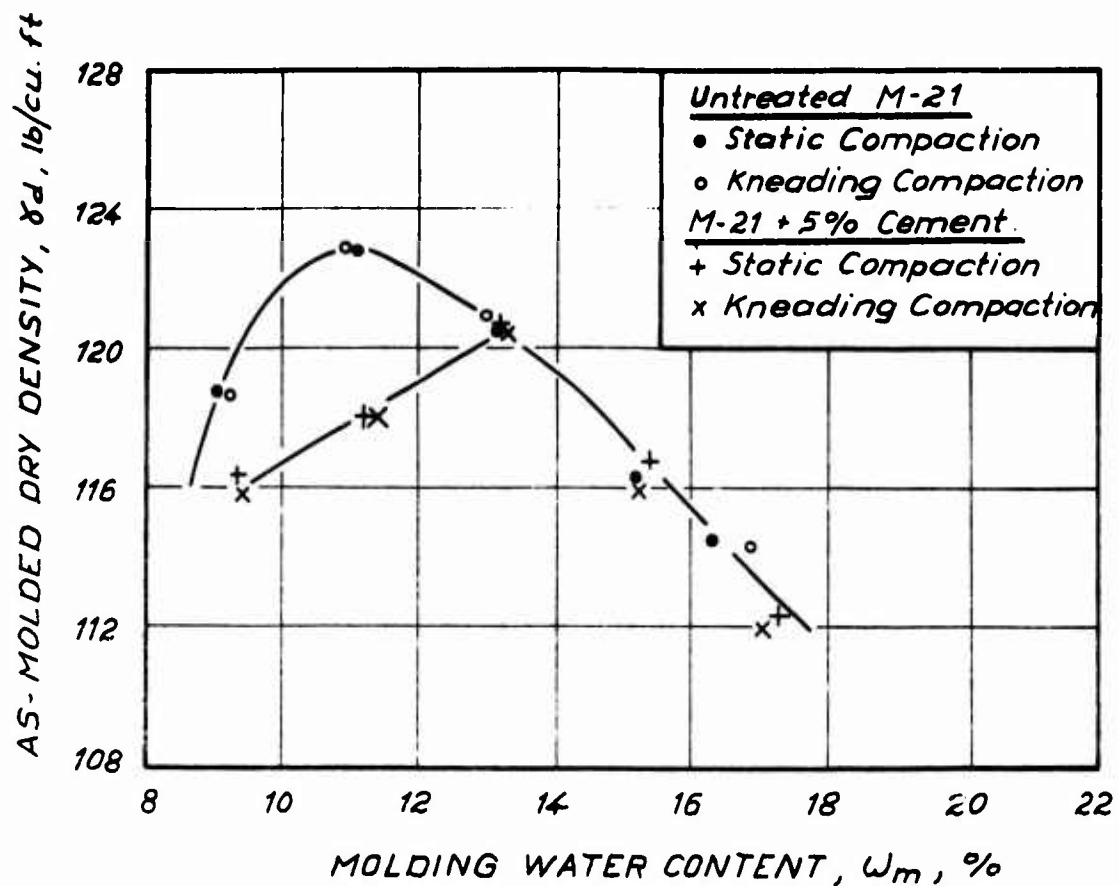


FIG. 3.1. MOISTURE-DENSITY RELATIONS OF
UNTREATED AND CEMENT STABILIZED
SAMPLES USED IN THE MAJOR
TESTING PROGRAM

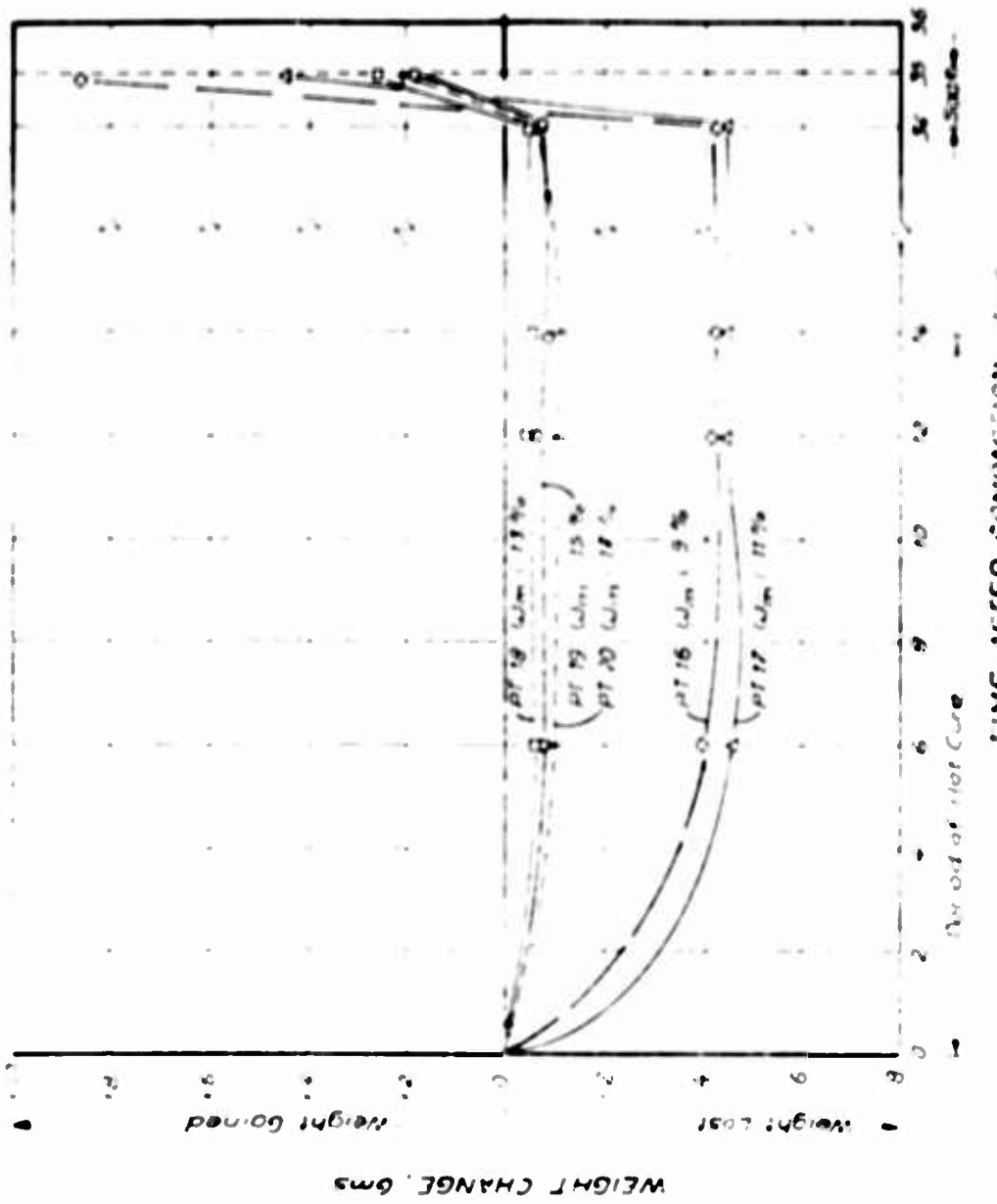


FIG 32 WEIGHT CHANGES DURING CURE VERSUS TIME FOR
STATIC STABILIZED SAMPLES

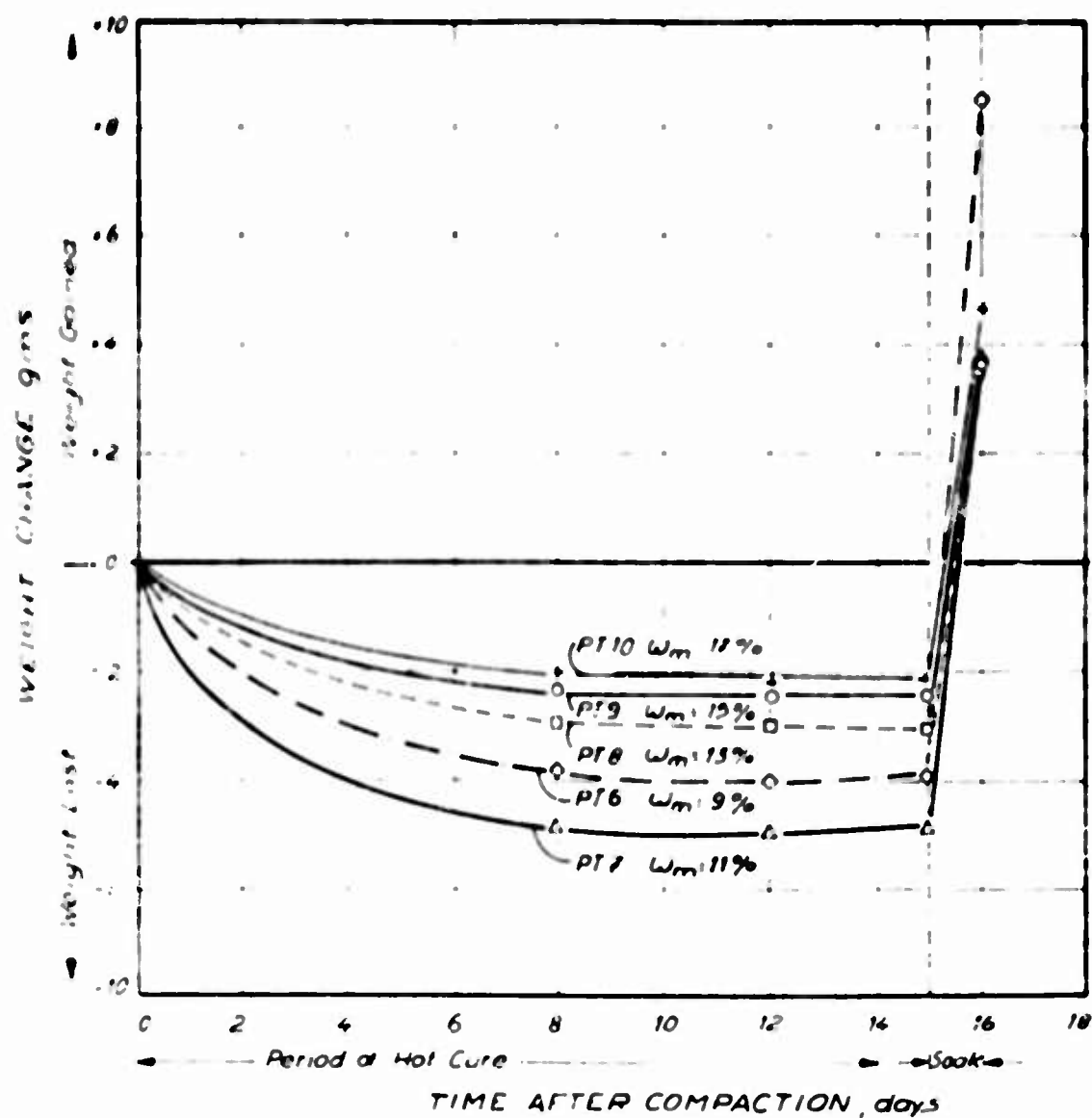


FIG 33 WEIGHT CHANGES DURING CURE VERSUS TIME FOR KNEADING STABILIZED SAMPLES.

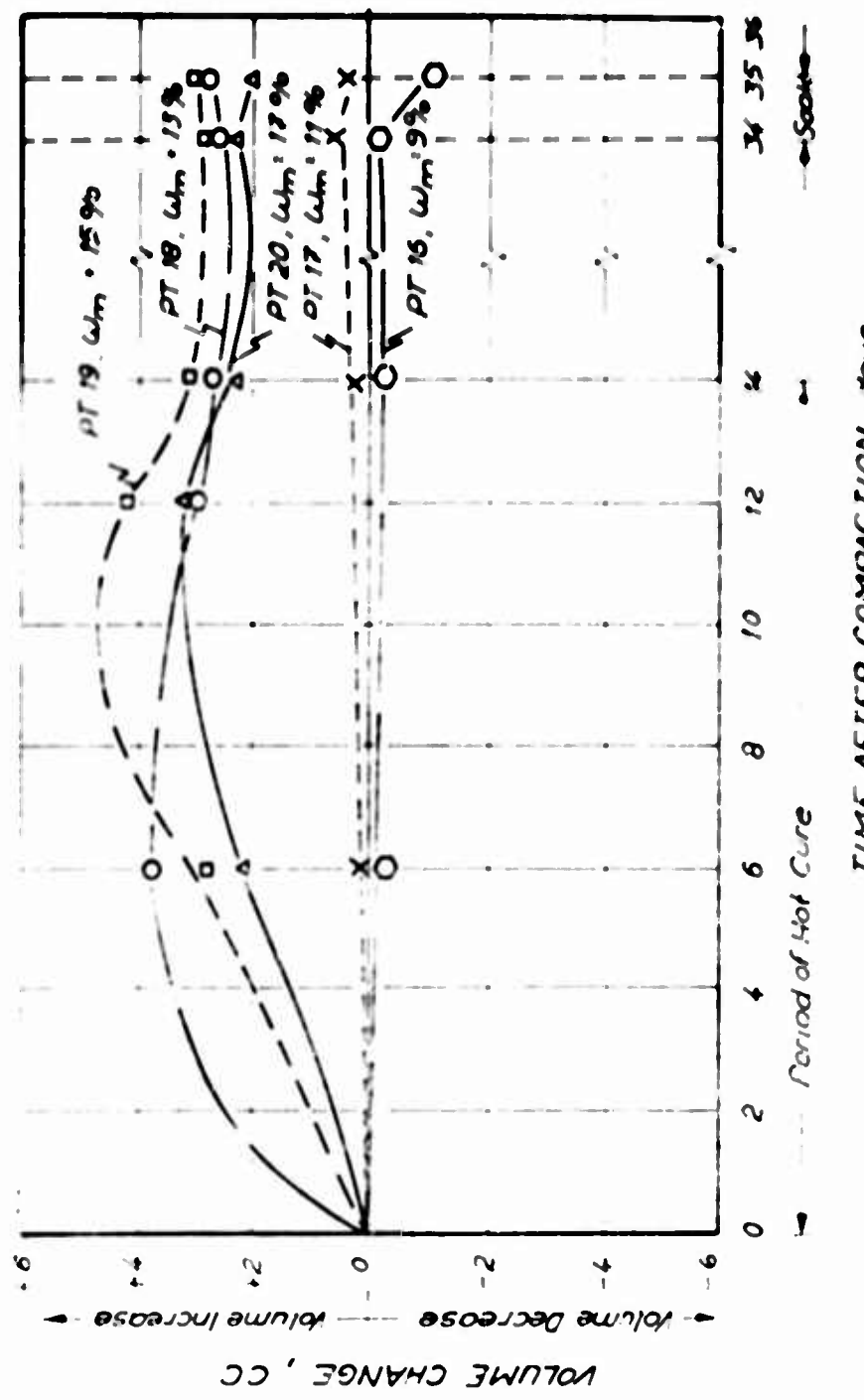


FIG. 34 VOLUME CHANGE DURING CURING FOR STATIC STABILIZED SAMPLES

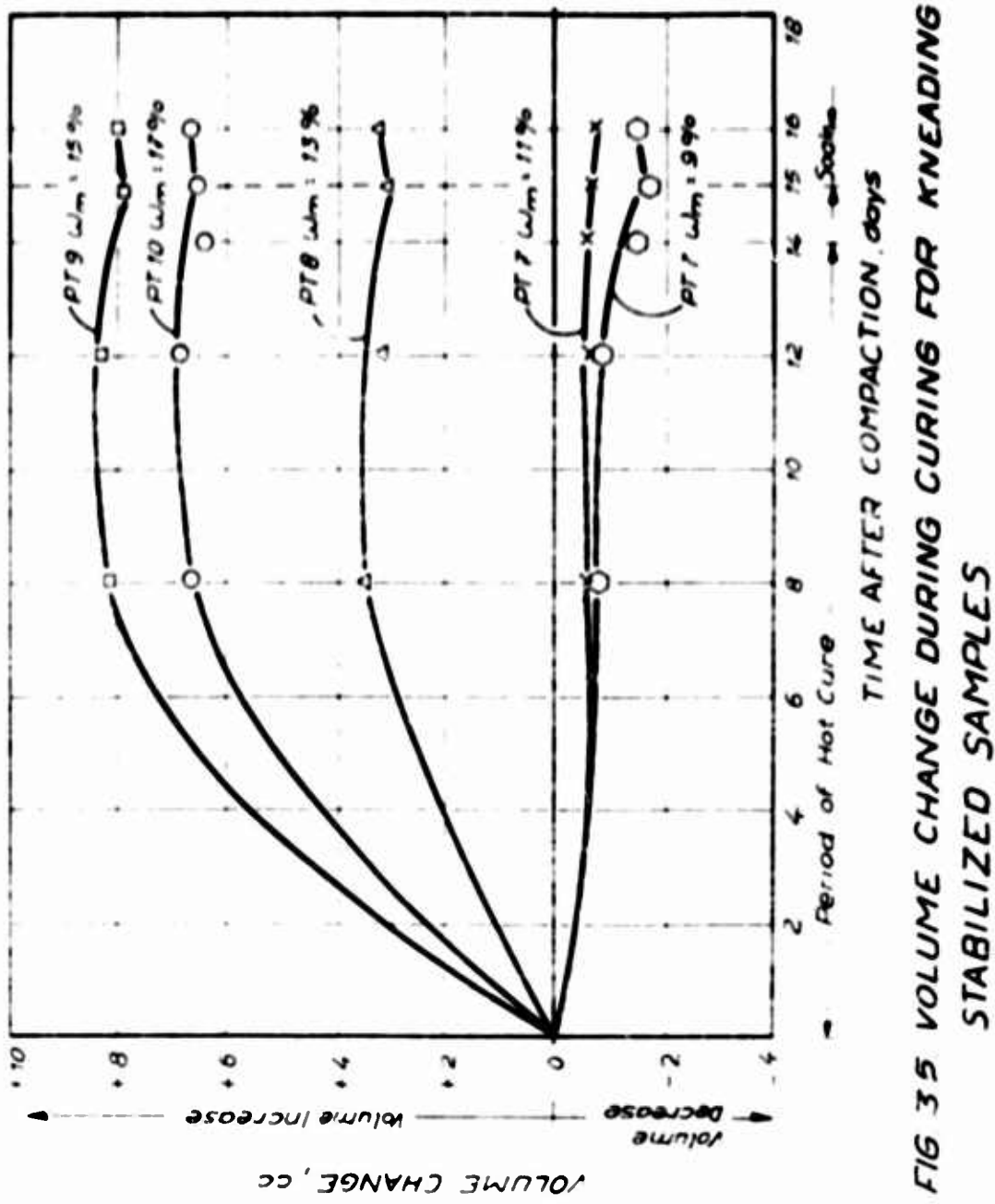


FIG 35 VOLUME CHANGE DURING CURING FOR KNEADING STABILIZED SAMPLES

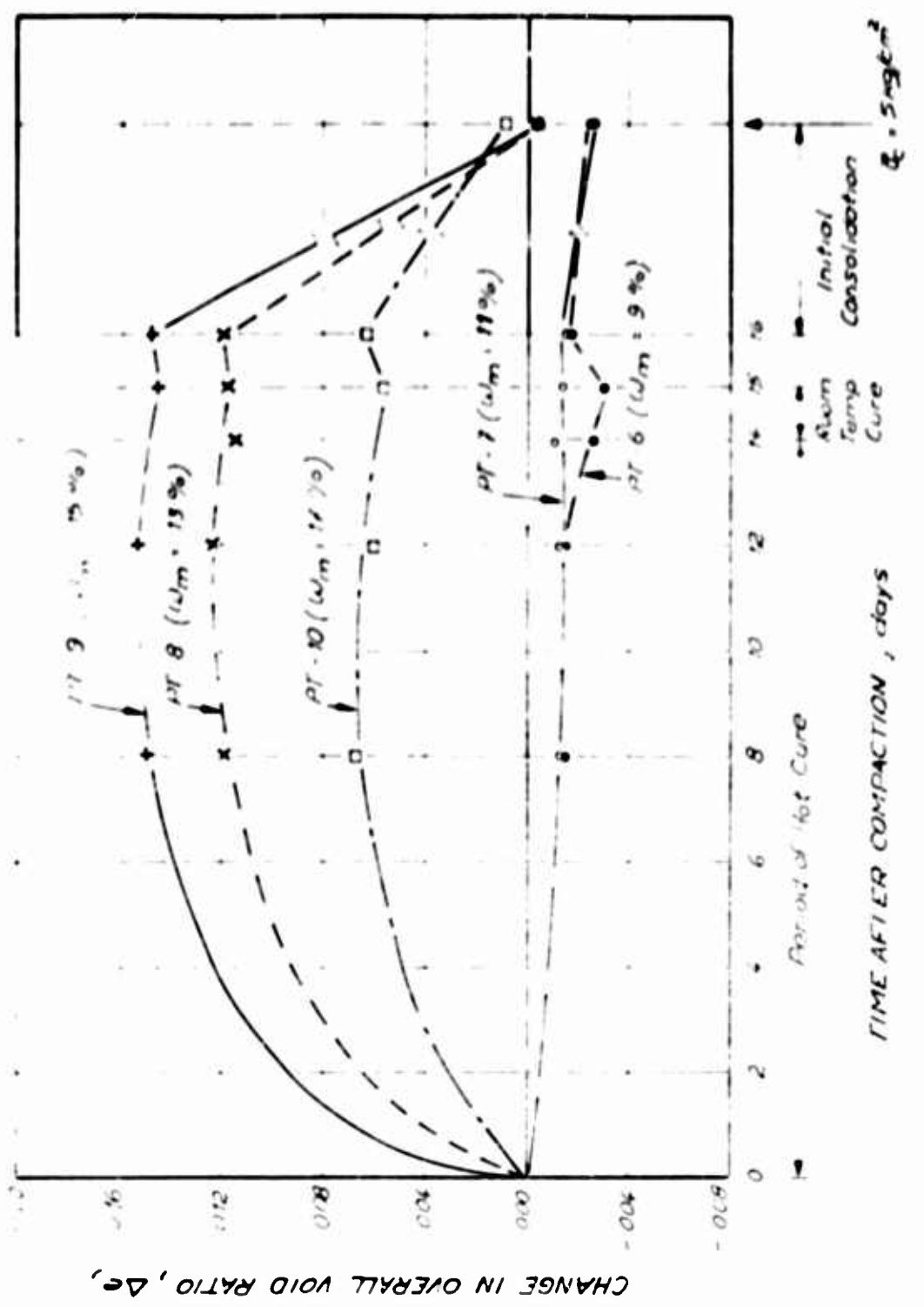


FIG. 36. CHANGE IN OVERALL VOID RATIO VERSUS CURING TIME FOR KNEADING STABILIZED SAMPLES

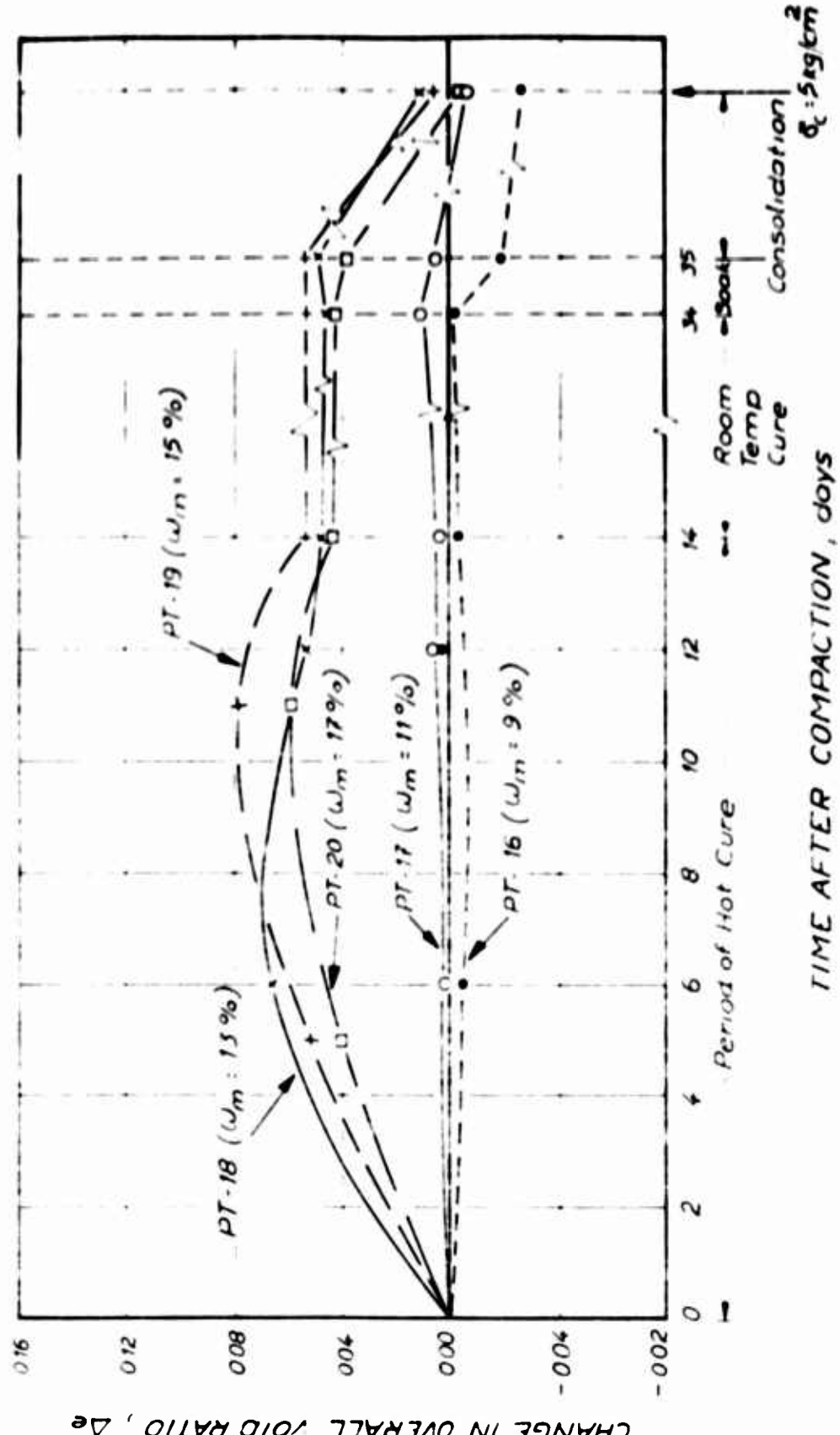


FIG. 3.7 CHANGE IN OVERALL VOID RATIO VERSUS CURING TIME FOR STATIC STABILIZED SAMPLES.

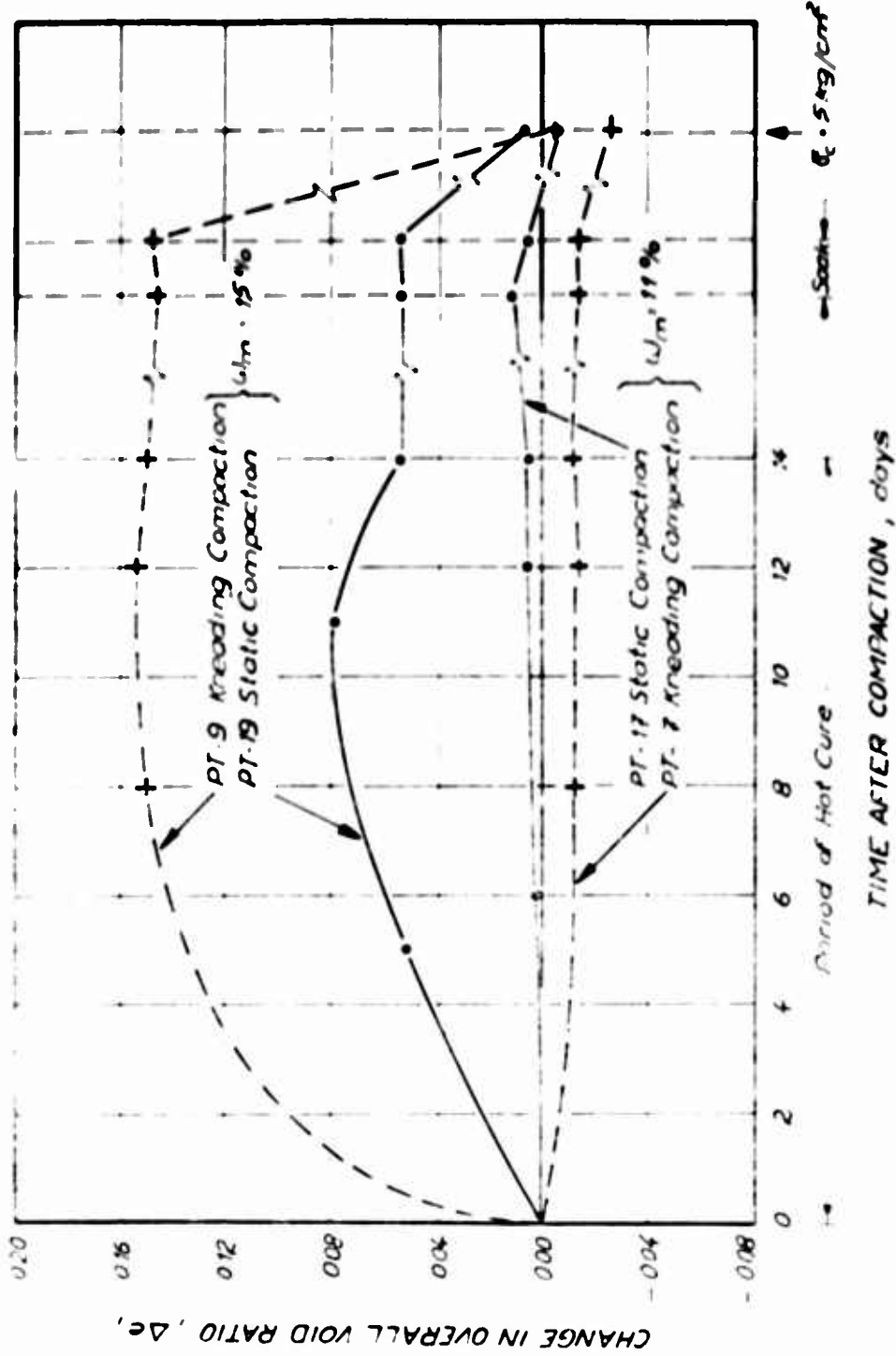


FIG. 3.8 INFLUENCE OF TYPE OF COMPACTION ON OVERALL VOID RATIO CHANGE DURING CURING FOR STABILIZED SAMPLES COMPACTED DRY AND WET OF OPTIMUM

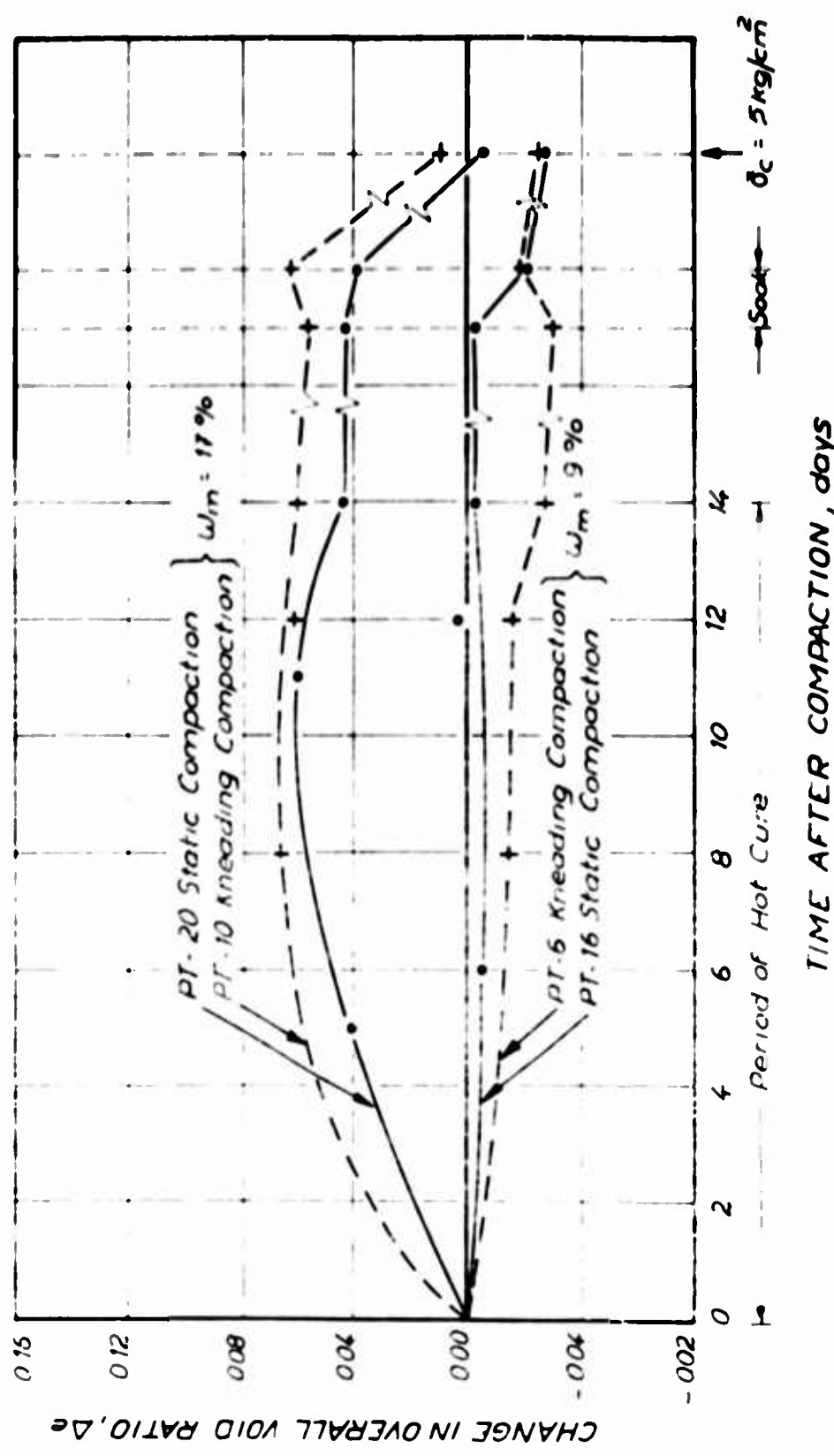


FIG. 3.9. INFLUENCE OF TYPE OF COMPACTION ON OVERALL VOID RATIO CHANGE DURING CURING FOR STABILIZED SAMPLES COMPACTED VERY DRY AND VERY WET OF OPTIMUM

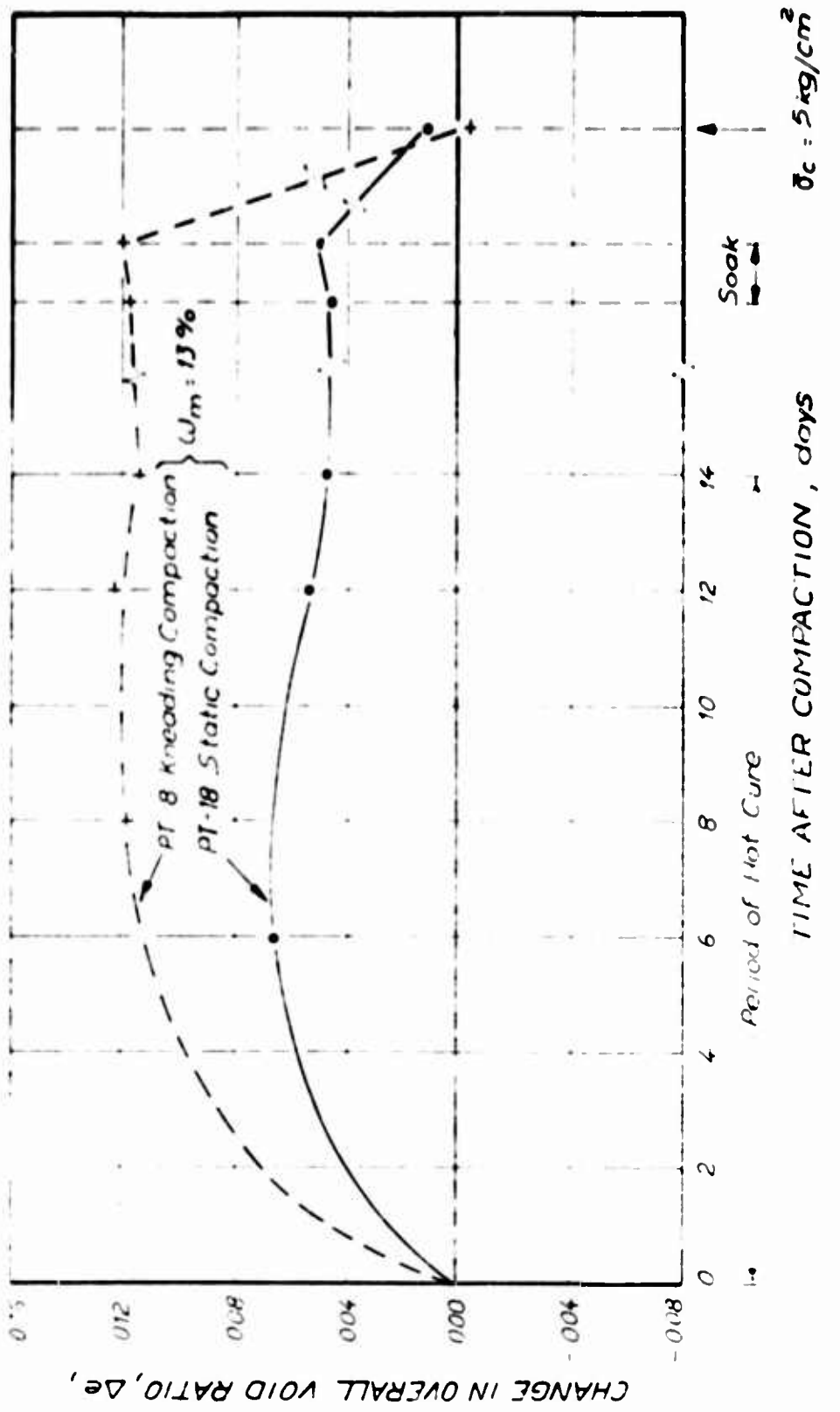


FIG. 3.10 INFLUENCE OF TYPE OF COMPACTION ON OVERALL VOID RATIO CHANGE DURING CURING FOR STABILIZED SAMPLES COMPACTED AT OPTIMUM

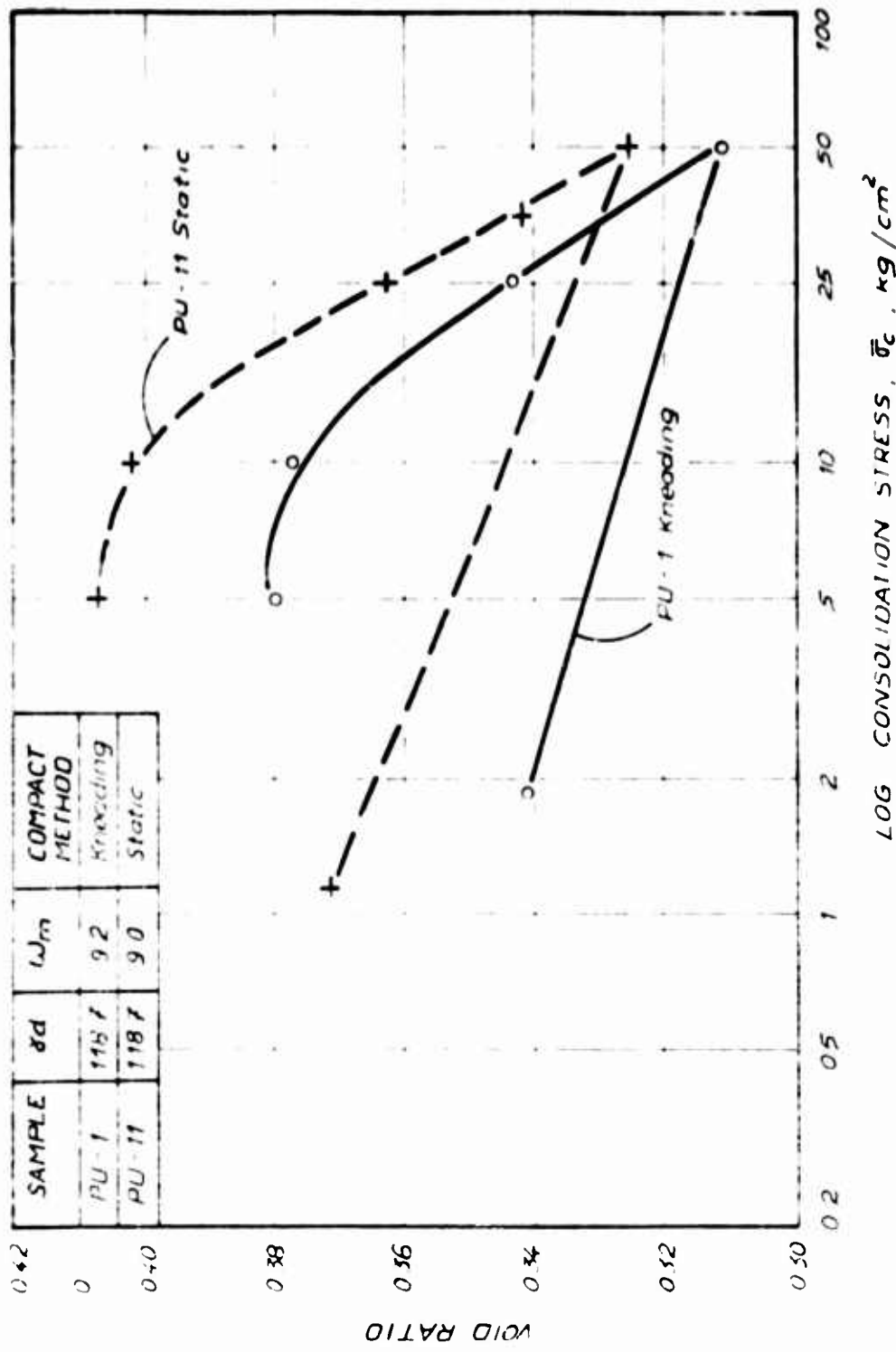


FIG. 3.11a VOID RATIO VERSUS CONSOLIDATION PRESSURE FOR UNTREATED
M-21 COMPACTED DRY OF OPTIMUM ($w_m = 9\%$)

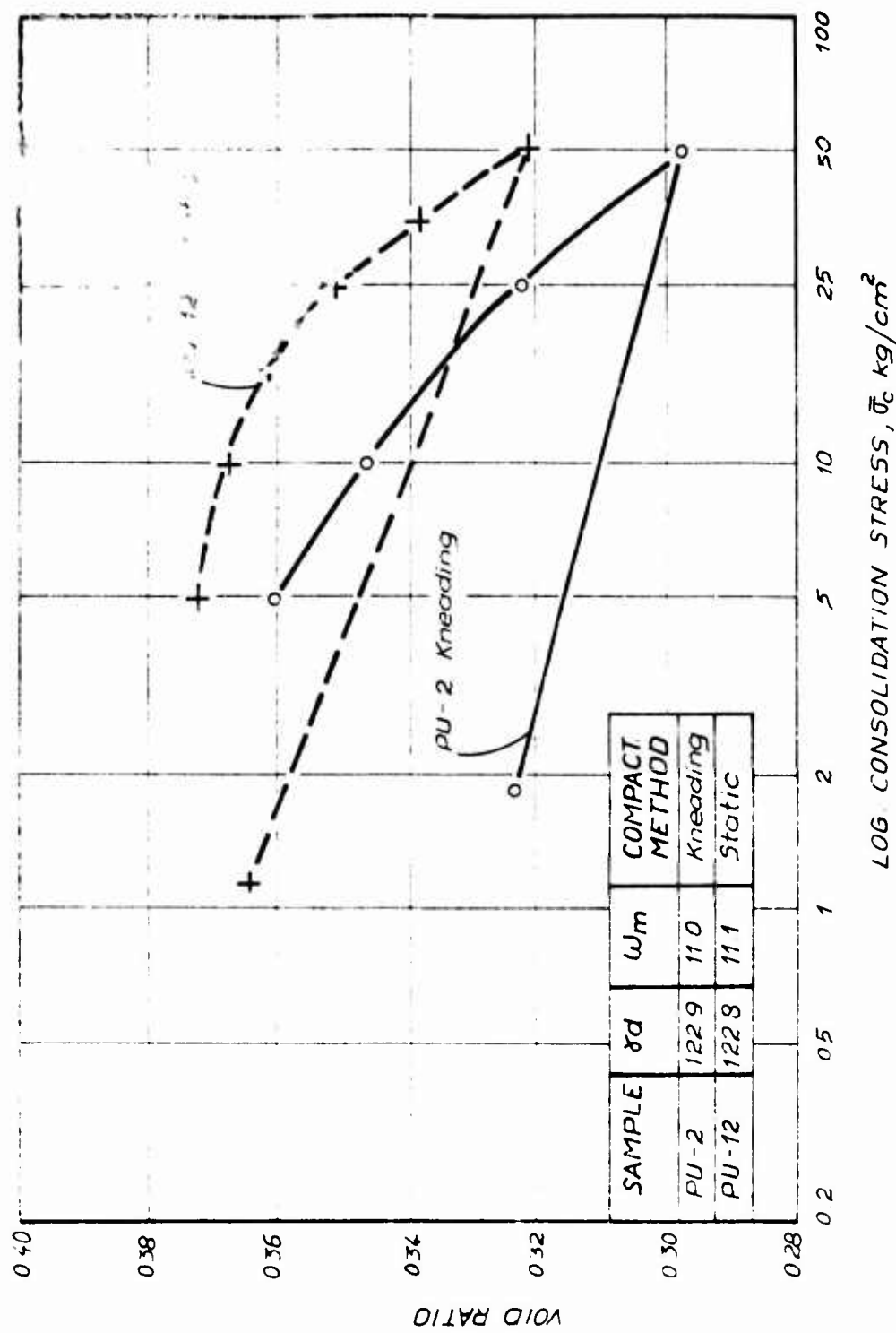


FIG. 3.11b VOID RATIO VERSUS CONSOLIDATION PRESSURE FOR
UNTREATED M-21 COMPACTED AT OPTIMUM ($w_m = 11\%$)

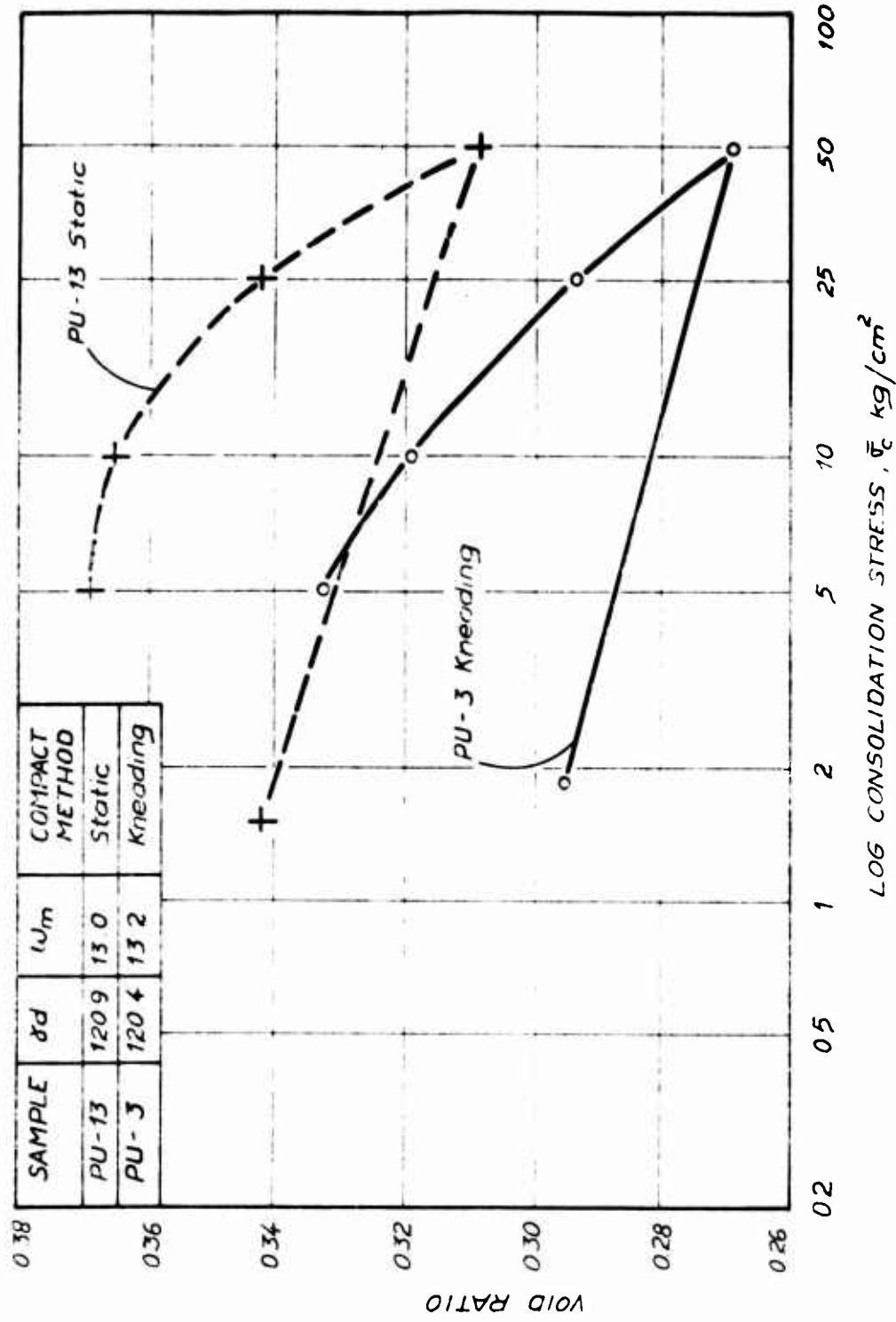


FIG. 3.11C VOID RATIO VERSUS CONSOLIDATION PRESSURE FOR UNTREATED
M-21 COMPACTED SLIGHTLY WET OF OPTIMUM ($\omega_m = 13\%$)

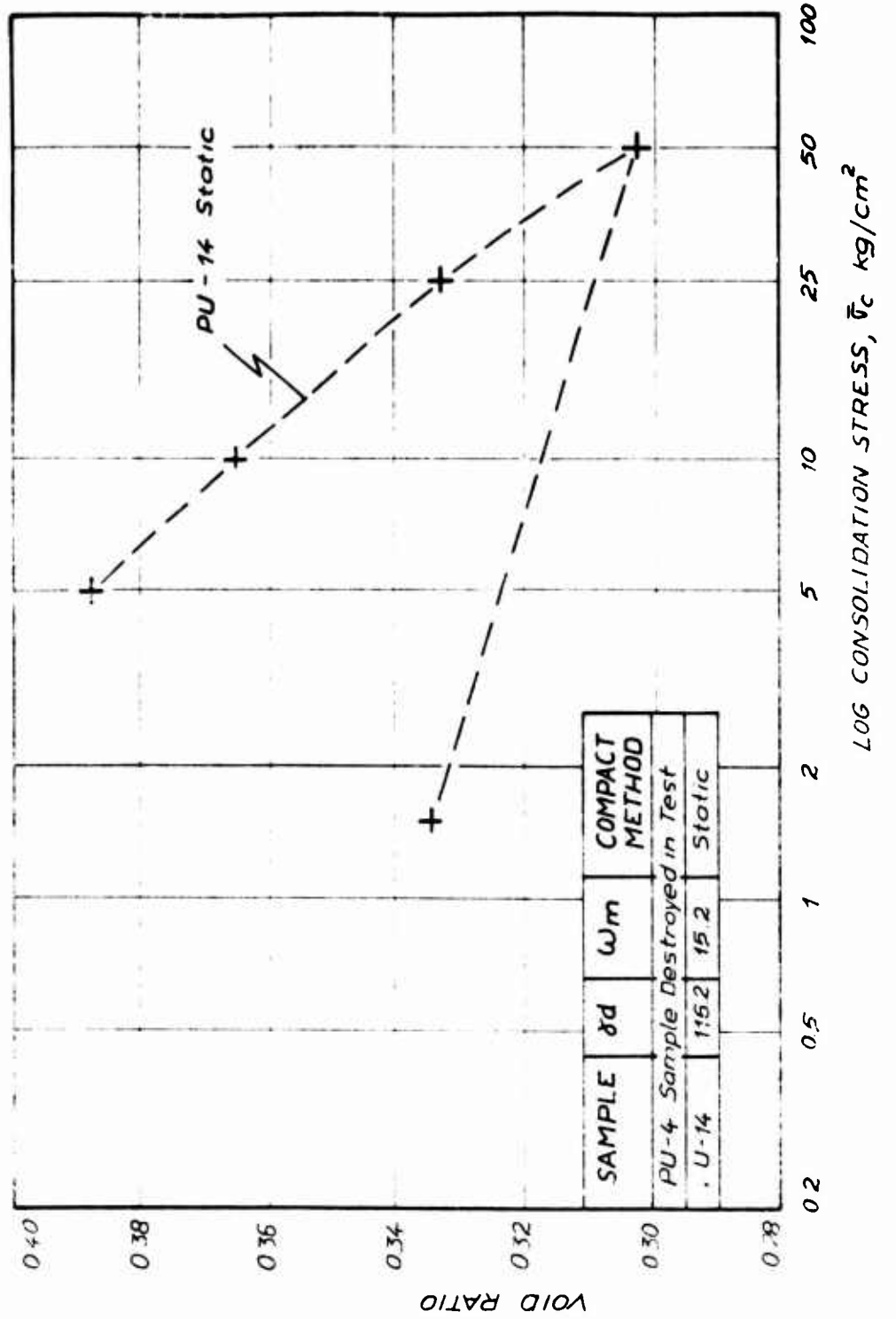


FIG. 3.11d VOID RATIO VERSUS CONSOLIDATION PRESSURE FOR
UNTREATED M-21 COMPACTED WET OF OPTIMUM ($\omega_m = 15\%$)

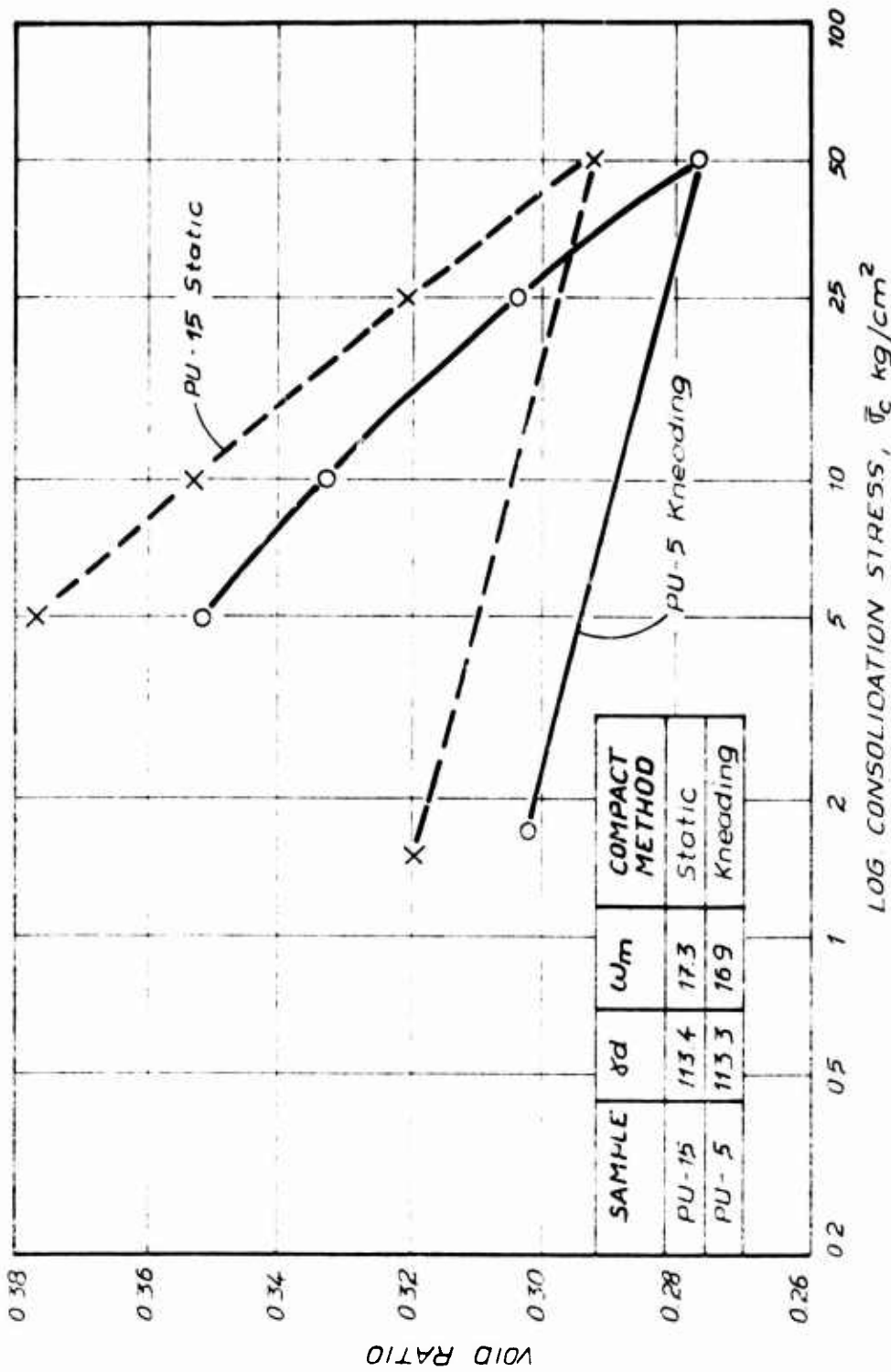


FIG. 3.11e VOID RATIO VERSUS CONSOLIDATION PRESSURE FOR
UNTREATED M-21 COMPACTED VERY WET
OF OPTIMUM ($\omega_m = 17\%$)

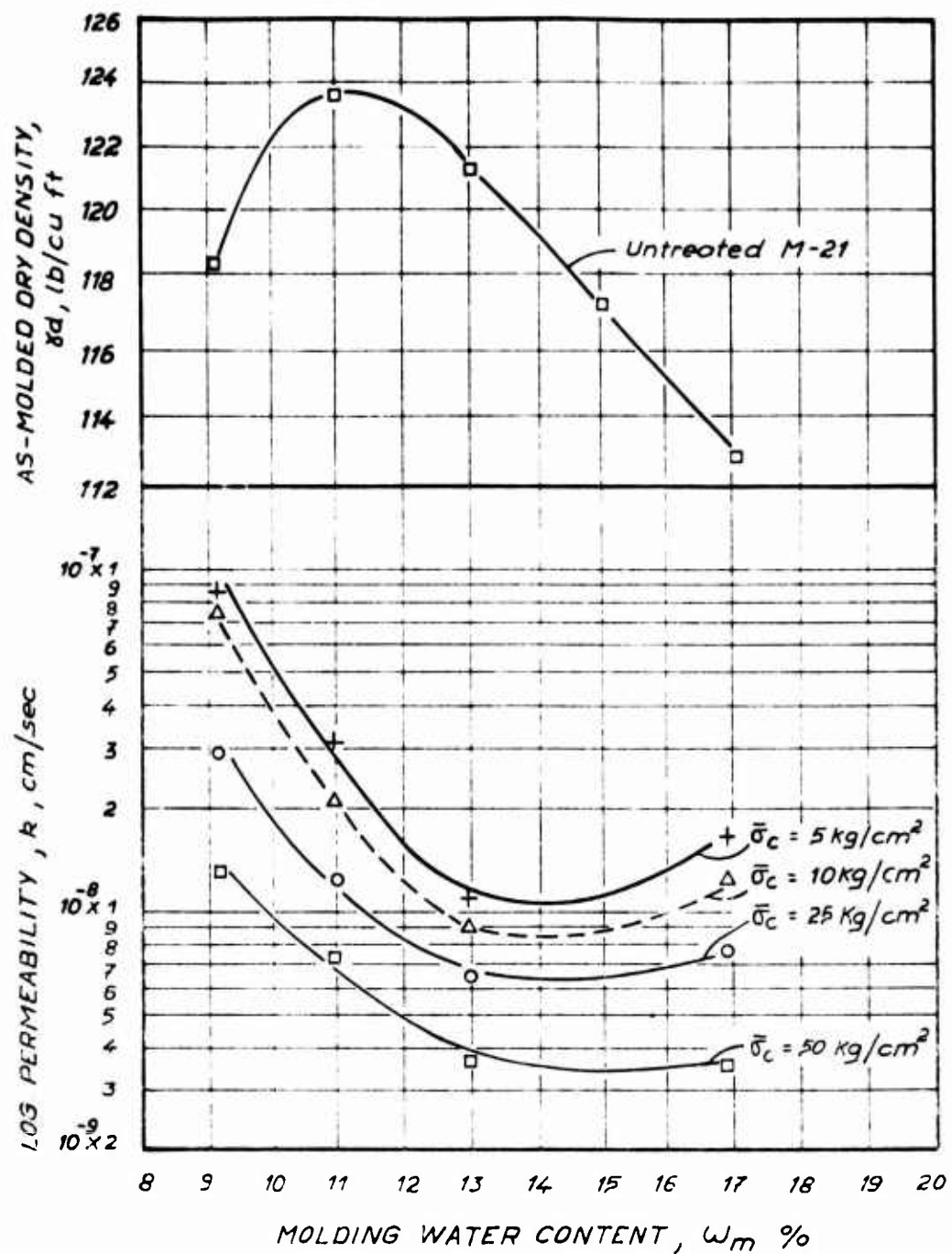


FIG. 3.12. PERMEABILITY VERSUS MOLDING WATER CONTENT FOR KNEADING COMPACTION UNTREATED M-21 SPECIMENS

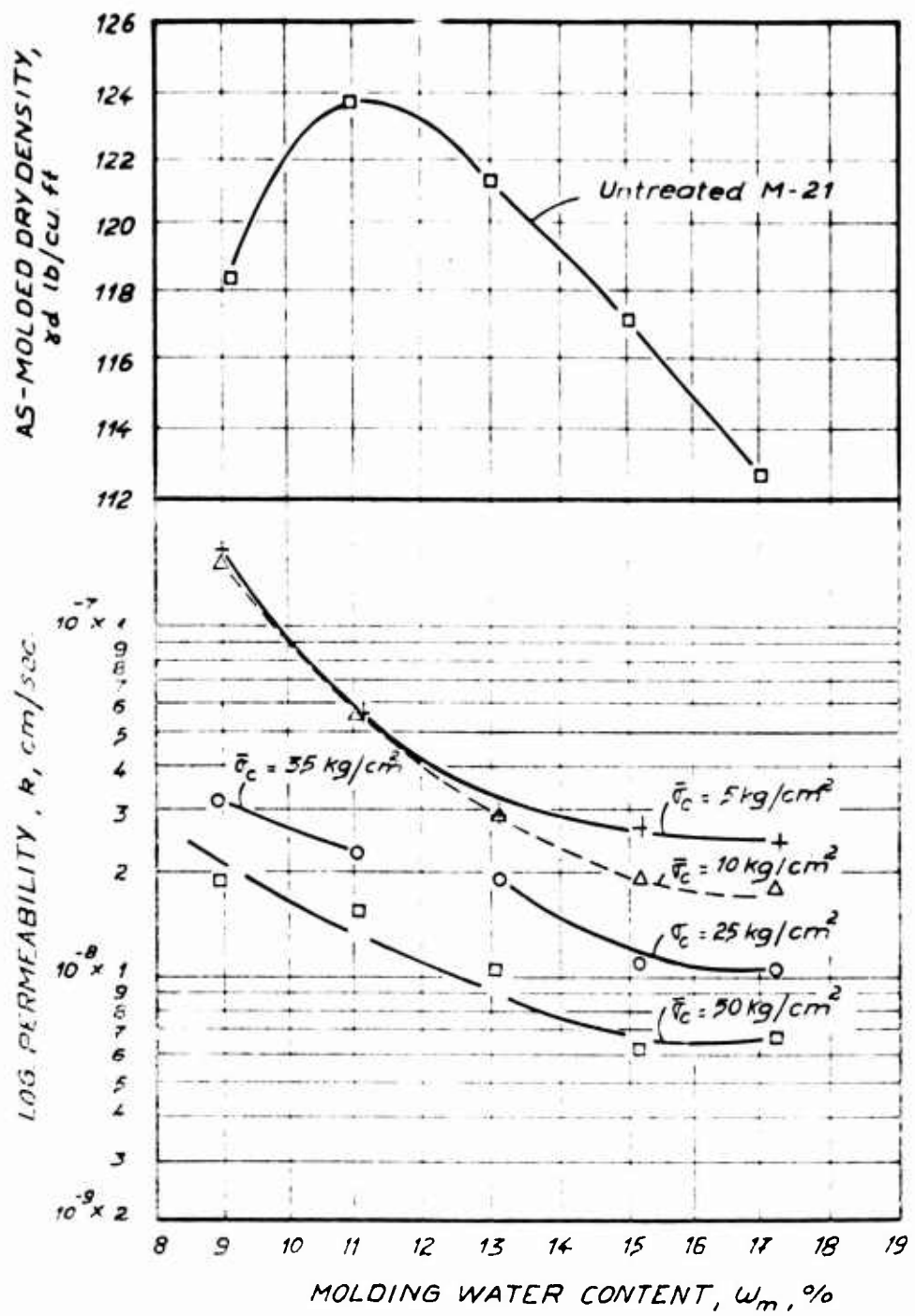


FIG. 3.13. PERMEABILITY VERSUS MOLDING WATER CONTENT FOR STATIC COMPACTION UNTREATED M-21 SPECIMENS.

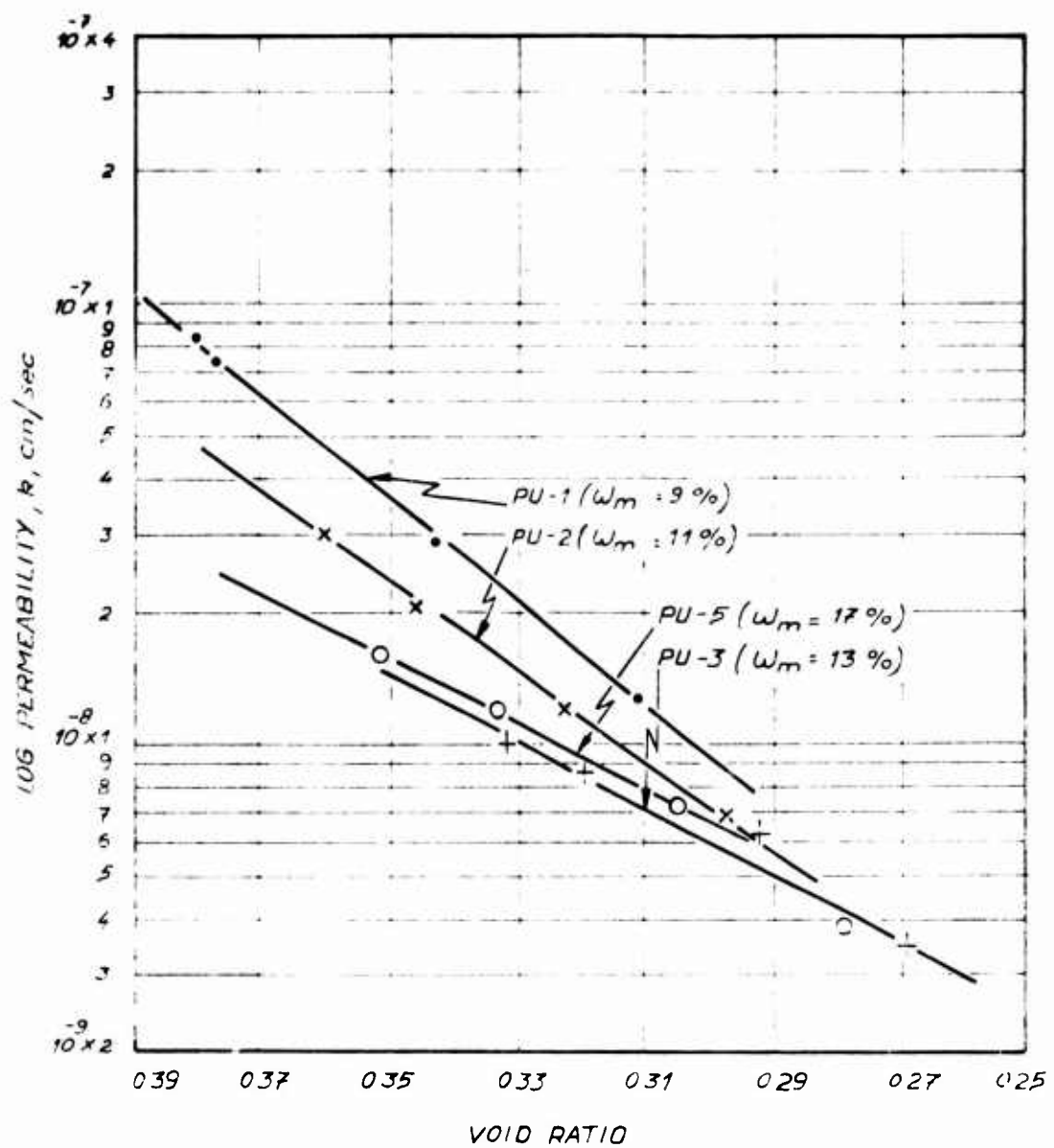


FIG. 3.14 INFLUENCE OF VOID RATIO ON THE PERMEABILITY OF KNEADINGLY COMPACTED M-21.

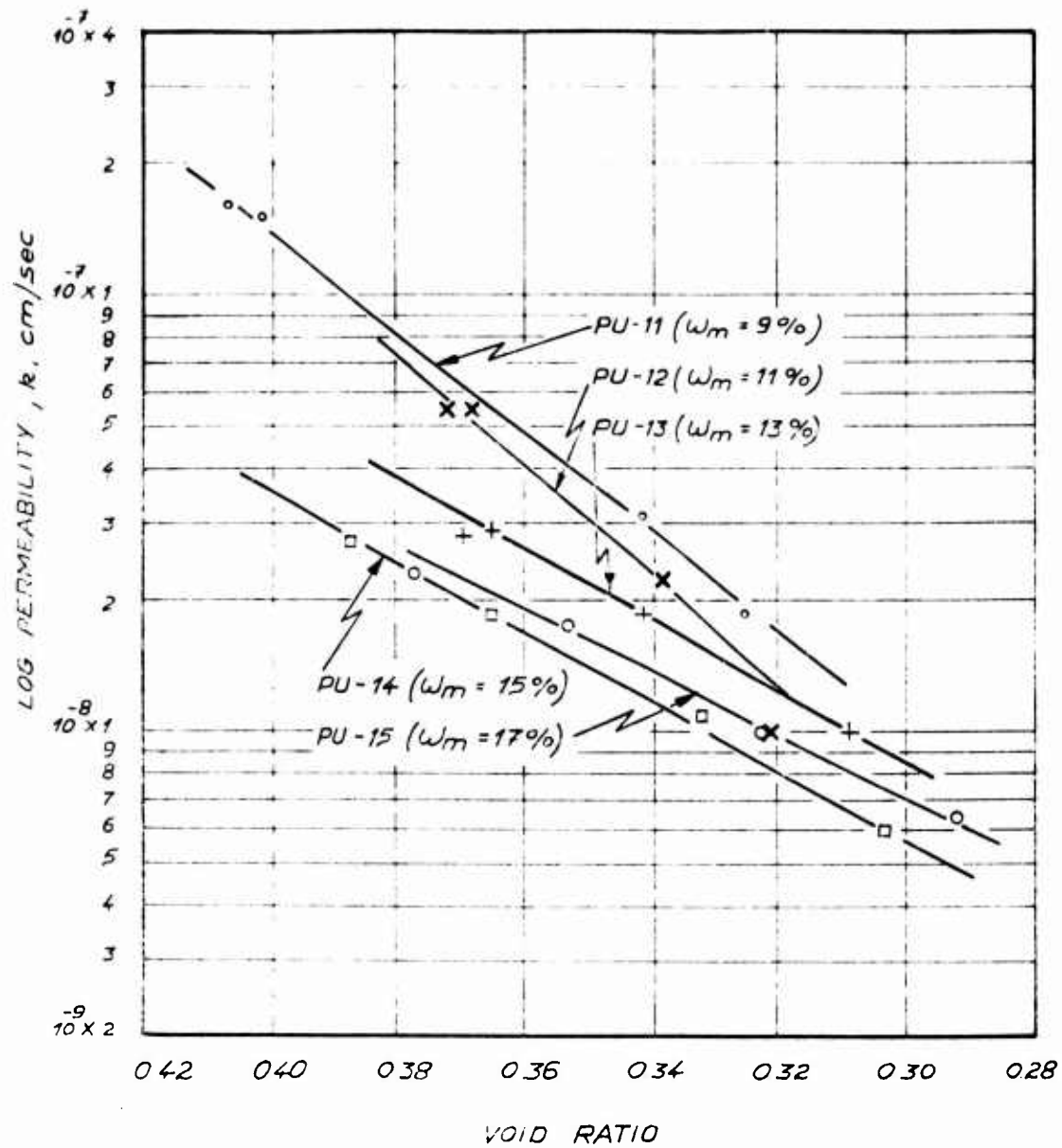


FIG. 3.15. INFLUENCE OF VOID RATIO ON THE PERMEABILITY OF STATICALLY COMPACTED M-21

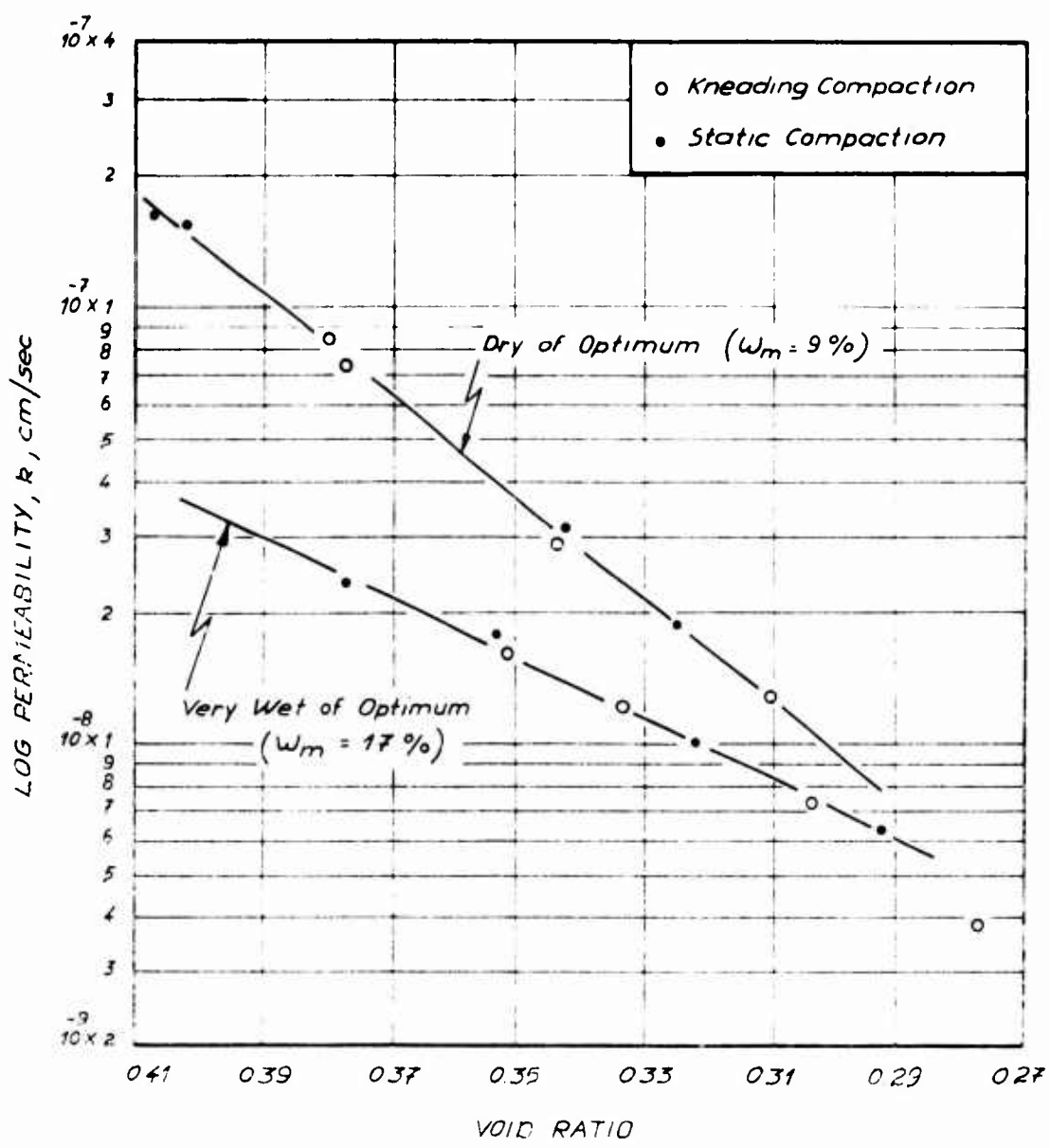


FIG 3.16a INFLUENCE OF TYPE OF COMPACTION ON THE PERMEABILITY OF UNTREATED M-21

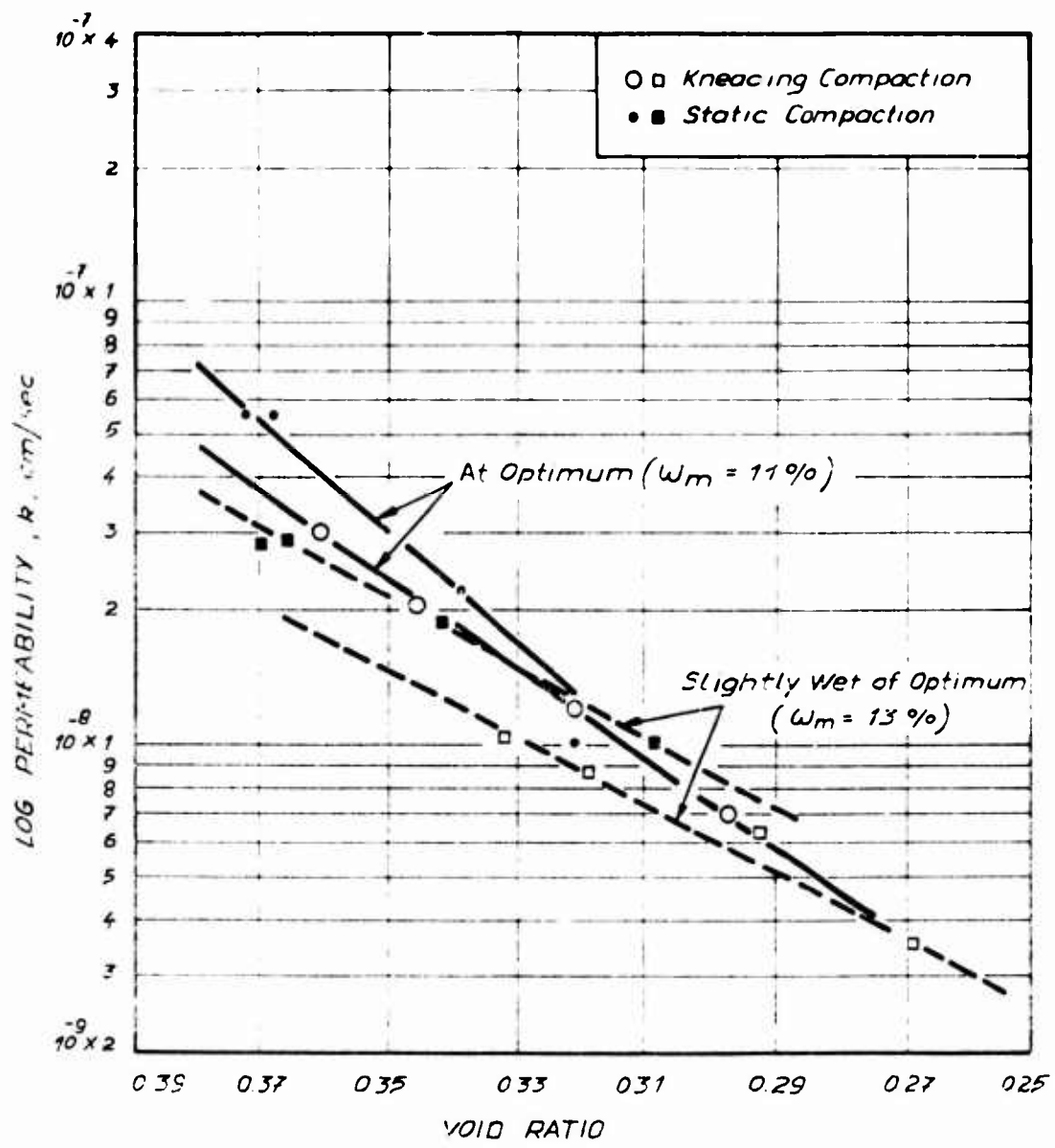


FIG. 3. 16 b. INFLUENCE OF TYPE OF COMPACTION ON THE PERMEABILITY OF UNTREATED M-21 (CONT'D)

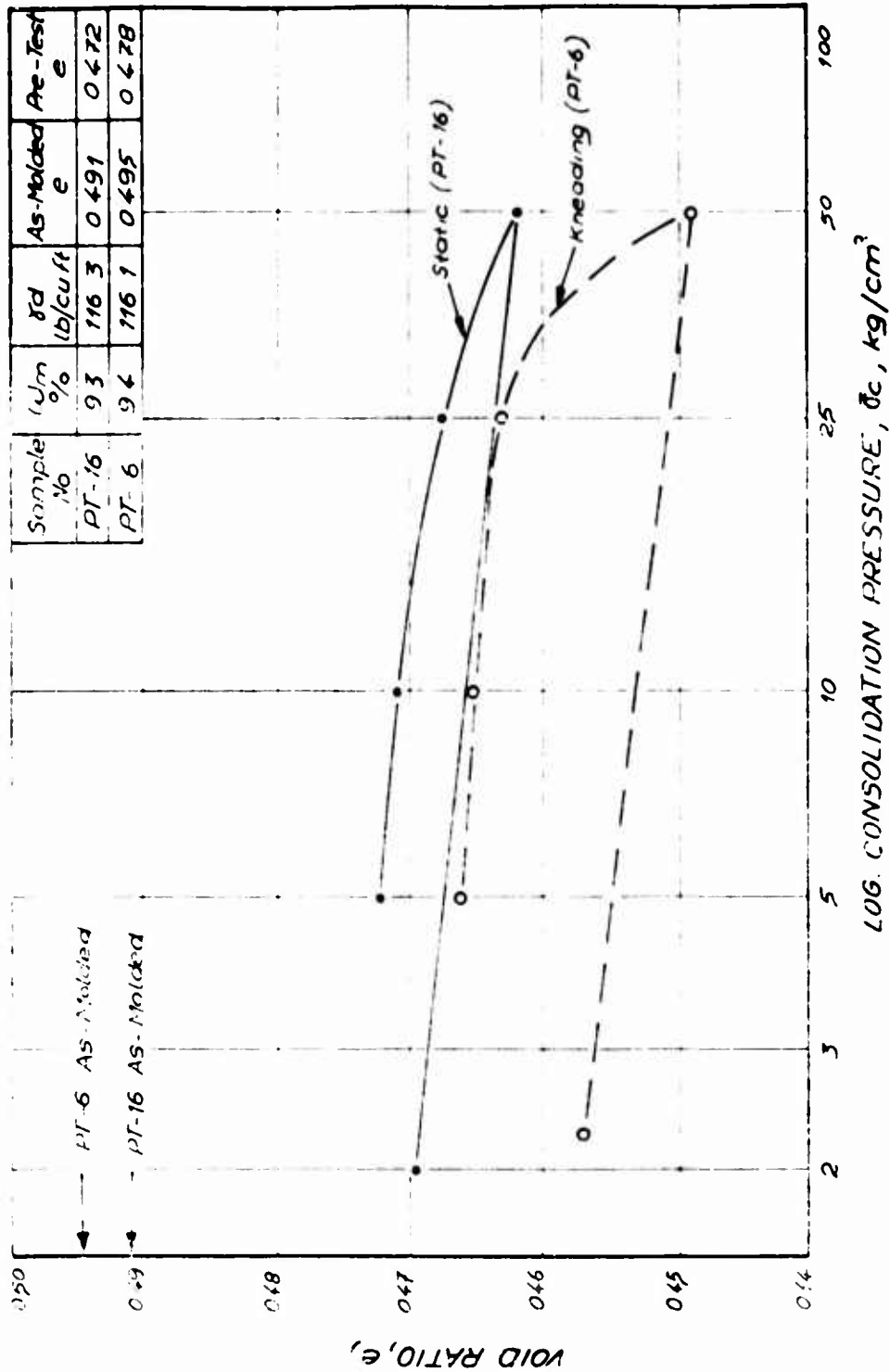
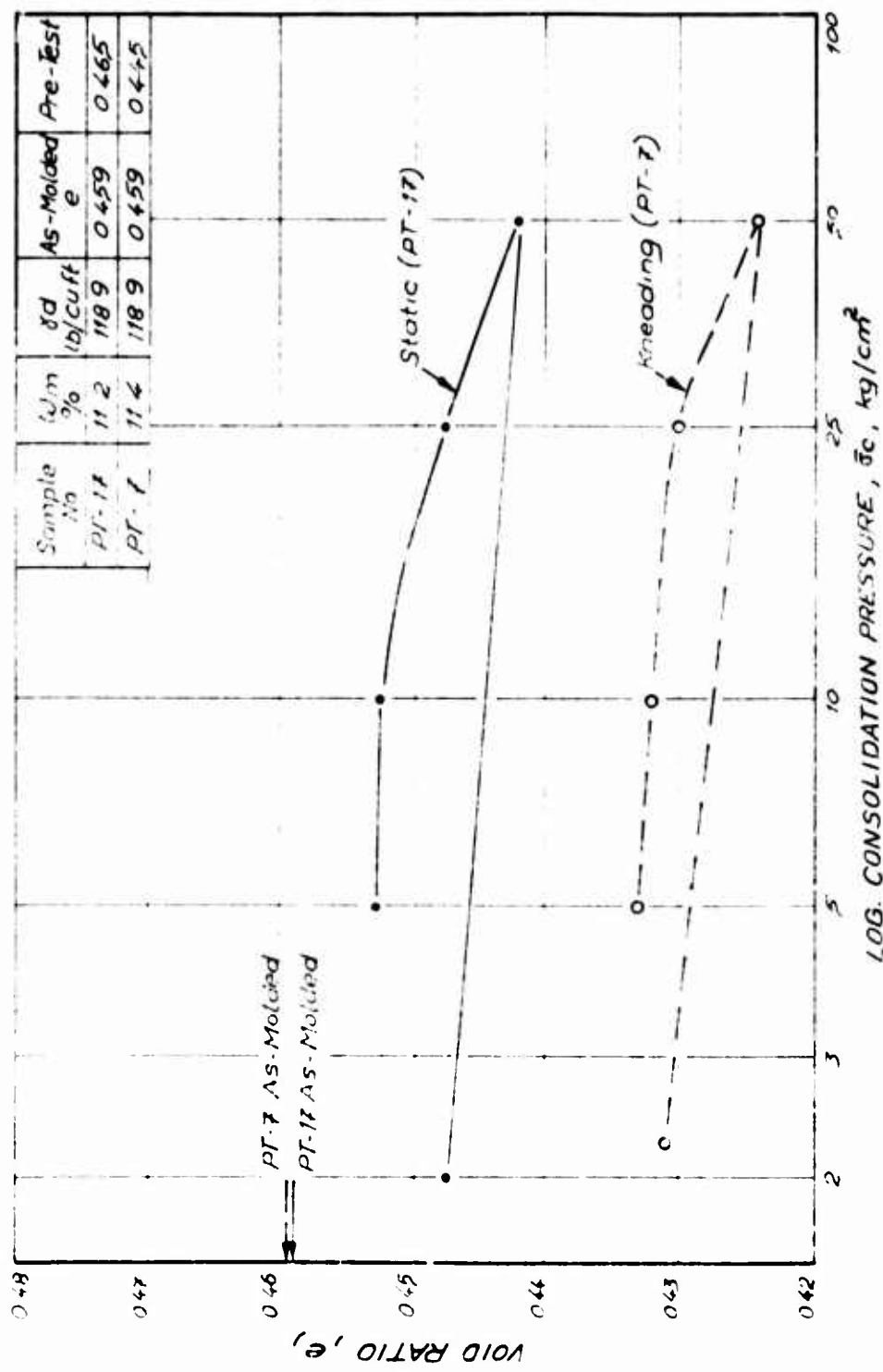


FIG 3.17a VOID RATIO VERSUS CONSOLIDATION PRESSURE, σ_c , kg/cm²
M-21+5% CEMENT COMPACTED VERY DRY OF OPTIMUM ($w_m = 9\%$)



VOID RATIO VERSUS CONSOLIDATION PRESSURE FOR M-21+5% CEMENT COMPACTED DRY OF OPTIMUM ($\omega_{opt} = 11\%$)

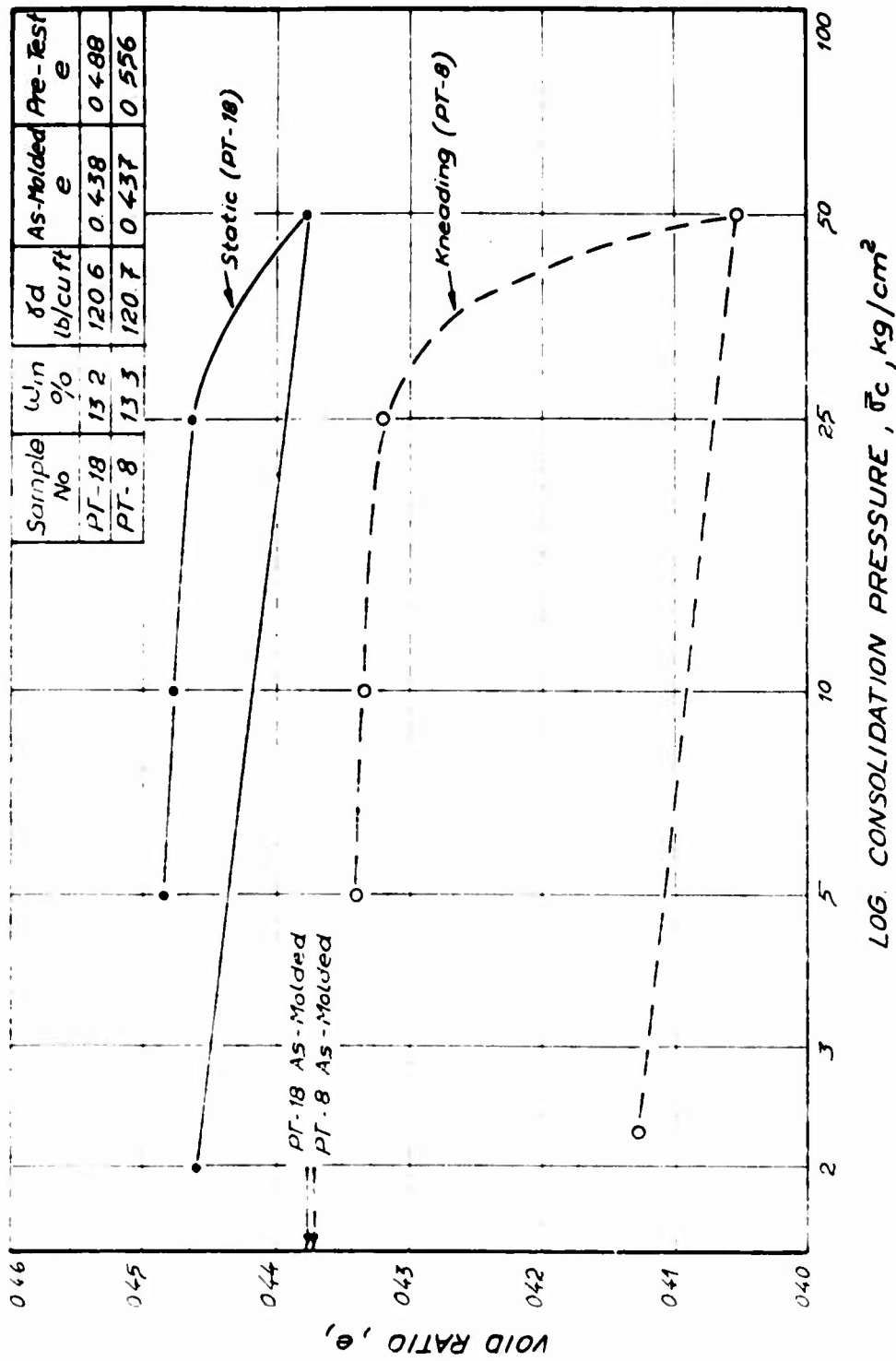


FIG. 3.17C VOID RATIO VERSUS CONSOLIDATION PRESSURE FOR
M-21+5% CEMENT COMPACTED AT OPTIMUM ($\omega_m = 13\%$)

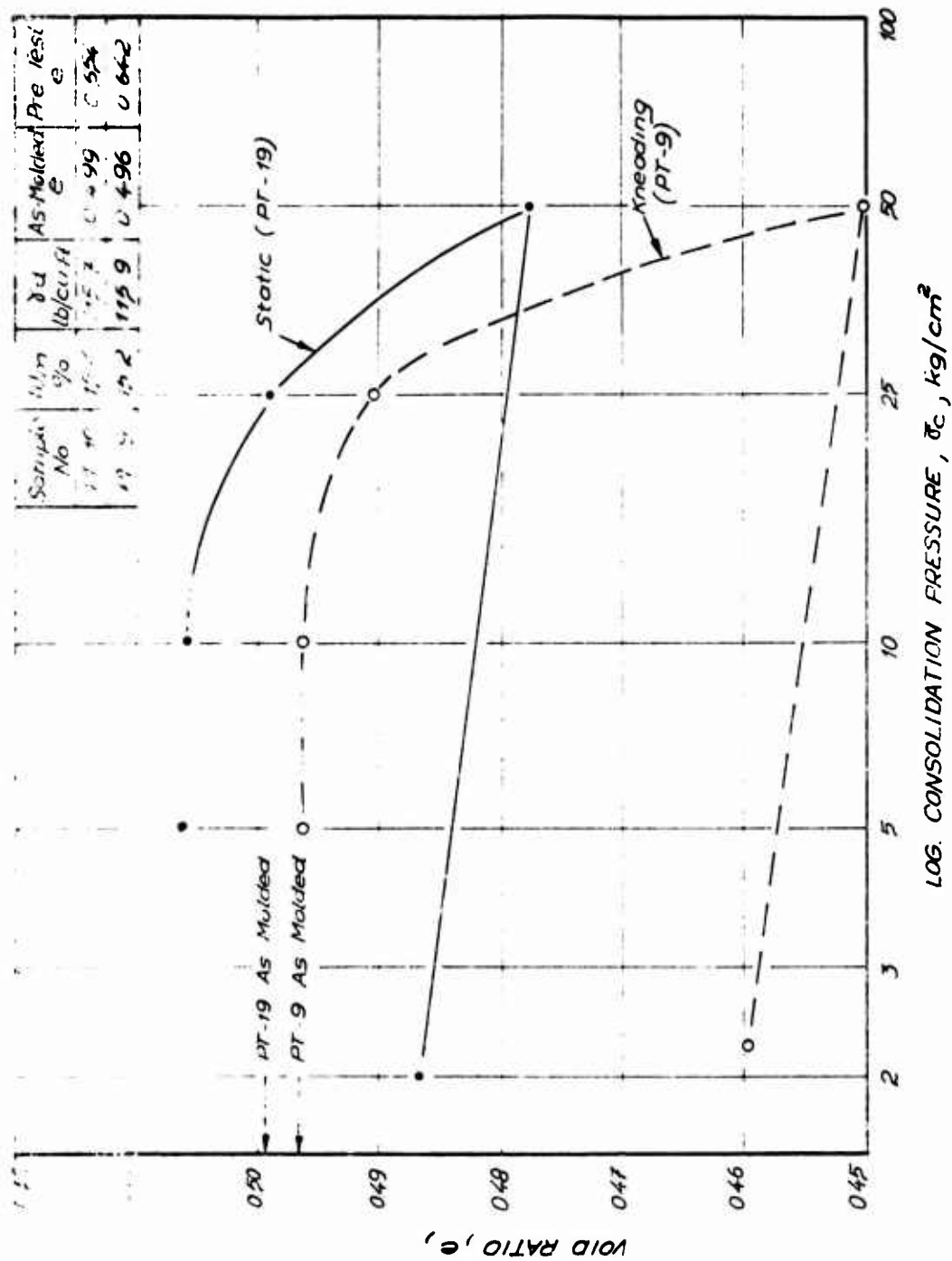


FIG. 3. 17d. VOID RATIO VERSUS CONSOLIDATION PRESSURE FOR
M-21+5% CEMENT COMPACTED WET OF OPTIMUM ($w_{Lm} = 15\%$)

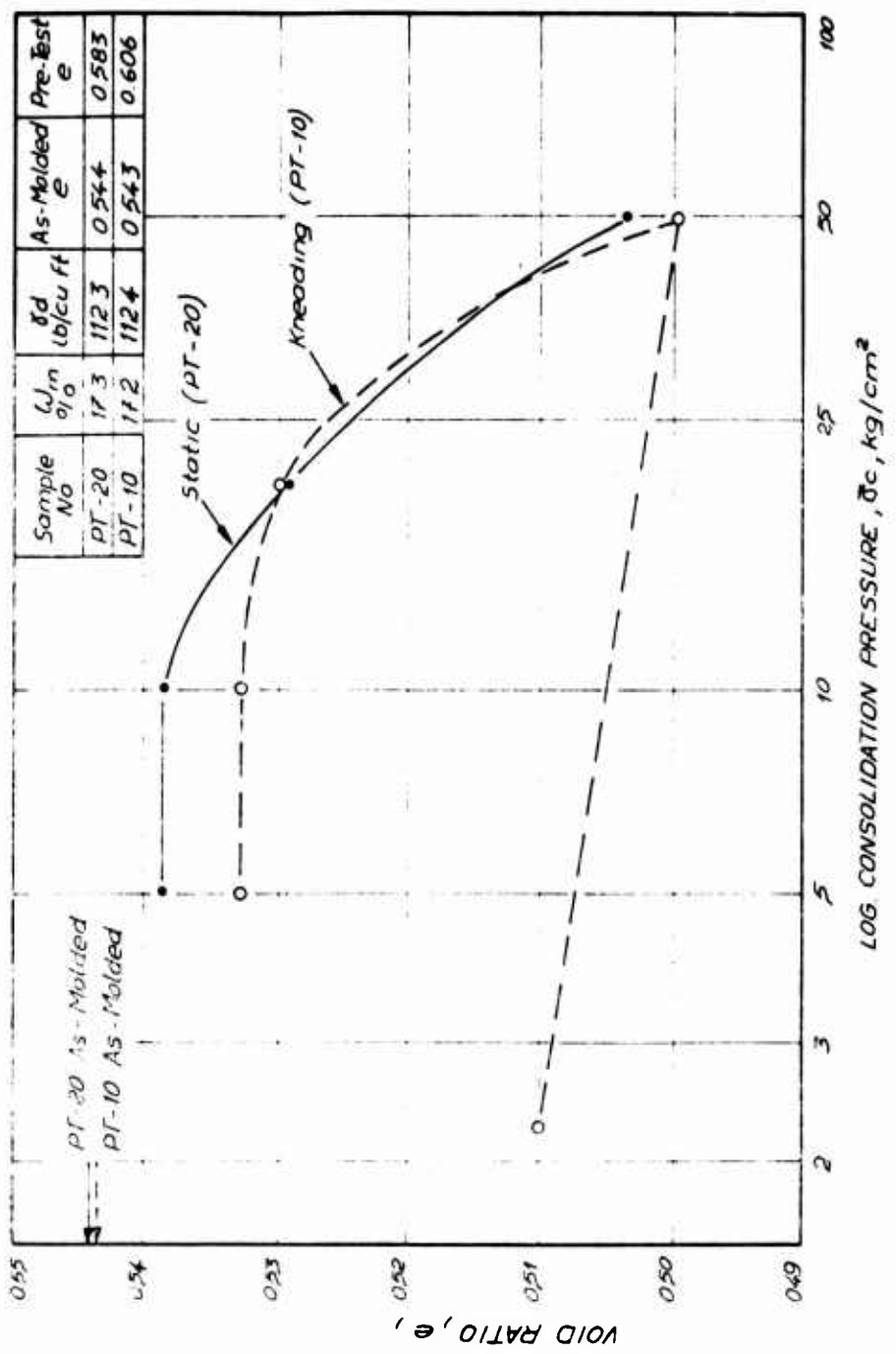


FIG. 3.17e. VOID RATIO VERSUS CONSOLIDATION PRESSURE FOR
M-21+5% CEMENT COMPACTED VERY WET OF
OPTIMUM ($\omega_m = 17\%$)

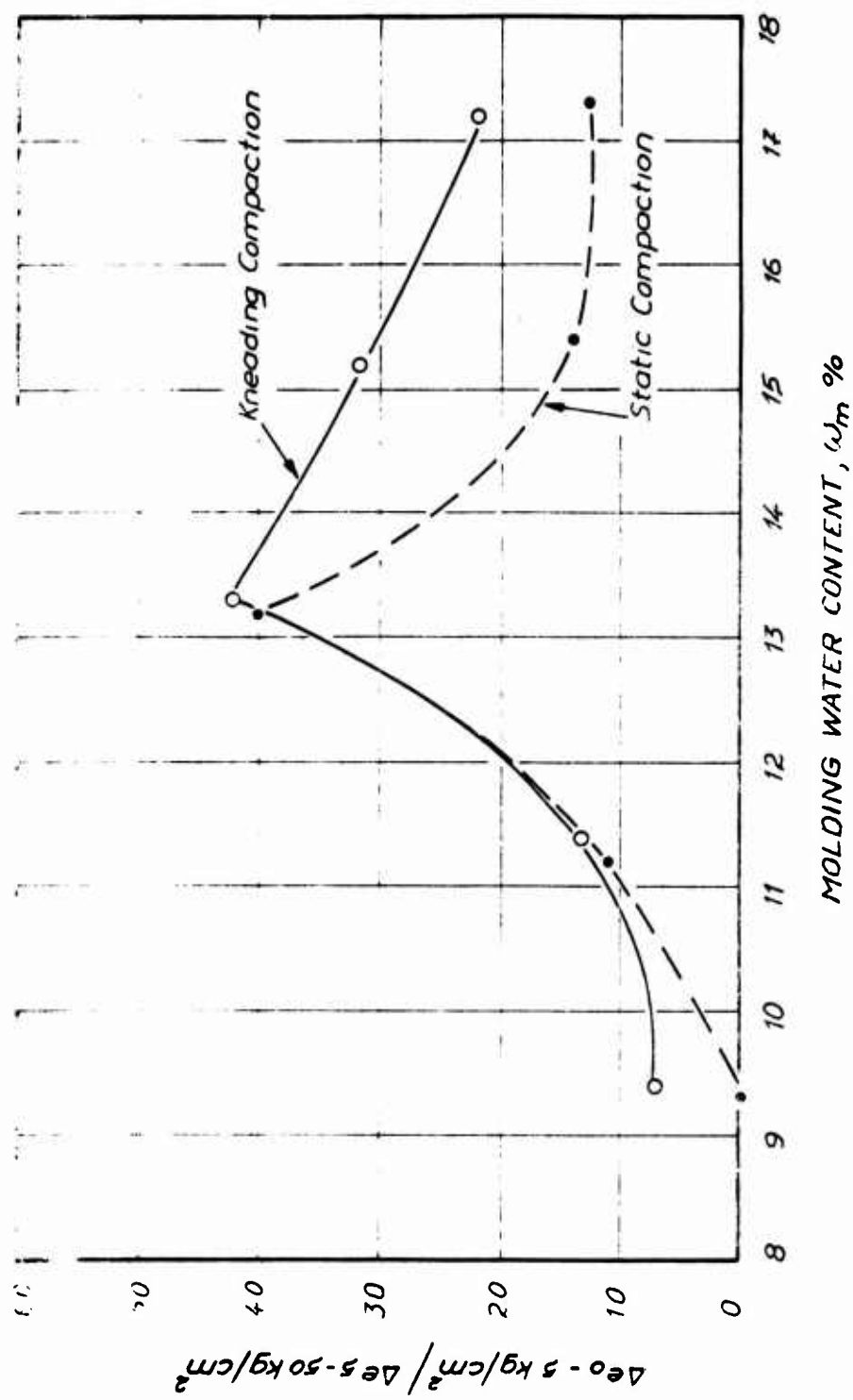


FIG. 3.18. RATIO OF VOID RATIO CHANGE DURING INITIAL CONSOLIDATION TO VOID RATIO CHANGE DURING CONSOLIDATION TO 50 kg/cm² VERSUS MOLDING WATER CONTENT.

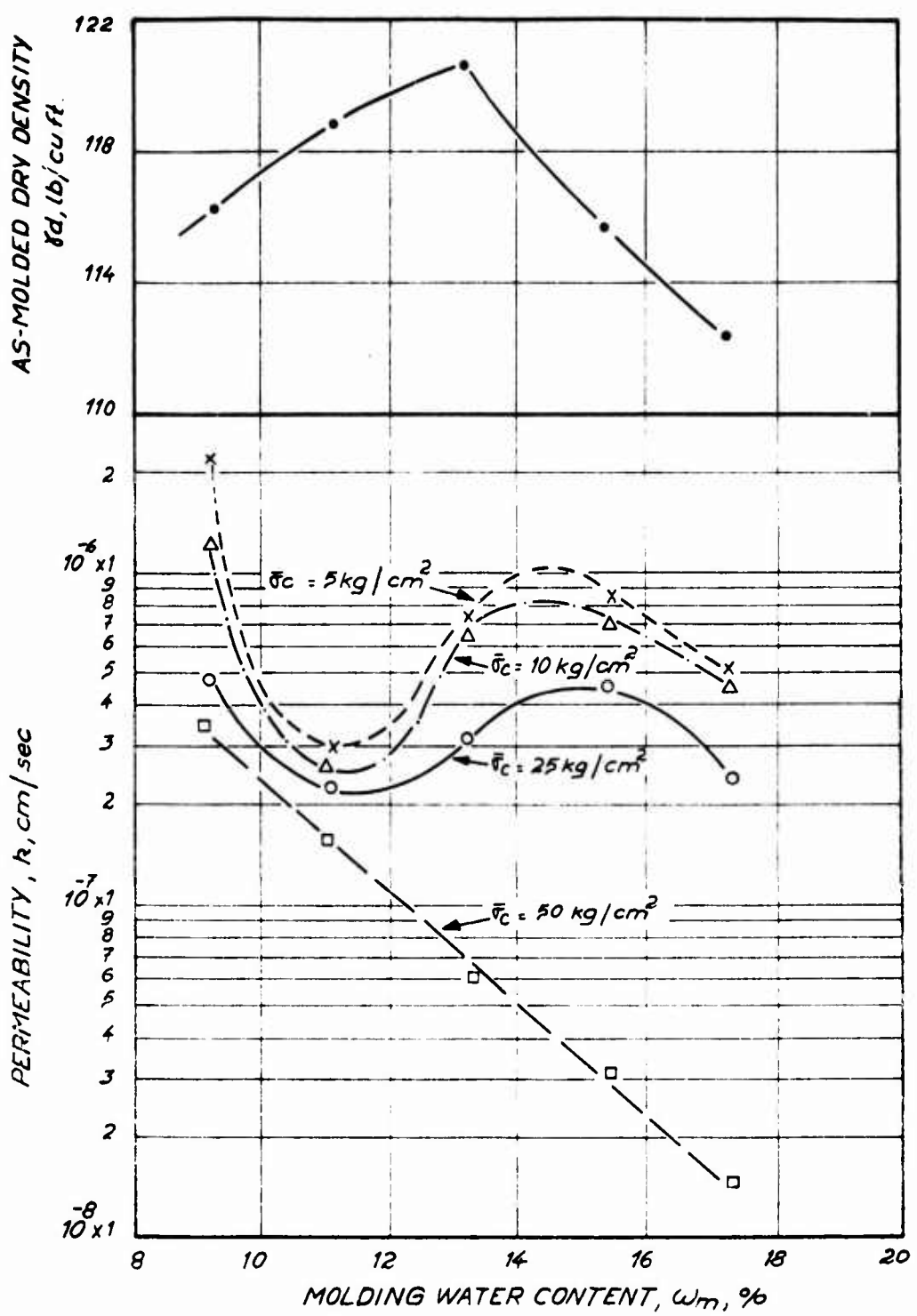


FIG. 3.19 PERMEABILITY VERSUS MOLDING WATER CONTENT FOR STATIC COMPACTION STABILIZED SAMPLES.

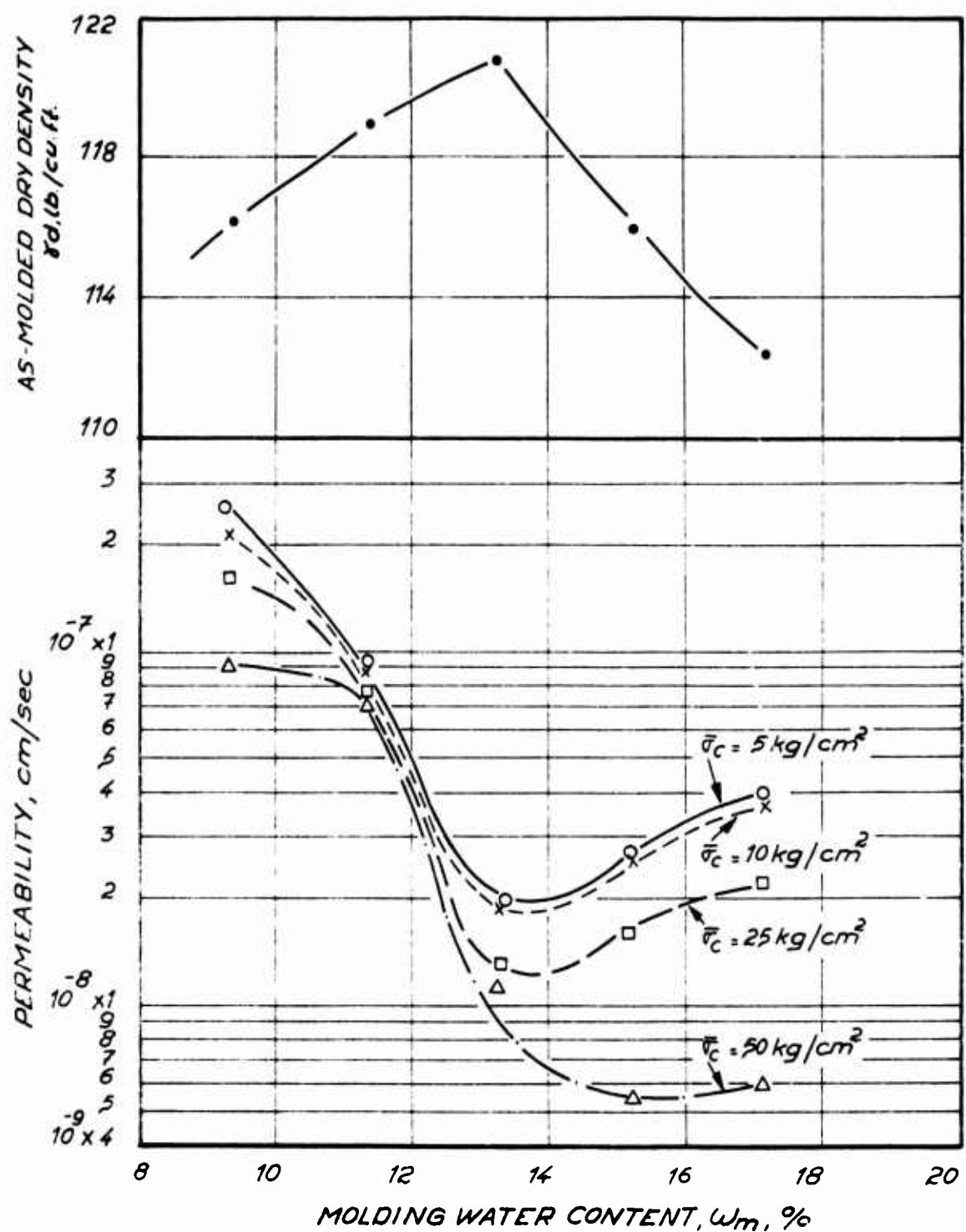


FIG. 3.20 PERMEABILITY VERSUS MOLDING WATER
CONTENT FOR KNEADING COMPACTION
STABILIZED SAMPLES

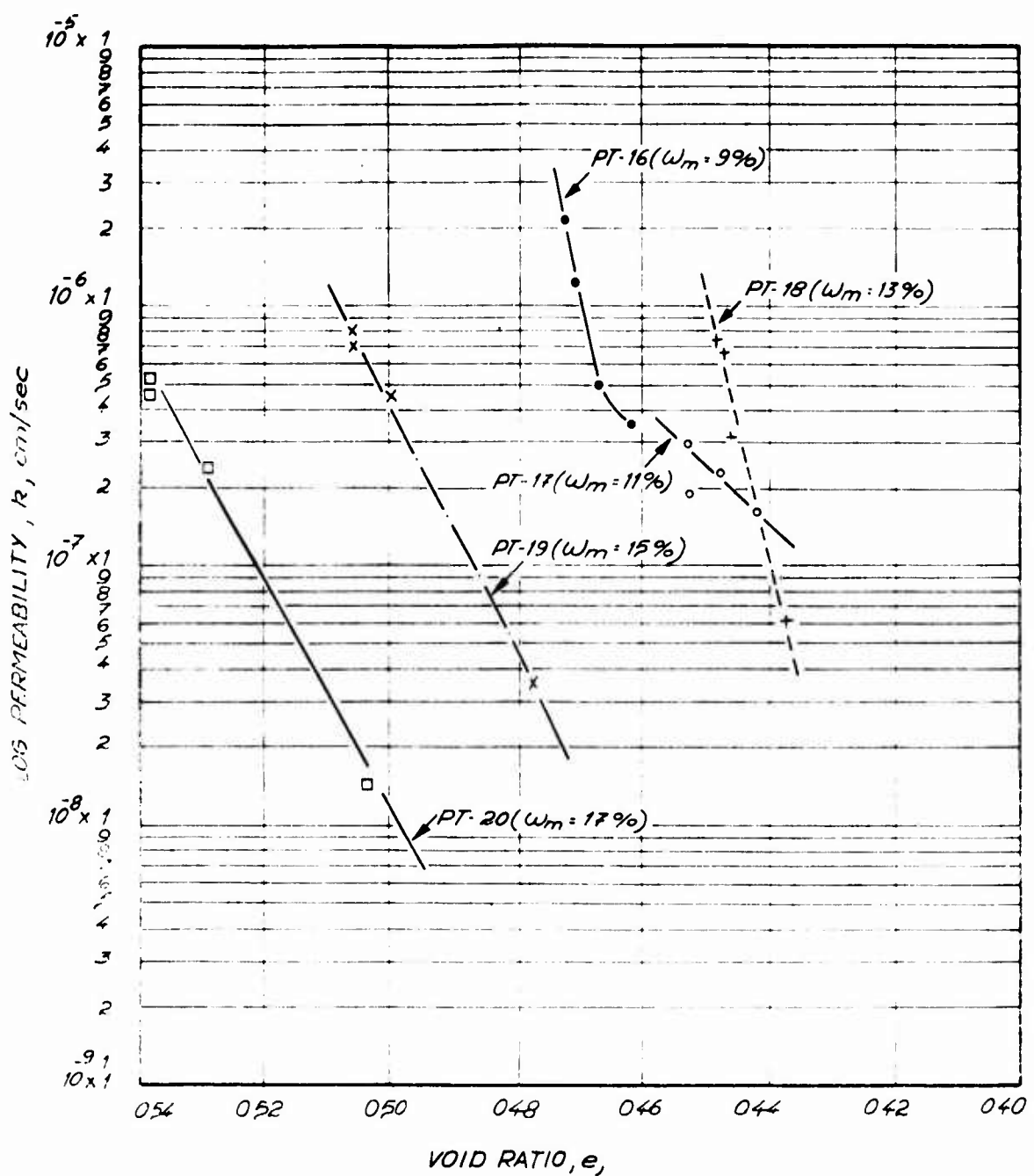


FIG. 3.21. PERMEABILITY VERSUS VOID RATIO FOR STATIC COMPACTION STABILIZED SAMPLES.

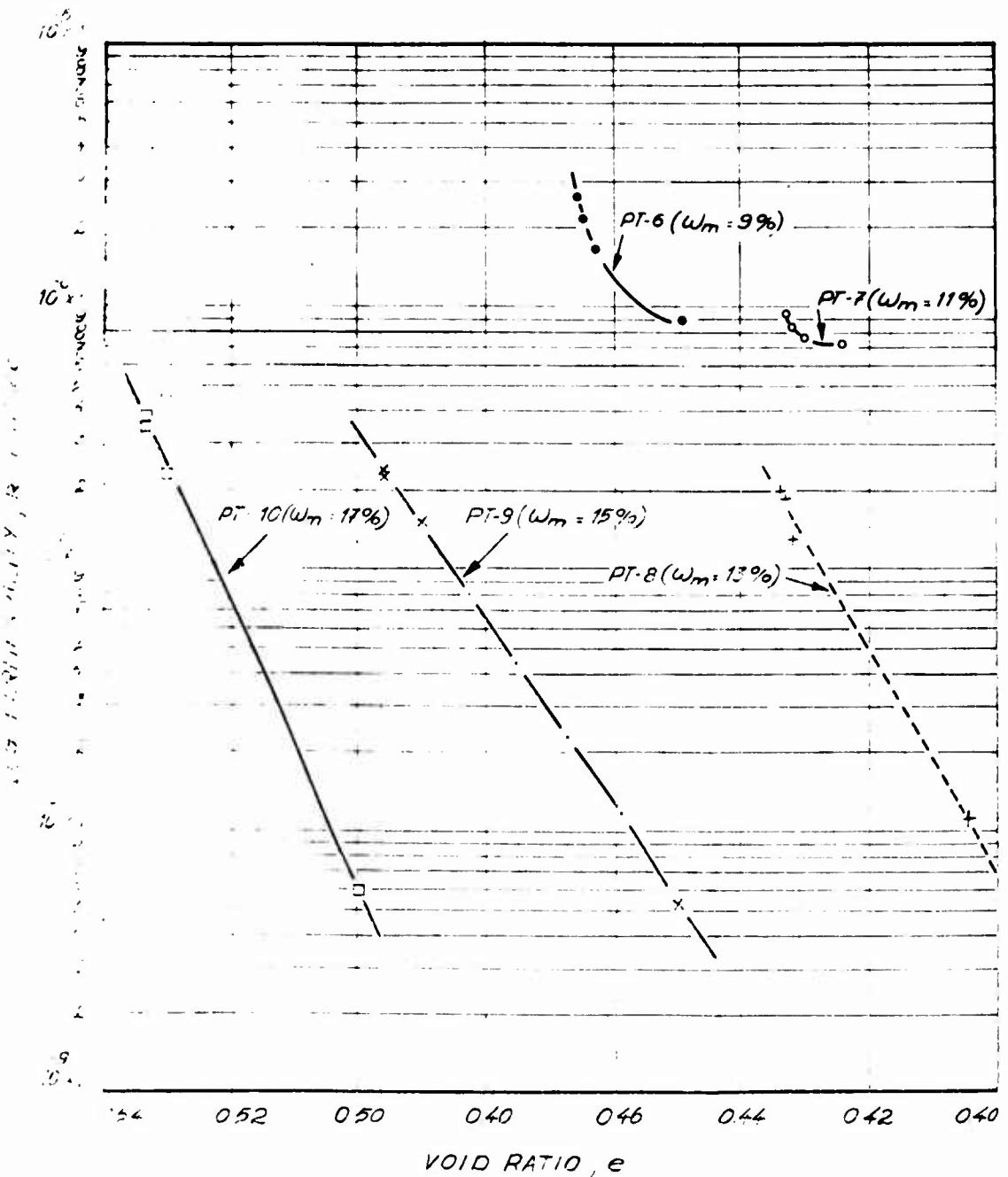


FIG 3.22 PERMEABILITY VERSUS VOID RATIO FOR KNEADING COMPACTION STABILIZED SAMPLES

Chapter IV

DISCUSSION OF TEST RESULTS FROM THE MAJOR TESTING PROGRAM

4.1 Introduction

From the results presented in the preceding chapter, it can be seen that several trends in the permeability and consolidation behavior of the stabilized soil are similar to those observed with untreated compacted soil. However, several significant deviations from such behavior were also reported. The following, therefore, attempts to explain the reasons for the observed similarities and differences between the stabilized and the untreated soil.

4.2 Behavior During Standard Curing

Klem (1964) showed that even after 28 days of humid curing at room temperature, the permeability of M-21 stabilized with 5% cement decreases with time. Clare and Pollard (1954) have shown that the unconfined compressive strength of cement-stabilized soils increases with increasing curing temperature. Therefore, it was decided in this investigation to accelerate curing of the stabilized test specimens by humid curing them for two weeks at 70°C (see Art. 2.3.1) in order to minimize the decrease in permeability that would occur during the testing period.

During curing at 70°, all samples lost water (Figures 3.2 and 3.3) even though they were cured at high relative humidity. As shown in Figure 4.1, the samples compacted dry of optimum lost the most water (4 to 5 cc) while the samples compacted wet of optimum lost the least water (1 to 3 cc). From Figure 4.1 it is seen that the samples compacted dry of optimum underwent relatively little volume change during the curing period (three of the four test specimen shrunk slightly while one sample expanded slightly); while the samples compacted at optimum and wet of optimum expanded significantly during the curing period. The samples that underwent large expansions during curing also developed fairly large circumferential cracks especially between compaction layers.

Soil-cement is known to shrink during curing, especially if loss of moisture also occurs during this period. The observed expansion of the test specimens is therefore not due to expansion of the soil-cement; rather, it is caused by non-uniform shrinkage, especially between compaction layers, that results in the opening up of cracks and by gross volume increase of the test specimens. The more severe the differential shrinkage, the greater the cracking and consequently the larger the overall expansion during curing.

The samples compacted at optimum or wet of optimum,

therefore, underwent the greatest differential shrinkage during curing since they showed the largest overall expansion (Figure 4.1). As with untreated fine-grained soils, stabilized soil compacted dry of optimum apparently has a more flocculated fabric than when compacted wet of optimum and therefore undergoes less shrinkage. This appears to be especially true for the stabilized soil used in this investigation, since the samples compacted dry of optimum lost the most water during curing but showed the smallest volume change during curing.

Since the cracking is caused by differential shrinkage, another factor that could contribute to the observed behavior is differences in the soil fabric between the top and bottom of the compacted layers. As with untreated soil, when soil-cement is dry of optimum, compaction does not significantly alter its fabric and, therefore, the fabric of the top and bottom of the compacted layer is similar. However, wet of optimum, compaction can significantly alter the fabric, in which case the fabric of the soil close to the top of the layer will be less flocculated than that at the bottom of the layers. This can result in large differential shrinkage between layers causing severe cracking. Further, static compaction causes less change in fabric than kneading compaction and therefore the differential shrinkage should be greatest in samples compacted wet of optimum using kneading

compaction. This was the case for M-21 + 5% cement since the kneading samples compacted wet of optimum showed larger expansion during curing than the corresponding static samples compacted at the same water content and dry density (Figure 4.1).

In conclusion, based on the behavior during curing, it is seen that the fabric of stabilized soils, like untreated soils, is influenced by molding water content and type of compaction. Stabilized samples compacted wet of optimum are less flocculated than samples compacted dry of optimum and therefore undergo more differential shrinkage during curing. Further, wet of optimum, kneading compaction produces a less flocculated fabric than static compaction, causing the kneading compaction samples to shrink more than the corresponding static compaction sample.

4.3 Void Ratio Versus Consolidation Pressure

4.3.1 Untreated Soil

From Figure 4.2 it can be seen that the initial compressibility (the decrease in void ratio during saturation and consolidation to 5 kg/cm²) is to a large extend dependent on the as-molded void ratio (dry density). The higher the as-molded void ratio, i.e., the lower the as-molded dry density, the larger the initial compressibility. Further, at a given as-molded void ratio (dry density), the initial compressibility

is greater for the soil compacted wet of optimum than for the soil compacted dry of optimum. This was to be expected since the soil wet of optimum has a less flocculated fabric and is therefore more compressible. Similarly, kneading compaction produces a less flocculated fabric than static compaction and, therefore, at any given molding condition the initial compressibilities of the kneading samples are greater than those of the corresponding static samples.

However, at very high consolidation pressures (25 to 50 kg/cm²), the more flocculated the fabric, the more compressible the soil since a flocculated fabric will gradually collapse at these high pressures. Therefore, at high consolidation pressures samples compacted dry of optimum have a higher compression index than samples compacted wet of optimum at the same dry density (see top of Figure 4.2). Similarly, the samples compacted statically have a higher compression index than the corresponding kneading compaction samples since they have more flocculated fabrics.

4.3.2 Stabilized Soil

From Figure 4.3 it is seen that the shapes of the curves for initial compression (decrease in void ratio) during saturation and consolidation to 5 kg/cm² versus molding water content bear striking similarities to the shapes of the curves of volume increase during curing. This strongly suggests that

this initial compression is primarily caused by the closing of cracks that developed during curing.

At high consolidation pressures (from 25 kg/cm² to 50 kg/cm²) the compressibility of the stabilized soil is lower dry of optimum than wet of optimum. This is contrary to the behavior of the untreated soil and the compressibility may still be due to cracking during curing since the samples dry of optimum underwent less volume change during curing than did the samples wet of optimum. Similarly, the kneading samples were more compressible than the static samples, which again could be due to the fact that the kneading samples expanded more than the static samples during curing.

4.4 Permeability Behavior

4.4.1 Untreated Soil

According to Lambe (1954b and 1958) and Mitchell et.al. (1965), the permeability of compacted fine-grained soils is primarily controlled by the as-molded soil fabric. The less flocculated the as-molded soil fabric, the lower the permeability of the soil. For example Michaels and Lin (1954) and Lambe (1954a) have shown that the permeability of fine-grained soils at a given dry density (void ratio) can be reduced 6 to 10 times by adding a chemical dispersant to the molding water prior to compaction. As stated by Lambe, the decrease in permeability is due to a higher

degree of particle orientation (less flocculation) which causes the soil to have a more tortuous seepage path.

Lambe (1958) and Seed et.al. (1960) have shown that molding water content and type of compaction also influence the as-molded soil fabric. For example kneading compaction produces a less flocculated fabric than static compaction, especially when the soil is wet of optimum. Further, a soil is less flocculated when compacted wet of optimum than when compacted dry of optimum.

The influence of molding water content on the permeability of untreated M-21 was shown in Figures 3.12 and 3.13. The results given in Figure 3.12 were obtained using a constant kneading compaction effort and are similar to those reported in the literature, i.e., the permeability decreases rapidly with increasing molding water content and reaches a minimum slightly wet of optimum, beyond which there is a slight increase in permeability with increasing molding water content. In the case of the static compaction test specimens (Figure 3.13), the permeability also decreased with increasing molding water content. However, there was not a significant increase in permeability wet of optimum. This may be due to the fact that the static compaction samples were not compacted at a constant effort but rather the compaction effort was varied in order to obtain the same as-molded dry densities as the corresponding kneading

samples at the same molding water content.

The permeability results given in Figures 3.12 and 3.13 were obtained after the test specimens were saturated and consolidated to 5, 10, 25 and 50 kg/cm². Void ratio changes that are dependent on molding conditions took place during saturation and consolidation, and therefore the permeability results shown in the figures include the influence of these void ratio changes. Figures 3.14 and 3.15 showed the influence of void ratio on the kneading and static compaction samples, respectively. For a given as-molded soil fabric (i.e. for a given molding water content and type of compaction), a linear relation existed between log permeability and void ratio. The rate of decrease in permeability with decreasing void ratio was greatest for samples compacted dry of or at optimum, because these samples were initially more flocculated and therefore could undergo larger changes in fabric during isotropic consolidation. For samples compacted wet of optimum, the rate of decrease in permeability with decreasing void ratio was less than for samples dry of optimum, and it was not very sensitive to molding water content.

Using Figures 3.14 and 3.15, it is possible by interpolation to determine the permeability as a function of molding water content at constant void ratio, thus eliminating the influence of void ratio on the results that were

shown in Figures 3.12 and 3.13. This has been done in Figure 4.4, which is a plot of log permeability versus molding water content at a void ratio of 0.350. When the influence of void ratio differences is eliminated, the permeability of the soil decreases with increasing molding water content* because wet of optimum the soil is less flocculated than dry of optimum. However, it should be noted that the decrease in permeability with increasing molding water content at constant void ratio (Figure 4.4) is considerably less than that observed when the results were not corrected for differences in void ratio (Figures 3.12 and 3.13).

As was shown in Figure 3.16a, type of compaction had no significant influence on the permeability of the untreated soil when it was compacted dry or very wet of optimum. Apparently, static and kneading compaction produce the same fabric when the soil is stiff (dry of optimum) and when the soil is very weak (very wet of optimum). However, between these two extremes, kneading compaction produces a less flocculated fabric than static compaction and consequently the kneading compaction samples had lower permeabilities at a given void ratio (Figure 3.16b). The influence of

*The samples compacted at $W_m = 17\%$ (very wet of optimum) had slightly higher permeabilities than samples compacted at $W_m = 15\%$.

type of compaction on the permeability of M-21 at a void ratio of 0.350 is also shown in Figure 4.4.

From a practical point of view, it is useful to know the influence of molding water content on permeability as a function of consolidation pressure. This is given in Figure 4.5, which is a plot of log permeability versus log consolidation pressure. The striking resemblance of these curves to the $e - \log \bar{\sigma}_c$ curves is due to the fact that linear relations exist between void ratio and log permeability. It is seen from Fig. 4.5 that large decreases in permeability (up to a factor of 10) can occur due to increasing the consolidation pressure from 5 to 50 kg/cm². The decrease in permeability is probably primarily due to the decrease in void ratio that occurs during consolidation rather than due to changes in the soil fabric.

4.4.2 Stabilized Soil

Before discussing the permeability behavior of the stabilized soil specimens, it should be recalled that cracks developed during the curing period. As mentioned in Art. 4.2, the kneading samples exhibited more severe cracking than the static samples and samples compacted wet of optimum cracked more than samples compacted dry of optimum. The existence of open cracks in a test specimen can significantly increase the permeability of the samples, especially if the cracks extend in the same direction as the applied hydraulic gradient.

The permeabilities of the stabilized soil samples as a function of molding water content were shown in Figures 3.19 and 3.20 for static and kneading compaction, respectively. At consolidation pressures up to 25 kg/cm^2 , the permeability decreased with increasing molding water content up to optimum ($W_m = 15\%$) for the kneading samples and up to $W_m = 13\%$ for the static samples, following which the permeability started to increase with increasing molding water content up to 15% for the static samples and up to 17% for the kneading samples. The static samples showed another permeability decrease when going from a molding water content of 15% to 17%. However, at a consolidation pressure of 50 kg/cm^2 , the permeability decreases with increasing molding water content over the whole range of molding water contents investigated, except for the kneading compaction sample at $W_m = 17\%$, which had a very slightly higher permeability than the kneading sample at $W_m = 15\%$.

The above results suggest that the cracks that developed during curing closed completely at a consolidation pressure of 50 kg/cm^2 and the cracks no longer influenced the permeability. Therefore, the results at $\bar{\sigma}_c = 50 \text{ kg/cm}^2$ suggest that for stabilized soil, the permeability decreases with increasing molding water content when cracking does not occur. At lower consolidation pressures, the observed increase in permeability around optimum water content is probably due to the existence of cracks that are still open.

Figures 3.21 and 3.22 showed the influence of void ratio on the permeability of the stabilized samples. It is interesting to note that the rate of decrease in log permeability with decreasing void ratio is greater for the stabilized samples than for the untreated samples (compare with Figures 3.14 and 3.15). This again suggests that the permeability of the stabilized samples was appreciably influenced by the existence of open cracks since if the decrease in void ratio is primarily due to the reduction in size of a few large pores (the cracks in the stabilized samples), they will cause a larger decrease in permeability than if the same decrease in void ratio was due to a uniform decrease in the size of most of the smaller pores when no cracks exist.

In order to eliminate the influence of void ratio differences on the permeability results shown in Figures 3.19 and 3.20 and to examine the influence of molding water content per se, Figures 3.21 and 3.22 can be used to estimate the permeabilities at a constant void ratio. Unfortunately, for the stabilized samples, it was necessary to extrapolate some of the curves in Figures 3.21 and 3.22 in order to estimate permeabilities at a given void ratio. This was done by linearly extrapolating the straight line portions of the log permeability versus void ratio curves. Figure 4.6 shows the results for the

kneading and static compaction samples at a void ratio of 0.470 obtained by this linear extrapolation. There is some question about the validity of the sudden large increase in permeability of the static compaction curve at $w_m = 13\%$; however, the results show that the permeability of the stabilized soil is much more sensitive than the untreated soil to molding water content. The permeability decreases by 4 to 5 orders of magnitude when going from $w_m = 9\%$ to $w_m = 17\%$ at constant void ratio. This compares with a factor of just over two for the untreated soil. Further, if one neglects the questionably high permeability of the static compaction sample at $w_m = 13\%$, kneading compaction results in higher permeabilities than static compaction. This is contrary to what was observed with the untreated soil, which showed higher permeabilities using static compaction. The higher permeability of stabilized soil using kneading compaction may be due to the fact that these samples showed more cracking than the static samples during curing (see Art. 4.2).

Figure 4.7 shows the influence of consolidation pressure on permeability of the stabilized soil. The samples dry of optimum show a relatively small decrease in permeability with increasing consolidation pressure; however, at optimum and wet of optimum, there is a sudden very

large decrease in permeability when going from a consolidation pressure of 25 kg/cm^2 to a consolidation pressure of 50 kg/cm^2 . The samples dry of optimum showed very little cracking during curing, while the samples that exhibited the large sudden decrease in permeability cracked considerably during curing. Therefore, the sudden decrease in permeability when going from $\bar{\sigma}_c = 25 \text{ kg/cm}^2$ to $\bar{\sigma} = 50 \text{ kg/cm}^2$ is further evidence that cracking has a major influence on the permeability behavior of the stabilized soil especially at low consolidation pressures.

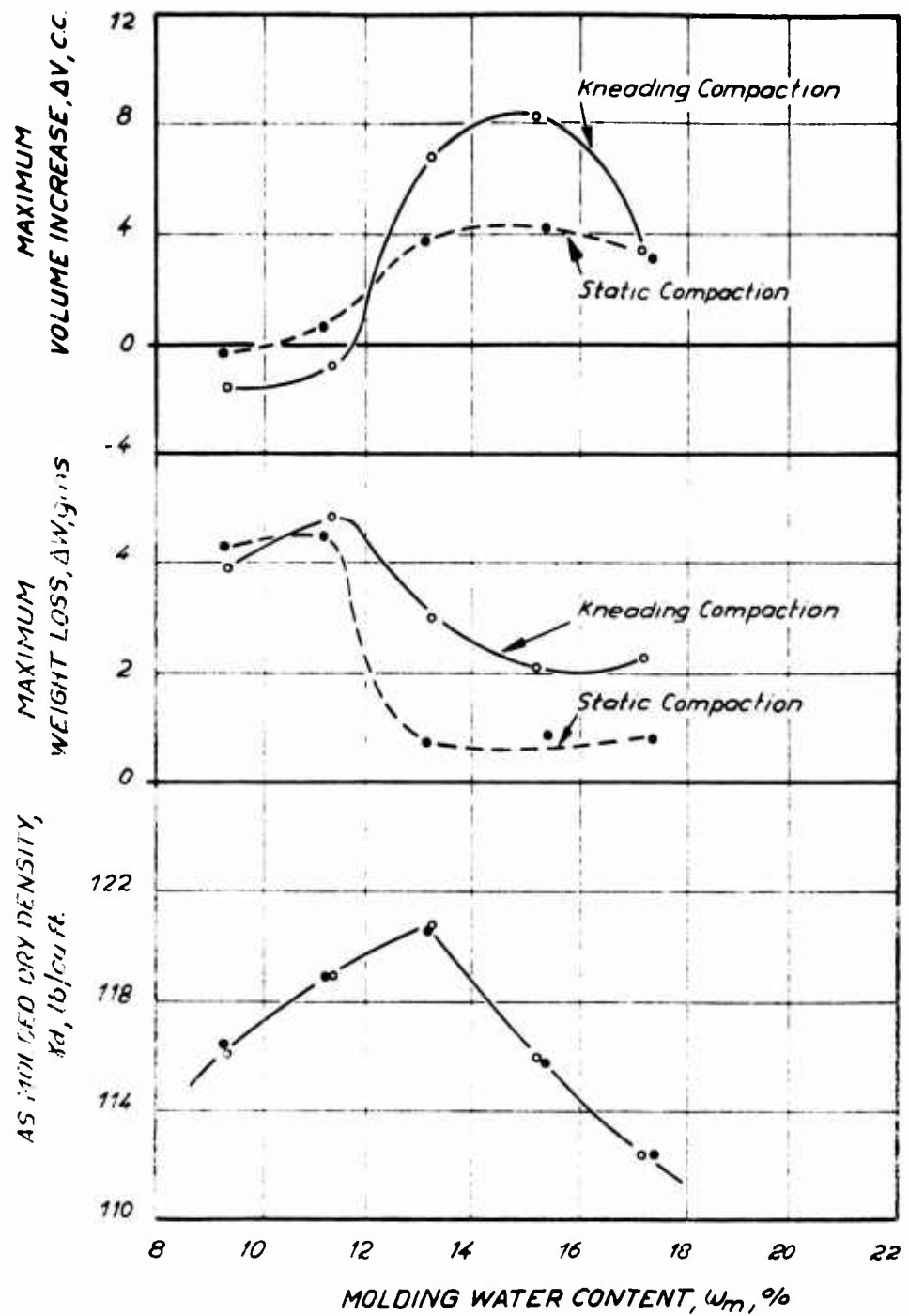


FIG. 4.1 INFLUENCE OF MOLDING WATER CONTENT AND TYPE OF COMPACTION ON THE BEHAVIOR OF THE STABILIZED SAMPLES DURING STANDARD HUMID CURE.

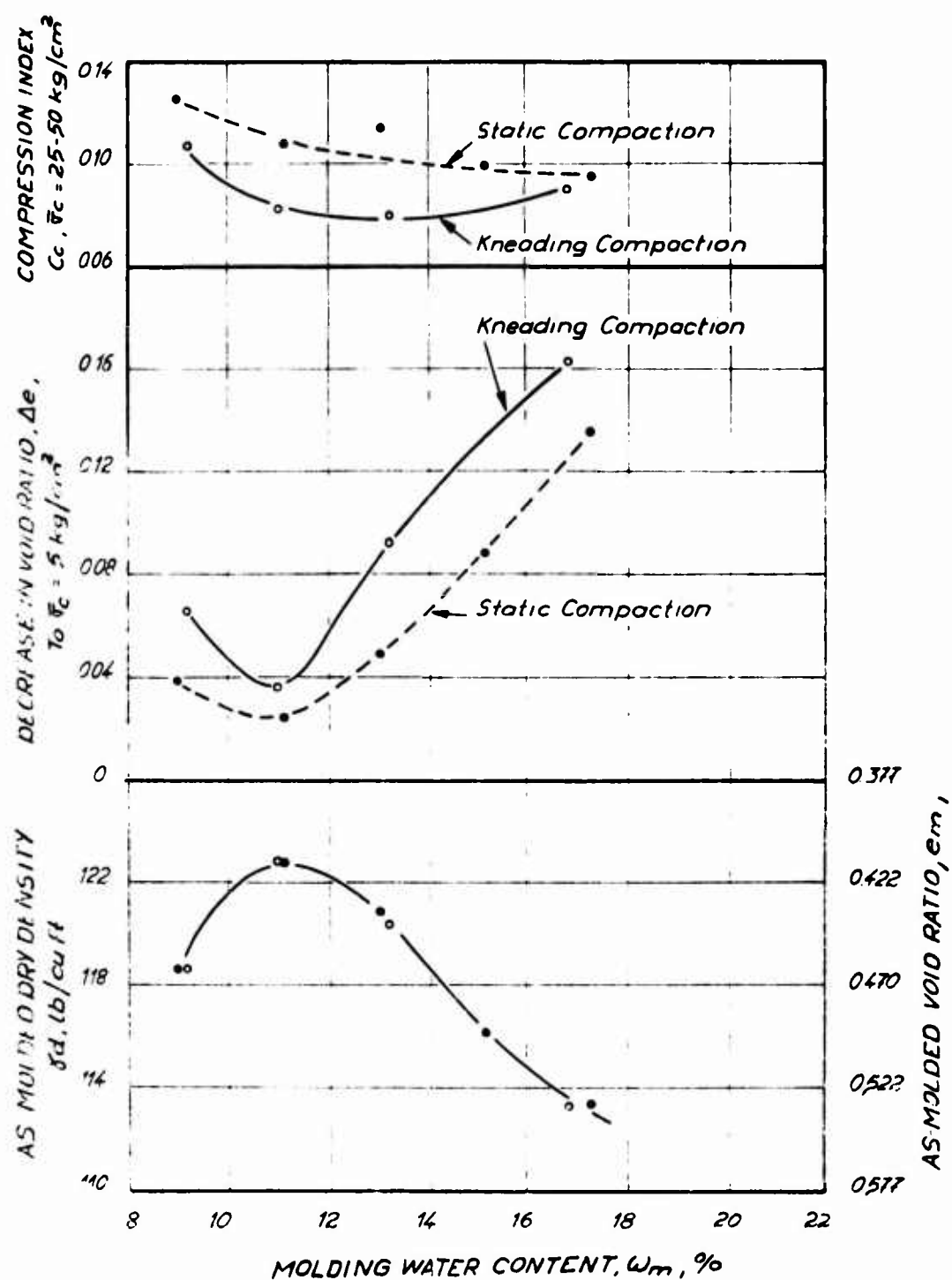


FIG. 4.2. COMPRESSIBILITY OF THE UNTREATED SOIL
AS A FUNCTION OF MOLDING WATER
CONTENT AND TYPE OF COMPACTION

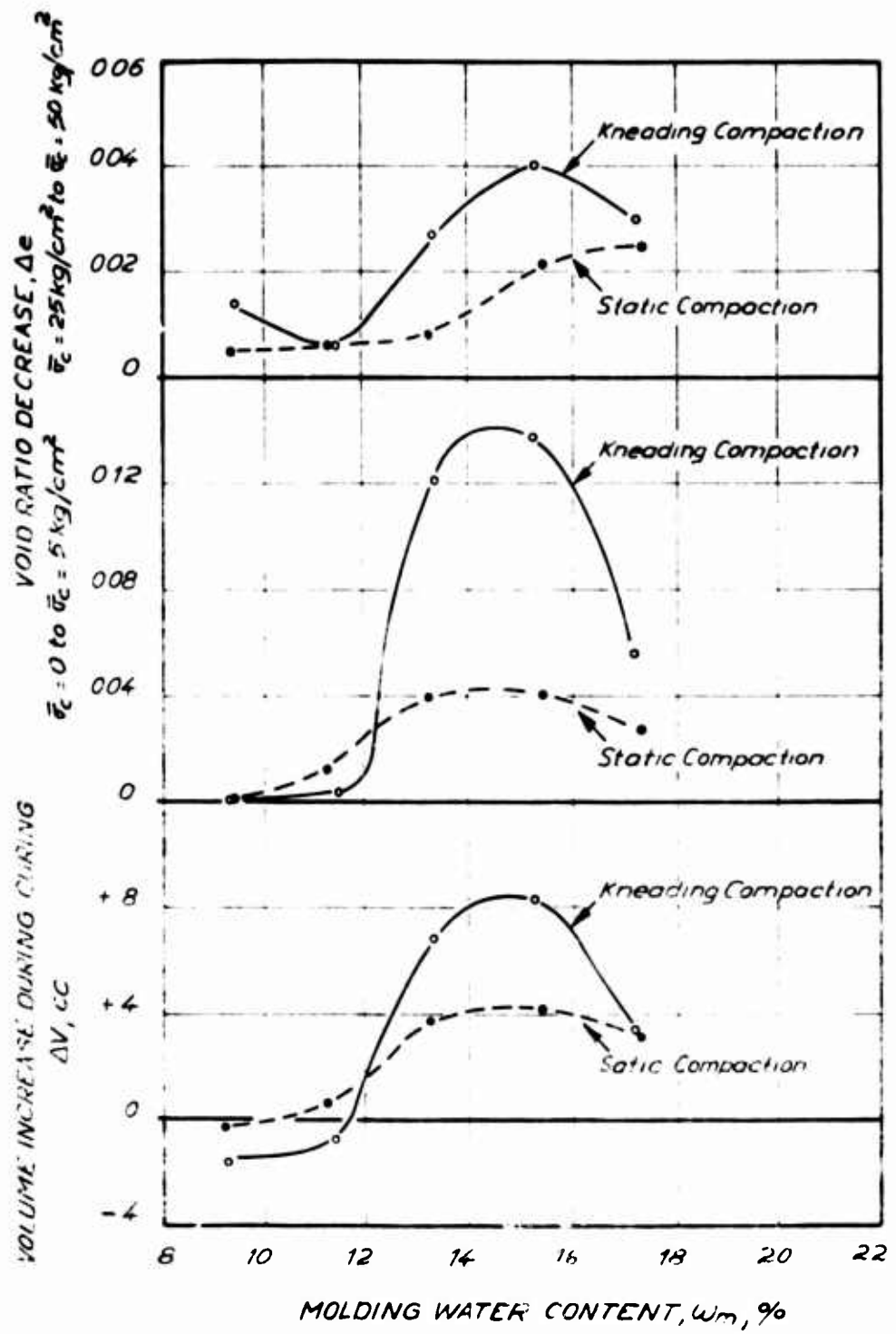


FIG. 4.3. COMPRESSIBILITY OF THE STABILIZED SOIL AS A FUNCTION OF MOLDING WATER CONTENT AND TYPE OF COMPACTION

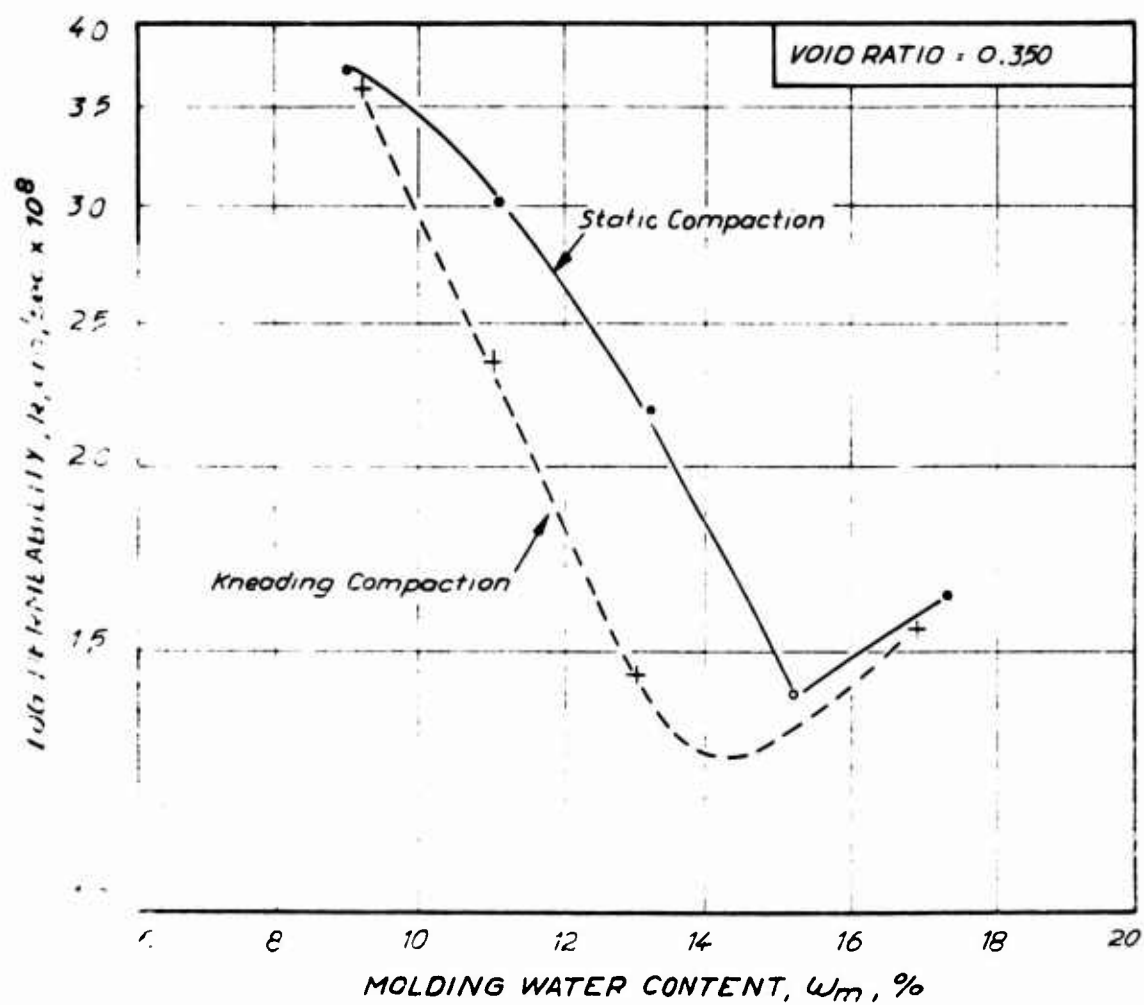


FIG. 4.4 INFLUENCE OF MOLDING WATER CONTENT AND
TYPE OF COMPACTION ON THE PERMEABILITY
OF UNTREATED M-21 AT A VOID RATIO OF 0.350

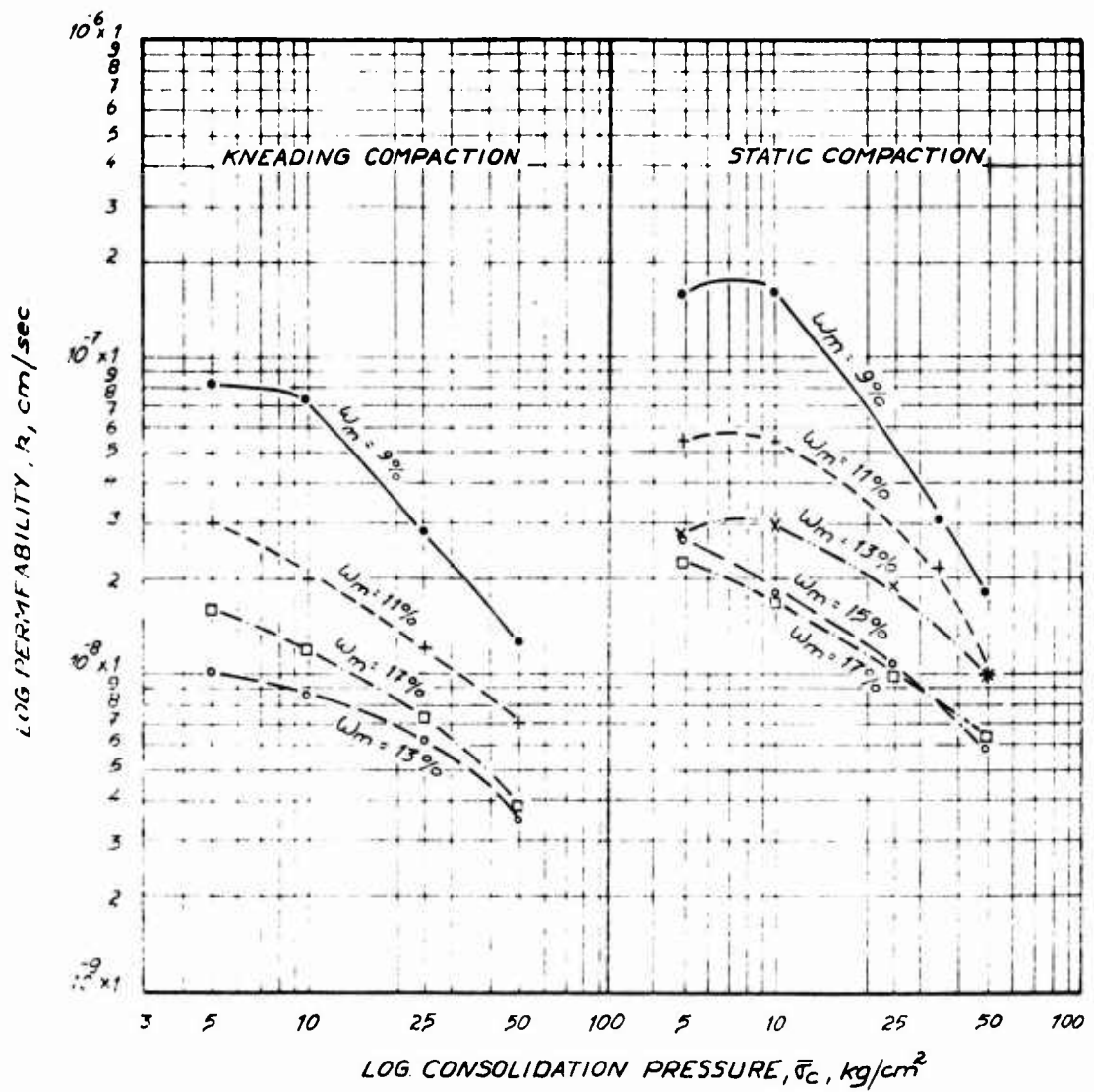


FIG. 4.5. INFLUENCE OF MOLDING WATER CONTENT AND
TYPE OF COMPACTION ON THE PERMEABILITY
OF UNTREATED M-21 ASA AS A FUNCTION OF
CONSOLIDATION PRESSURE

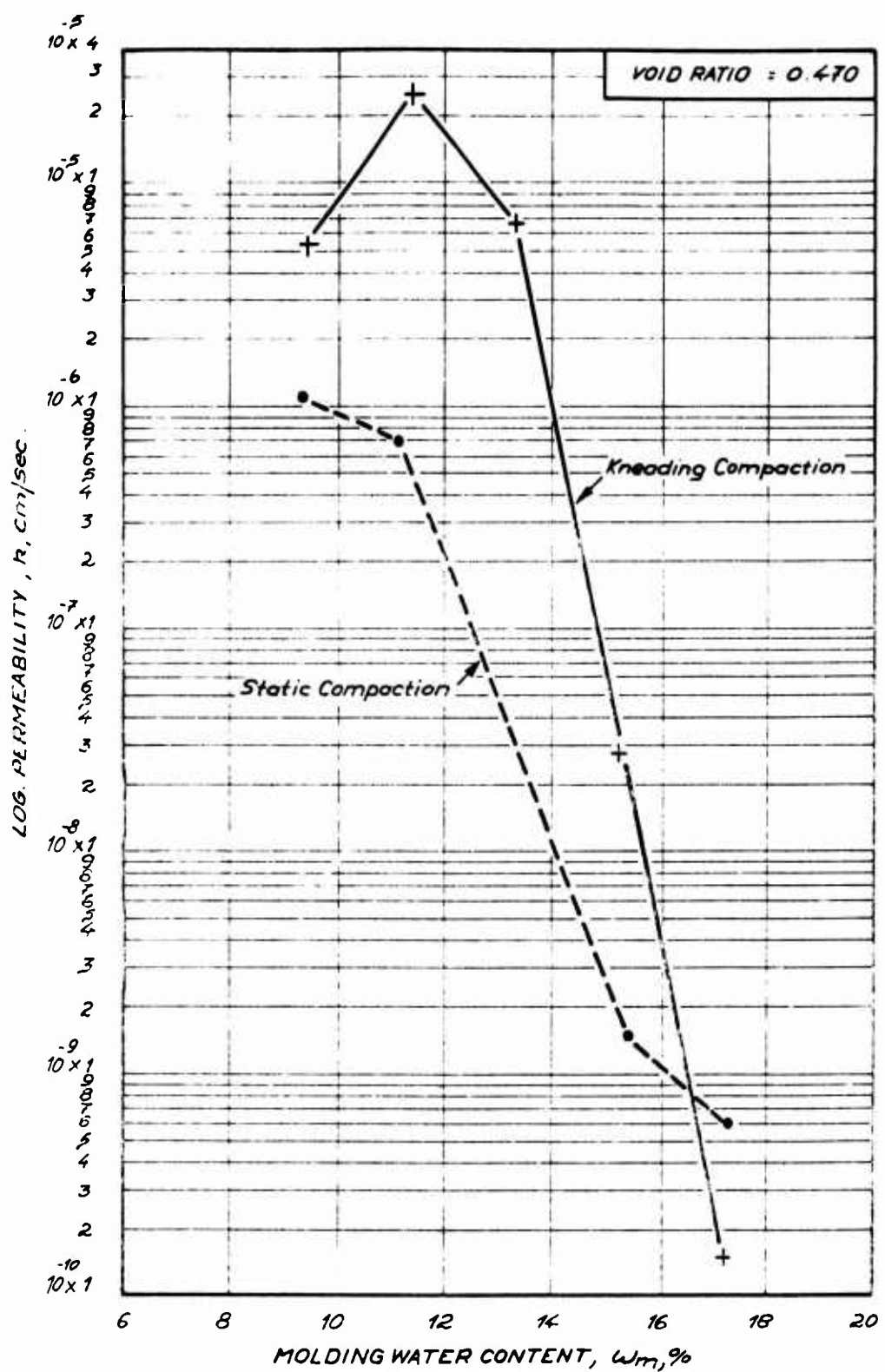


FIG. 4.6. INFLUENCE OF MOLDING WATER CONTENT AND TYPE OF COMPACTION ON THE PERMEABILITY OF M-21+5% CEMENT AT A VOID RATIO OF 0.470.

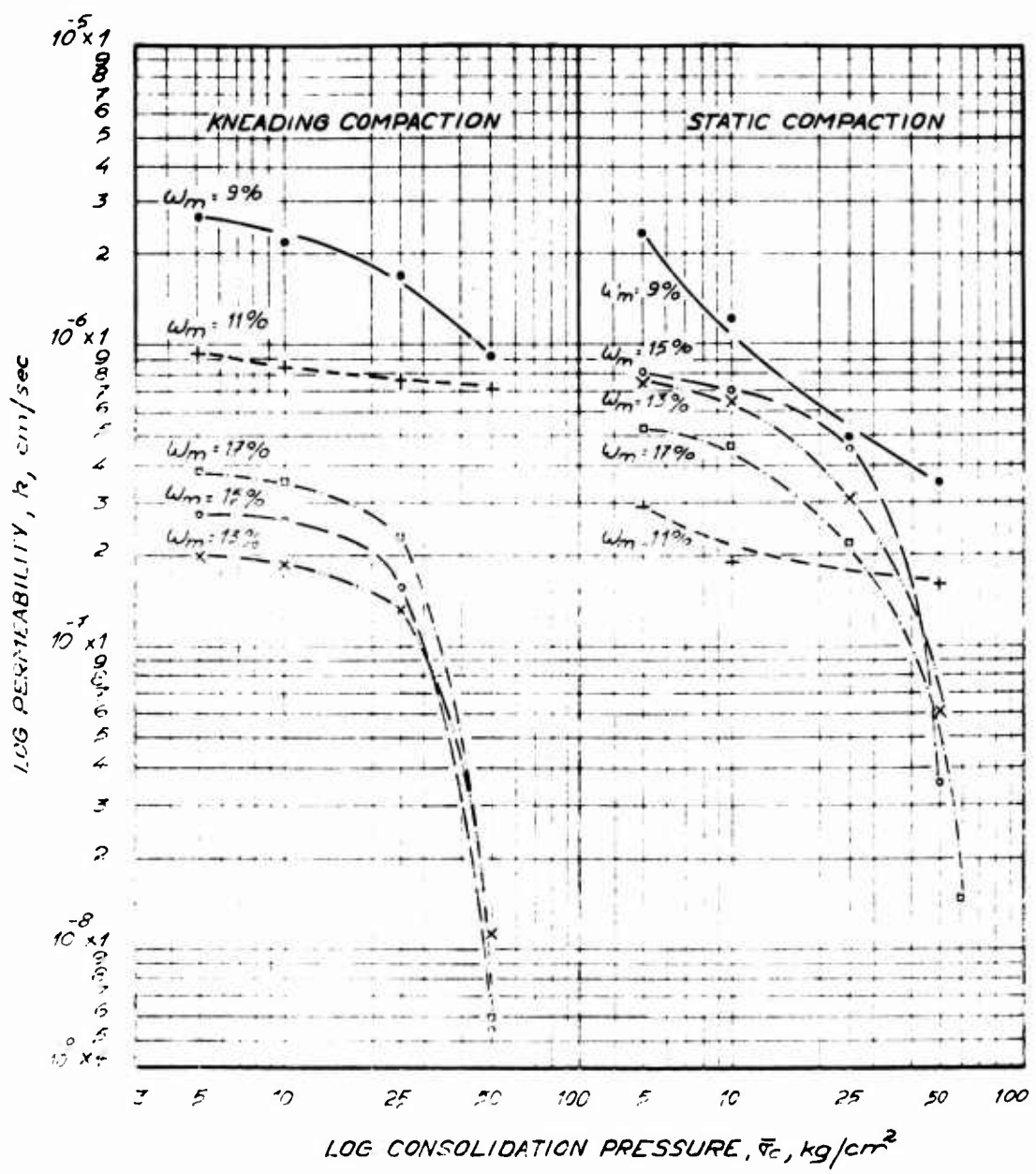


FIG. 4.7. INFLUENCE OF MOLDING WATER CONTENT AND TYPE OF COMPACTION ON PERMEABILITY OF M-21+5% CEMENT AS A FUNCTION OF CONSOLIDATION PRESSURE.

Chapter V

CLARIFICATION TESTS: RESULTS AND DISCUSSION

5.1 Objectives

The cracking that developed during curing of the stabilized test specimens used for the major testing program had a severe influence on their compressibility and permeability behavior. Since the amount of cracking was dependent on the molding water content and the type of compaction, it was not possible to determine the influence of molding conditions per se on the compressibility and permeability behavior of the stabilized soil. The clarification tests, therefore, consisted of measuring the compressibility and permeability behavior of stabilized test specimens in which cracking during curing was minimized or eliminated.

5.2 Testing Program

The loss of moisture that occurred during standard curing of the stabilized test specimens (see Art. 3.2.1) was apparently the primary cause for the severe cracking. For the clarification tests, moisture loss from the test specimens was prevented during curing by wrapping the samples, immediately after compaction, in a thin polyvinyl-chloride film sealed with nonshrinking wax. The

samples were then cured at 70° for 14 days. The wrapping was loose and therefore did not place any restraint on the samples: they were free to expand if the cause for such expansion existed. This type of curing is referred to as "sealed curing" (see Art. 2.3.2).

A few samples were also humid cured at room temperature (without being wrapped, see Art. 2.3.2) in order to study the influence of curing temperature on the compressibility and permeability behavior.

The clarification program consisted of ten stabilized test specimens. The molding water contents and as-molded dry densities of these test specimens are shown in Figure 5.1. For comparison purposes, the moisture-density relation for M-21 + 5% cement obtained from the major testing program is also shown in the figure. The appreciably lower as-molded dry densities of most of the clarification test specimens are probably due to a change in the composition of the soil caused by segregation of fines at the bottom of the barrel. This soil was used because it was the only soil remaining from the batch of M-21 used in the major testing program.

5.3 Curing Behavior

5.3.1 Sealed versus Unsealed Test Specimens

Four test specimens were compacted at optimum water

content ($W_m = 13.5\%$), two using kneading compaction and two using static compaction. One kneading and one static sample were subjected to standard curing (unsealed, 14 days at 70°C) and the other two samples were subjected to sealed curing (sealed, 14 days at 70°C). The sealed specimens lost essentially no moisture during curing and did not undergo a measurable change in length. The unsealed test specimens lost moisture and cracked, causing them to expand during curing. Figure 5.2 shows the weight and length changes of these test specimens during the hot-cure period of fourteen days. As previously shown, the kneading unsealed specimen expanded more during curing than the corresponding unsealed static specimen, i.e. the kneading sample underwent more severe cracking. Figure 5.3 is a photograph of the cracked unsealed samples and uncracked sealed samples after the fourteen days of hot curing.

5.3.2 Room Temperature versus Hot Cure

The two samples compacted dry of optimum ($W_m = 10\%$) and humid cured at room temperature for 35 days without sealing lost about 0.1 gms. of moisture during the curing period. This compares with 4 to 5 gms. of moisture lost by the dry samples cured at 70°C in the major testing program. The room temperature samples also showed no measurable

expansion during curing. The two samples compacted wet of optimum ($W_m = 15\%$) lost 0.5 to 0.8 gms. of moisture during 35 days of humid curing at room temperature, which is of the same order of magnitude as the loss in moisture experienced by the hot-cure samples compacted wet of optimum. However, the room-temperature-cure samples did not undergo visible cracking nor did they measurably increase in length during curing.

5.4 Compressibility Behavior

5.4.1 Sealed Versus Unsealed Test Specimens

The influence of cracking during curing on the compressibility behavior of M-21 plus 5% cement was investigated using two static compaction and two kneading compaction test specimens having about the same molding water content and dry density. The four samples were cured for fourteen days at 70°C. One kneading compaction and one static compaction sample were wrapped and sealed during curing to prevent moisture losses and cracking while the other two samples were cured in the standard way. The void ratio changes during curing and initial consolidation of the four samples are shown in Figure 5.4.

The compressibility behaviors of the four samples at consolidation pressures up to 50 kg/cm^2 are shown in Figure

5.5. Even at the higher consolidation pressures, the sealed specimens showed much smaller void ratio decreases with increasing consolidation pressures than the corresponding unsealed specimens. Also void ratios of the unsealed specimens at a consolidation pressure of 50 kg/cm² were considerably higher than those of the corresponding sealed specimens. Both of these observations clearly indicate that the cracks that developed during curing of the unsealed specimens remain partially open even at the very high consolidation pressure of 50 kg/cm². The engineering properties, especially the permeability, of stabilized soils can therefore be expected to be influenced by cracking during curing over the full range of consolidation pressure encountered in practice. Obviously, cracking will have the largest effect at low consolidation pressures where the cracks are largest.

5.4.2 Influence of Molding Water Content and Type of Compaction

The experimental results on the compressibility of the stabilized soil as a function of molding water content and type of compaction also included the influence of molding conditions on the degree of cracking that developed during curing. To eliminate the effects of cracking and to study the influence of molding conditions per se on

the compressibility, four stabilized test specimens were wrapped and sealed during the hot curing period. The compressibility behavior of these samples is given in Figure 5.6.

From Figure 5.6 it is seen that for the uncracked stabilized soil:

(1) The compressibility is greater dry of optimum than at optimum. This is opposite to that observed with standard cured, cracked samples (e.g. see Figure 4.3), which was due to the more severe cracking that occurred in the samples compacted at optimum. For the uncracked samples, the higher compressibility dry of optimum is probably due to these samples having a lower as-molded dry density (higher as-molded void ratio) than that of the samples at optimum and therefore will compress more easily.

(2) Dry of optimum type of compaction does not significantly influence the compressibility behavior, the kneading sample being slightly more compressible than the static sample. This was also observed with the unsealed test specimens compacted dry of optimum (see Figures 3.17a and 3.17b). Based on the volume change behavior during curing of the unsealed specimens dry of optimum, it was concluded that they did not undergo severe cracking during

curing. This is reinforced by the observation that the sealed samples dry of optimum showed larger void ratio decreases during consolidation than the corresponding unsealed specimens (compare Figure 5.6 with Figures 3.17a and 3.17b). The higher compressibility of the sealed specimens is due to their much lower as-molded dry densities.

(3) At optimum water content, the kneading sample was more compressible than the static sample especially at the higher range of consolidation pressures. This may be due in part to the slightly lower as-molded dry density of kneading samples; however, its less flocculated soil fabric is probably the primary cause.

5.4.3 Influence of Curing Conditions

Due to the fact that wrapping and sealing of stabilized soil test specimens prior to curing is a time-consuming operation and is not representative of field conditions, stabilized samples are frequently humid cured at room temperature by storing them in sealed containers at close to 100% relative humidity without wrapping the individual samples. This curing procedure is probably more representative of field conditions; however, samples cured in this manner do undergo some moisture and volume changes. These changes are much smaller than those observed when unwrapped samples were cured at 70°C.

Figures 5.7 and 5.8 compare the compressibility behavior of unsealed samples humid cured at room temperature for 35 days with sealed and unsealed specimens cured for fourteen days at 70°C. The results show that, with the exception of sample PK-R2*, the unsealed room-temperature-cured samples are less compressible than the corresponding unsealed hot-cured samples, even though the cementation in the hot-cured samples was probably stronger than that of the room temperature cured samples (14 days curing at 70°C produces more hydration of cement than 35 days curing at 23°C). This strongly suggests that cracking is probably not a major problem when unsealed samples are cured at room temperature.

The fact that from Figure 5.8 the room temperature sample was slightly more compressible than the hot sealed sample can be due to its much lower as-molded dry density and/or its weaker cementation. It does not necessarily mean that the room-temperature sample underwent cracking during curing.

5.5 Permeability Behavior

5.5.1 Sealed Test Specimens

Figure 5.9 shows the influence of molding water content on permeability. These results are questionable.

tent and type of compaction on the void ratio-permeability behavior of hot-cured, sealed M-21 specimens stabilized with 5% portland cement. The three orders of magnitude higher permeability of the samples compacted dry of optimum cannot be due to the slightly higher void ratios of these samples. The very large decrease in permeability going from dry of optimum to optimum molding water content is probably due to large differences in the soil fabric that occur with increasing molding water content. Compacting dry of optimum apparently produces a much more flocculated fabric than compacting at or wet of optimum.

Dry of optimum, compaction method has very little influence on the fabric of stabilized soils since the permeabilities of the kneading and static compaction samples were about the same (sample nos. PS-W2 and PK-W2 in Figure 5.9). At optimum, kneading compaction produces a less flocculated fabric than static compaction since kneading sample No. PK-W1 had a higher void ratio than the static sample No. PS-W1; whereas both samples had about the same permeability.

The relatively large decrease in permeability due to an extremely small decrease in void ratio for the samples compacted wet of optimum is probably not a direct effect of the observed decrease in void ratio. Rather, the

in permeability is caused by a time effect* that had been observed in a preliminary investigation conducted several years ago (Klem, 1964). Some of these results are presented in the following articles.

5.5.2 Influence of Curing and Permeation Time

The influence of curing time and time of permeations on the permeability behavior of M-21 stabilized with 5% portland cement were investigated in 1964 as part of a preliminary study. A different batch of M-21 was used for this investigation and the samples were prepared using two-end static compaction at a compaction pressure of 400 psi. The stabilized test specimens were cured at room temperature in the same manner as that used for the unsealed samples in this report. The samples were permeated in low pressure triaxial cells following consolidation to an effective pressure of 1.6 kg/cm^2 under a back pressure of 7.6 kg/cm^2 to ensure saturation. Figure 5.10 shows the influence due to the low permeability of the samples compacted at optimum, it was necessary to permeate them for at least a week at each consolidation pressure in order to be able to measure flow. This compares with one to two days of permeation needed for the samples compacted dry of optimum. The permeability of sample PK-W1 at $\bar{\sigma}_c = 50 \text{ kg/cm}^2$ shown in Figure 5.9 is probably in error since the equipment used is not accurate enough to reliably measure such low permeabilities.

of curing time and permeation time on the permeability of samples of M-21 plus 5% cement compacted at optimum water content. The results show that both time of permeation and curing time prior to permeation tend to decrease the permeability of the stabilized soil. The decrease in permeability due to increasing curing time is shown in Figure 5.11. The permeability results plotted in that figure are the initial permeabilities determined during the first day of permeation immediately after saturation and consolidation. This decrease in permeability is probably due to clogging of pores caused by the cement gel as it hydrated. From Figure 5.10 it is seen that the permeability of the untreated soil decreases slightly with increasing time of permeation and this is probably caused by segregation of fines due to the seepage gradients. For the stabilized soil the decrease in permeability with increasing permeation time is much larger than for the untreated soil. The effect is greatest at the initial stages of permeation and for samples having short curing times. The actual cause of this decrease in permeability has not been investigated but is probably due to segregation of some cement hydration products.

5.5.3 Influence of Curing Conditions

Figure 5.12 shows the influence of curing conditions

on the permeability behavior as a function of void ratio of M-21 plus 5% cement compacted at about optimum water content. Even at the highest consolidation pressure of 50 kg/cm^2 (lowest void ratios), the unsealed hot-cured samples. (Nos. Pk-N1 and PS-N1), which underwent severe cracking during curing, had permeabilities that were three orders of magnitude larger than the corresponding values for the hot-cured sealed specimens. This is further evidence that the cracks do not close completely even at $\bar{\sigma}_c = 50 \text{ kg/cm}^2$. At $\bar{\sigma}_c = 5 \text{ kg/cm}^2$, the cracked unsealed samples had permeabilities five orders of magnitude larger than the sealed uncracked specimens.

The unsealed samples cured at room temperature* had permeabilities that were lower than the unsealed hot-cured samples but they were higher than those of the hot-cured sealed samples. This does not necessarily mean that the room-temperature samples developed cracks during curing since hot-curing for fourteen days at 70°C causes more hydration of the cement than thirty-five days at 23°C , and it was shown above that the permeability of cement-stabilized M-21 decreases with increasing curing time.

Figure 5.13 comp res the permeability behavior of

*The void ratios of sample No. PS-R1 are questionable.

sealed and unsealed samples of M-21 plus 5% cement compacted dry of optimum and hot cured for fourteen days. The sealed samples had higher permeabilities than the unsealed samples because they had significantly lower as-molded dry densities. These results suggest that cracking was not a problem with the unsealed samples compacted dry of optimum.

Wet of optimum (Figure 5.14), the permeabilities of the unsealed hot-cured samples and the unsealed room-temperature cured samples were of the same order of magnitude. This suggests that cracking may be a problem when unsealed samples are cured at room temperature, or it may be due to less hydration of the cement at room temperature.

5.5.4 Influence of Molding Conditions

Due to the limited amount of soil that remained from this batch of M-21, it was not possible to study the influence of sealed hot curing and unsealed room temperature curing on the permeability behavior of M-21 plus 5% cement over the full range of molding water contents used in the major testing program. However, the permeability behavior of treated and untreated M-21 as a function of molding water content was investigated in 1964 using a

different batch of soil. Further, in that investigation two-end static compaction at a constant compaction pressure of 400 psi was used to prepare the test specimens. This compares with five-layer static compaction at varying compaction efforts (to reproduce the same densities as the kneading samples) that was used in the recent (1967-1968) investigation. The stabilized test specimens in the 1964 investigation were unsealed and humid cured at room temperature for one week, followed by one-day soaking prior to consolidation and saturation in the triaxial cells. All 1964 samples were consolidated to an effective pressure of 1.7 kg/cm^2 prior to permeation.

Even though the procedures used in the 1964 investigation differed from those used in the recent program, it is possible, at least in a qualitative manner, to study the influence of curing temperature on the permeability behavior of M-21 plus 5% cement.

Figure 5.15 compares the moisture-density-permeability behavior of the 1964 and 1967-1968 batches of untreated M-21. The differences in the moisture-density relations of the two batches is probably primarily due to the different number of layers and the different compaction pressures used in the two investigations. The molding water content-permeability relations for the two batches

are very similar. The 1964 samples had higher permeabilities because they were consolidated to a lower effective pressure (1.7 kg/cm^2 versus 5 kg/cm^2) and therefore had higher void ratios during permeation. Based on these results, it can be stated that the two batches of M-21 did not differ significantly.

Figure 5.16 compares the moisture-density-permeability behavior of the unsealed hot-cured samples of M-21 + 5% cement obtained in the recent (1967-1968) investigation with the behavior of the unsealed room-temperature-cured samples obtained in 1964. The permeability results for samples compacted dry of optimum indicate that the hot curing did not cause more severe cracking than room-temperature curing since in both cases the decrease in permeability with increasing molding water content was about the same. The hot-cure samples dry of optimum had lower permeabilities because they had higher as-molded densities and because they were more extensively cured than the room-temperature samples (14 days at 70°C versus 7 days at 23°C).

The permeability of the room-temperature samples decrease with increasing molding water content and reached a minimum close to the maximum water content investigated (wet of optimum). In contrast the hot-cured samples had higher permeabilities at optimum and wet of optimum than dry of optimum. As stated previously in this report,

this behavior is due to the severe cracking that occurred during hot curing of the samples compacted at and wet of optimum.

It is of interest to note that the sample compacted at 13.5% water content and cured at room temperature was considerably more pervious than the hot-cured sealed sample compacted at the same water content (sample No. PS-W1). The lower permeability of the sealed sample can in part be due to its higher as-molded dry density (121.4pcf versus 118.5 pcf) and the more extensive curing to which it was subjected. Nevertheless, the possibility that minor cracking occurred during room-temperature curing of the unsealed sample contributed to its higher permeability cannot be discarded.

TABLE 5.1 SUMMARY OF CLARIFICATION TEST RESULTS FOR M-21 + 5% CEMENT

Sample No.	Type of Compaction	Type of Cure	Molding Conditions			Consolidation Pressure, kg/cm ²	Void Ratio e	Permeability k, cm/sec.
			Water Content W, %	Dry Density 'd, p.c.f.	Void Ratio e			
PS-N ₁	Static	Standard	13.6	121.7	0.425	0.21	0.446	2.8×10^{-5}
						5.0	0.442	1.6×10^{-6}
						10.0	0.441	6.8×10^{-7}
						25.0	0.439	5.0×10^{-7}
						50.0	0.426	3.1×10^{-8}
						1.82*	0.433	-----
PK-N ₁	Kneading	Standard	13.5	120.8	0.436	0.21	0.480	4.5×10^{-5}
						5.0	0.462	2.4×10^{-6}
						10.0	0.460	1.3×10^{-6}
						25.0	0.458	8.5×10^{-7}
						50.0	0.439	1.5×10^{-7}
						1.82*	0.448	-----
PS-W ₁	Static	Sealed	13.5	121.4	0.429	2.0	0.414	7.7×10^{-10}
						5.0	0.414	6.0×10^{-10}
						10.0	0.413	4.8×10^{-10}
						25.0	0.413	2.8×10^{-10}
						50.0	0.412	2.7×10^{-10}
						2.0*	0.413	-----
PS-W ₂	Static	Sealed	10.7	112.7	0.526	5.0	0.471	5.7×10^{-7}
						10.0	0.471	6.1×10^{-6}
						25.0	0.469	4.5×10^{-7}
						50.0	0.459	3.2×10^{-7}
						1.6*	0.460	-----
						2.0*	0.473	-----
PK-W ₁	Kneading	Sealed	13.5	120.7	0.437	2.0	0.424	7.5×10^{-10}
						5.0	0.424	2.0×10^{-10}
						10.0	0.423	1.3×10^{-10}
						25.0	0.422	1.0×10^{-10}
						50.0	0.422	1.0×10^{-10}
						2.0*	0.423	-----
PK-W ₂	Kneading	Sealed	10.0	113.6	0.527	5.0	0.476	5.5×10^{-6}
						10.0	0.475	5.1×10^{-6}
						25.0	0.469	3.7×10^{-6}
						50.0	0.448	3.2×10^{-6}
						1.6*	0.450	-----
						2.0*	0.476	-----
PS-W ₃	Static	Room Temp.	12.0	115.0	0.497	5.0	?	2.5×10^{-6}
						10.0	?	2.0×10^{-6}
						25.0	0.421	1.3×10^{-7}
						50.0	0.400	1.0×10^{-7}
						2.0*	0.432	-----
						2.0*	0.476	-----
PS-W ₄	Static	Room Temp.	15.2	116.0	0.495	5.0	0.459	1.3×10^{-7}
						10.0	0.459	9.5×10^{-8}
						25.0	0.459	7.1×10^{-8}
						50.0	0.459	5.7×10^{-8}
						2.0*	0.451	-----
						2.0*	0.455	-----
PK-W ₃	Kneading	Room Temp.	12.5	115.7	0.499	5.0	0.455	3.3×10^{-7}
						10.0	0.452	2.0×10^{-8}
						25.0	0.448	2.0×10^{-9}
						50.0	0.436	1.1×10^{-9}
						2.0*	0.449	-----
						2.0*	0.476	-----
PK-W ₄	Kneading	Room Temp.	17.7	115.2	0.505	5.0	?	3.2×10^{-2}
						10.0	0.460	2.6×10^{-2}
						25.0	0.439	1.1×10^{-2}
						50.0	0.415	6.5×10^{-3}
						2.0	0.426	-----
						2.0*	0.476	-----

*Rebound consolidation pressure.

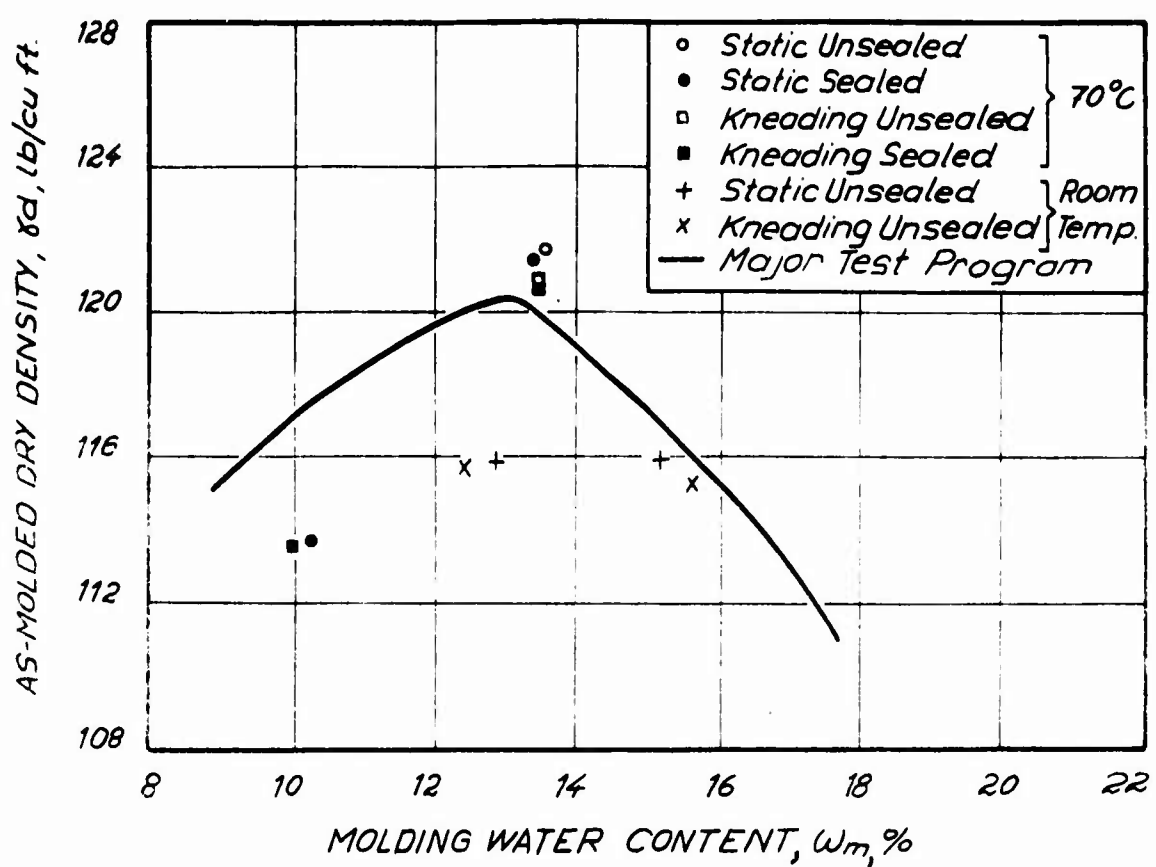


FIG. 5.1 MOLDING CONDITIONS OF CLARIFICATION
TEST SPECIMENS

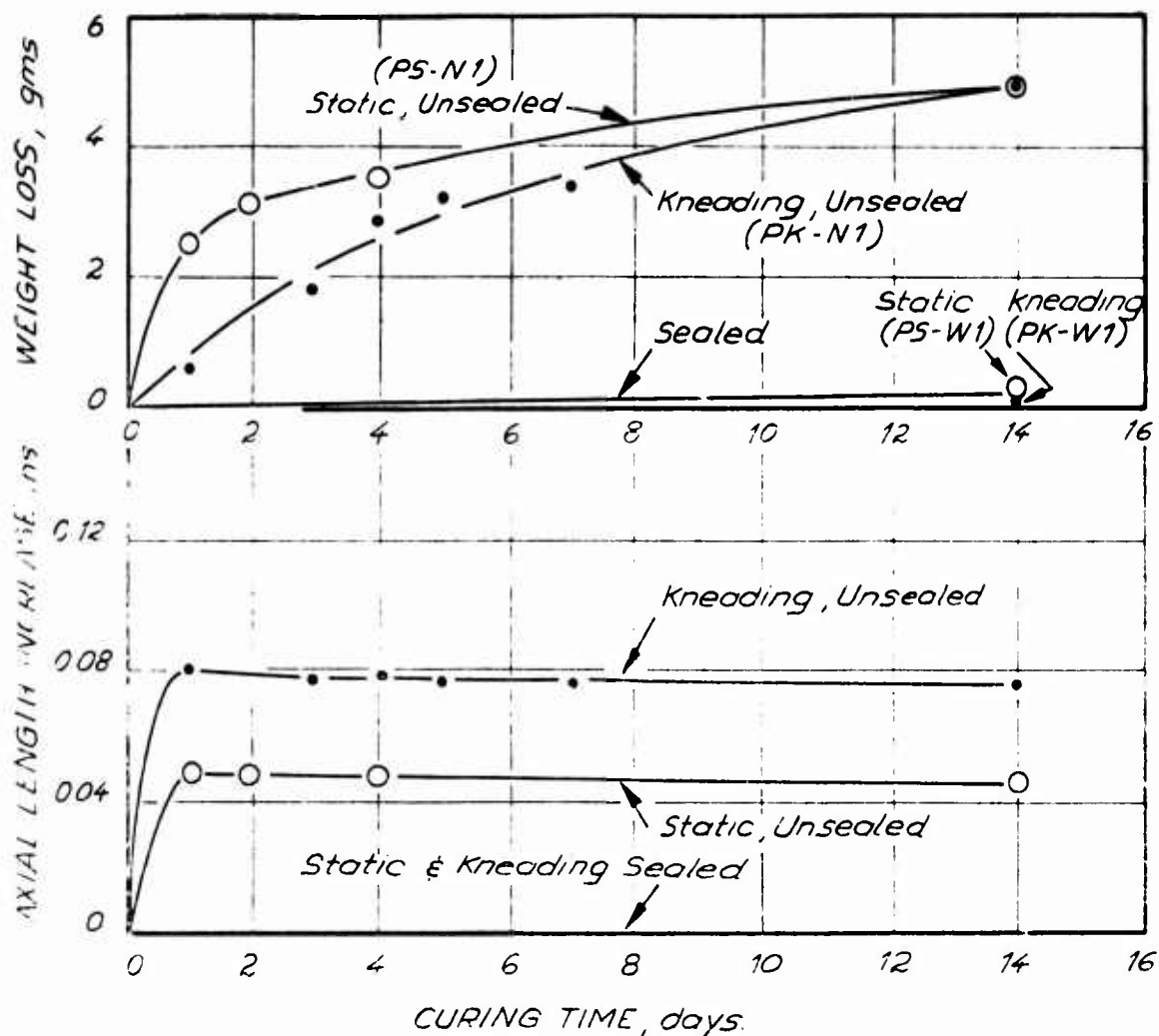


FIG. 5.2 INFLUENCE OF SEALING TEST SPECIMENS
ON WEIGHT AND LENGTH CHANGES
DURING HOT CURING.



FIG. 23 UNSEALED AND SEALED TEST SPECIMENS AFTER HOT CURING SHOWING CRACKING AND OVERALL EXPANSION OF UNSEALED SAMPLES

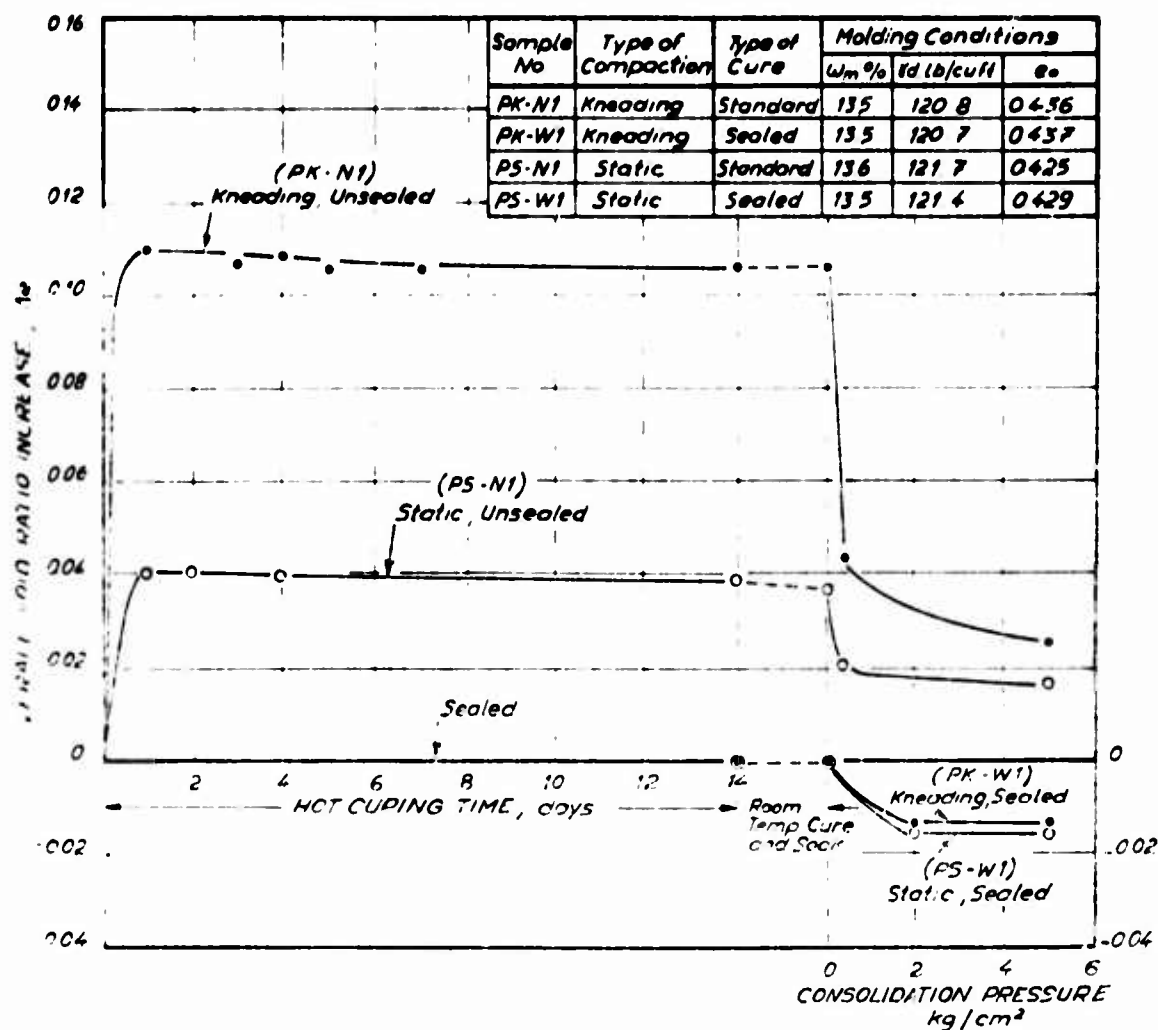


FIG 5 4 INFLUENCE OF CURING CONDITIONS ON OVERALL VOID RATIO CHANGE DURING CURING AND INITIAL CONSOLIDATION OF M-21+5% CEMENT COMPACTED AT OPTIMUM.

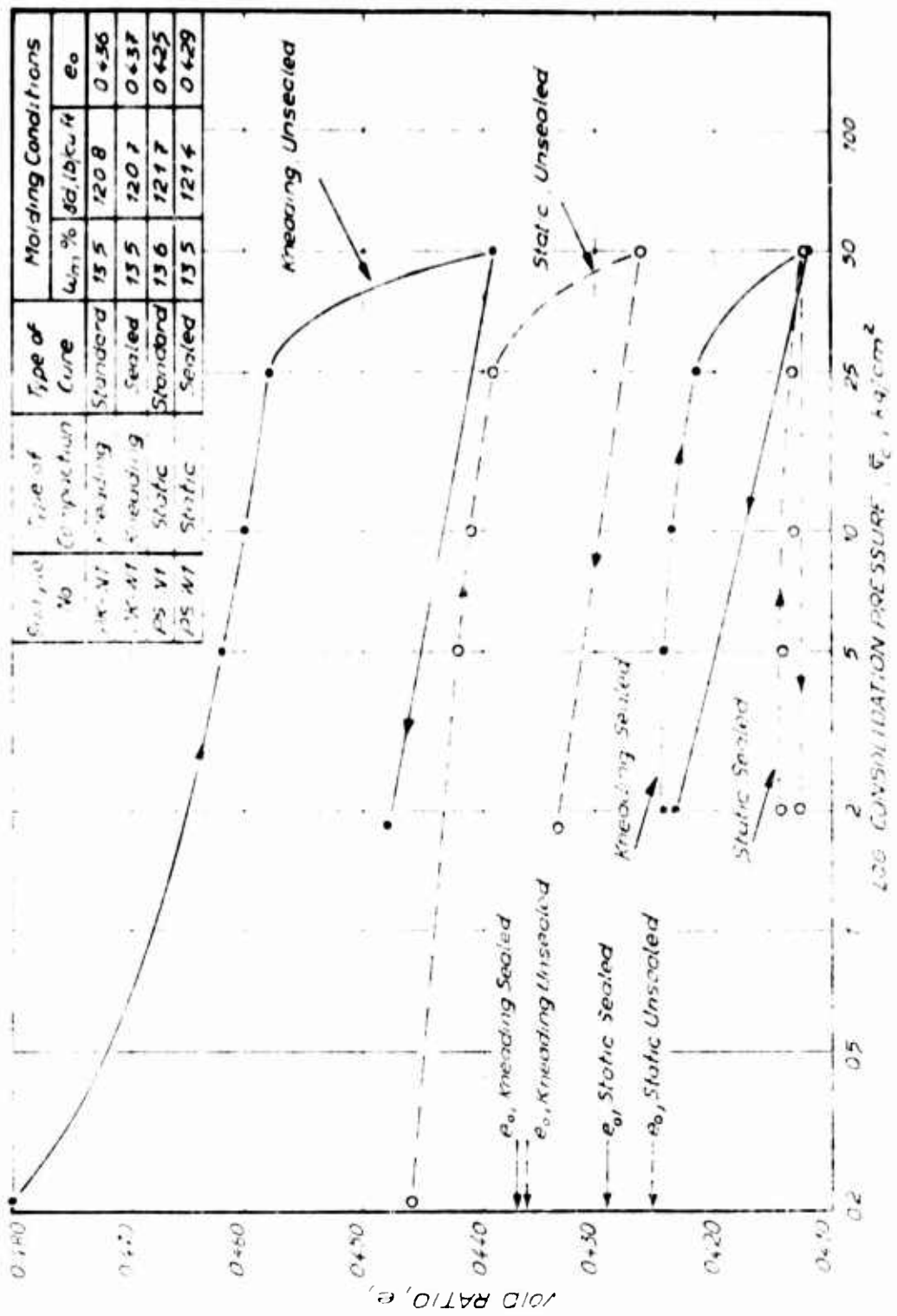


FIG 5.5 INFLUENCE OF CURING CONDITIONS ON THE COMPRESSIBILITY OF M-21+5% CEMENT COMPACTED AT OPTIMUM AND HOT CURED.

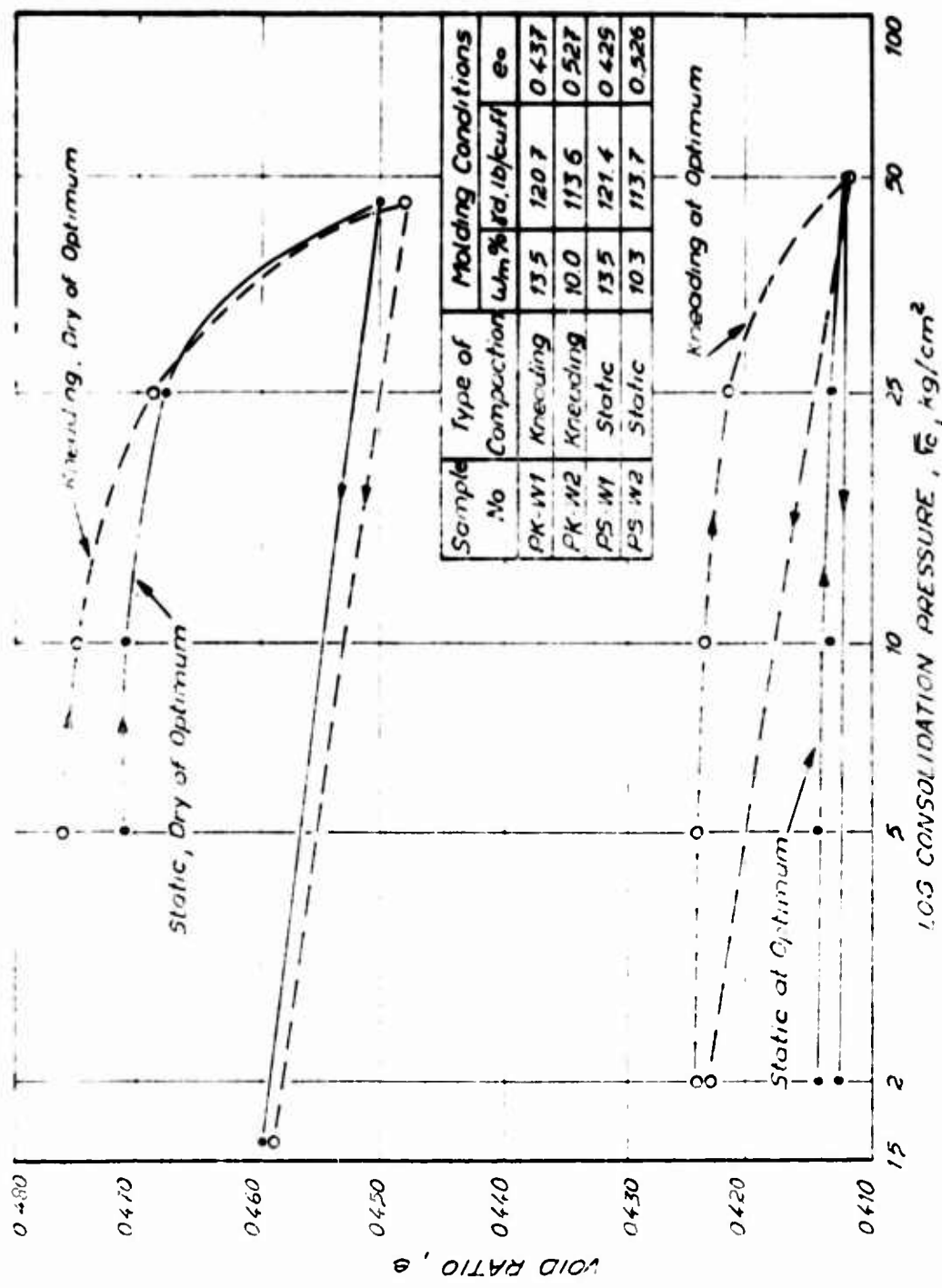


FIG. 5.6 INFLUENCE OF MOLDING CONDITIONS ON THE COMPRESSIBILITY OF SEALED M-21 + 5% CEMENT TEST SPECIMENS.

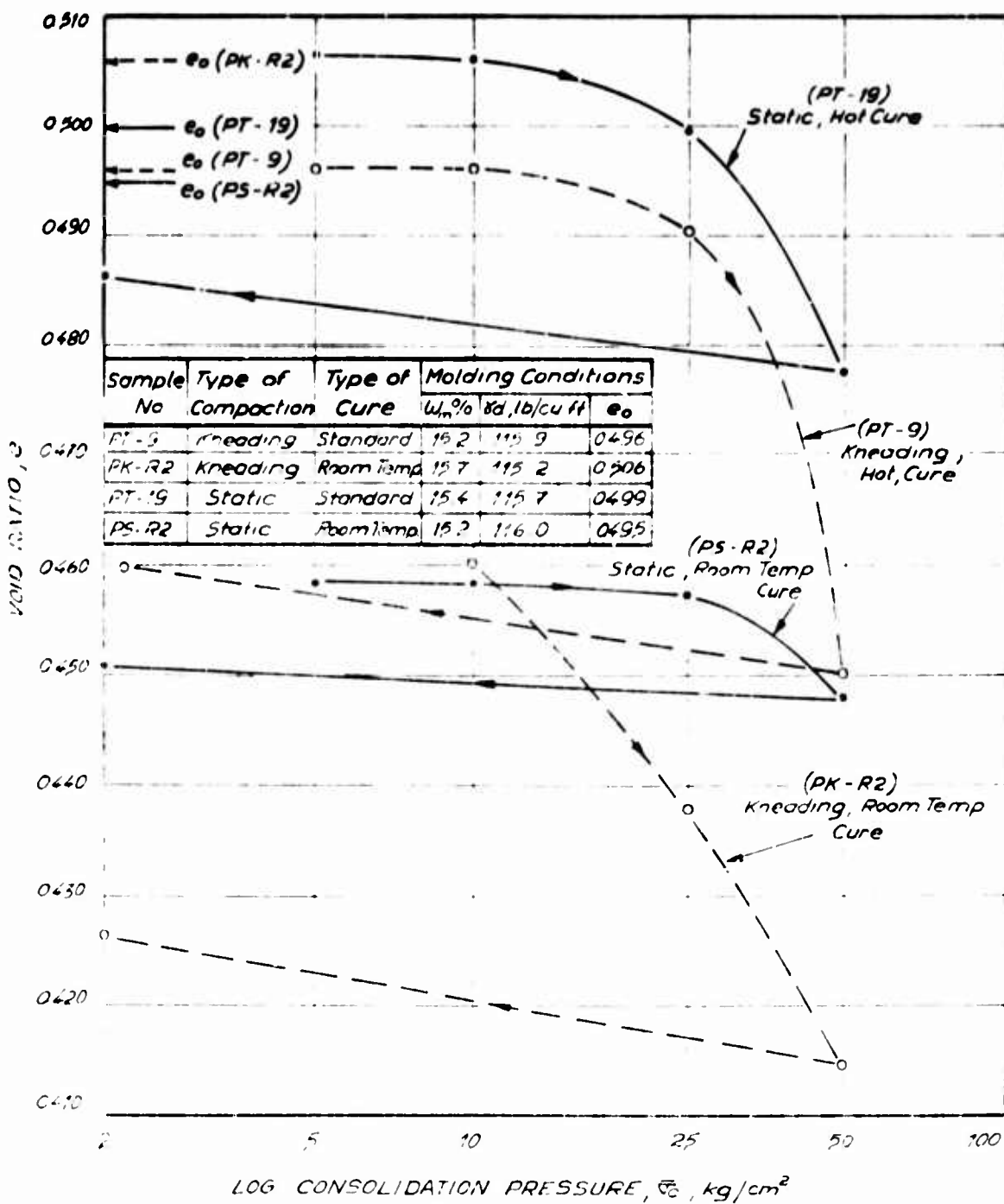


FIG 57. INFLUENCE OF CURING TEMPERATURE ON THE COMPRESSIBILITY OF M-21+5% CEMENT.

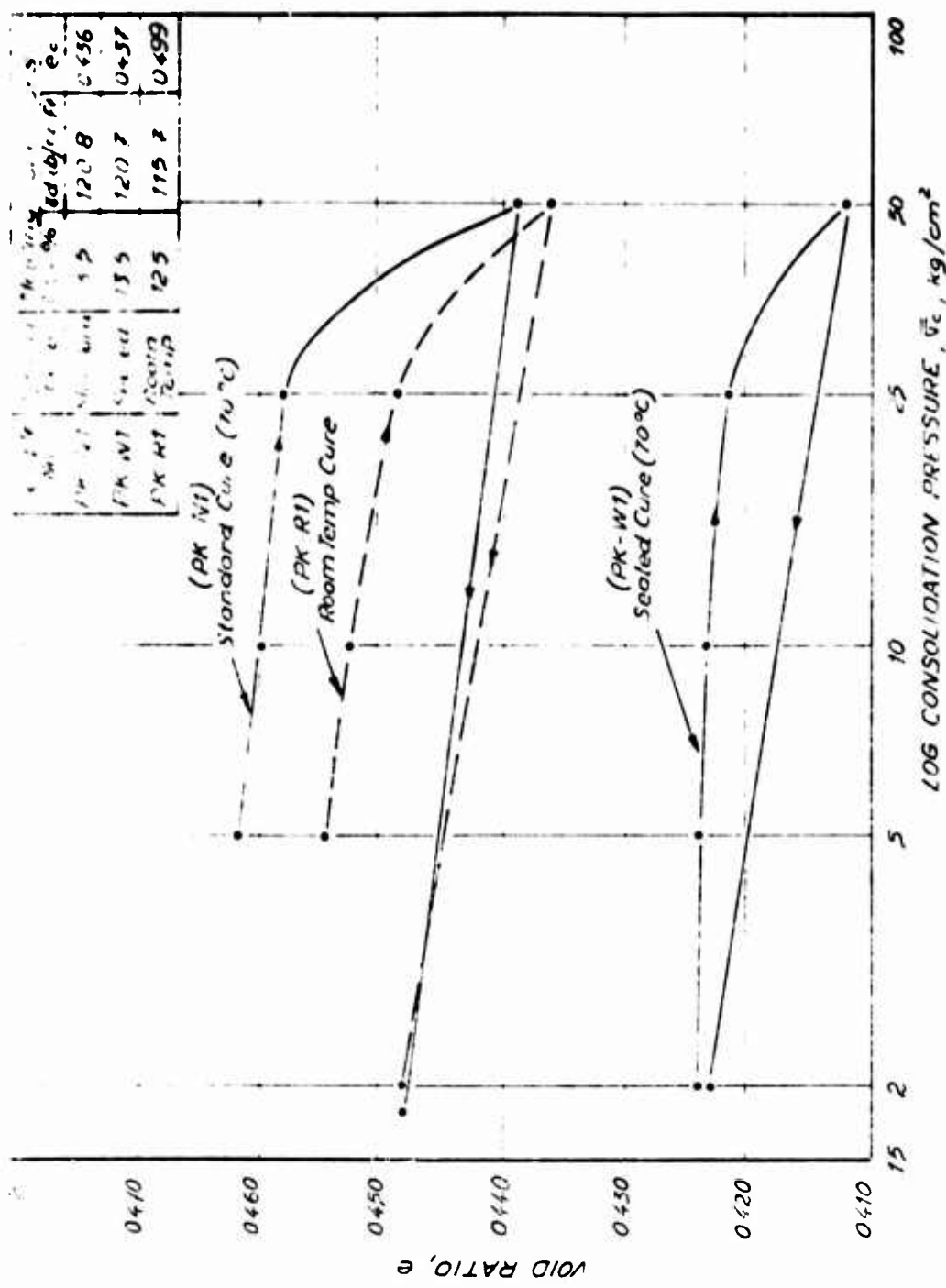


FIG. 5.8. INFLUENCE OF CURING CONDITIONS ON THE COMPRESSIBILITY OF M-21 + 5% CEMENT COMPACTED NEAR OPTIMUM WATER CONTENT USING KNEADING COMPACTION.

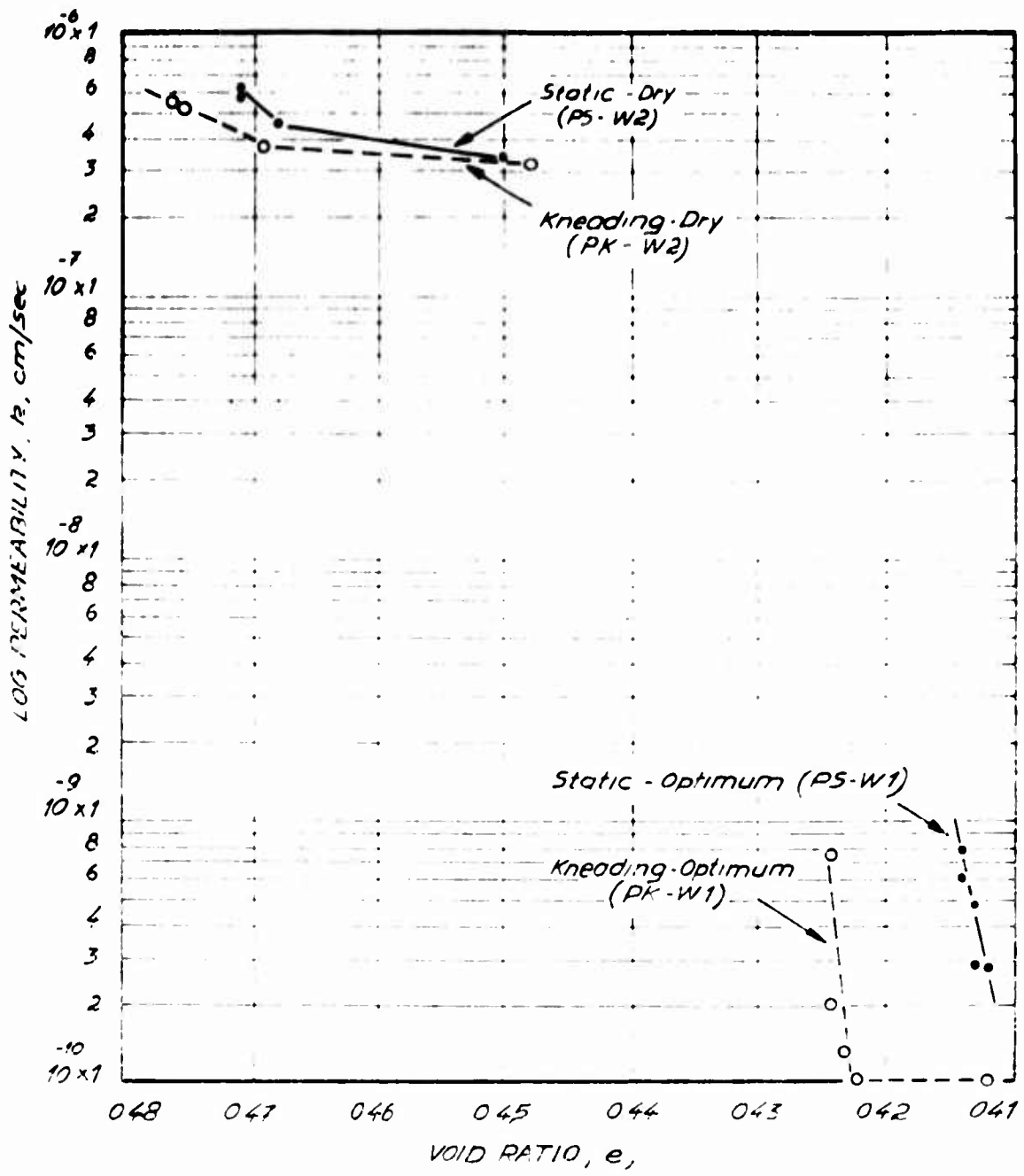
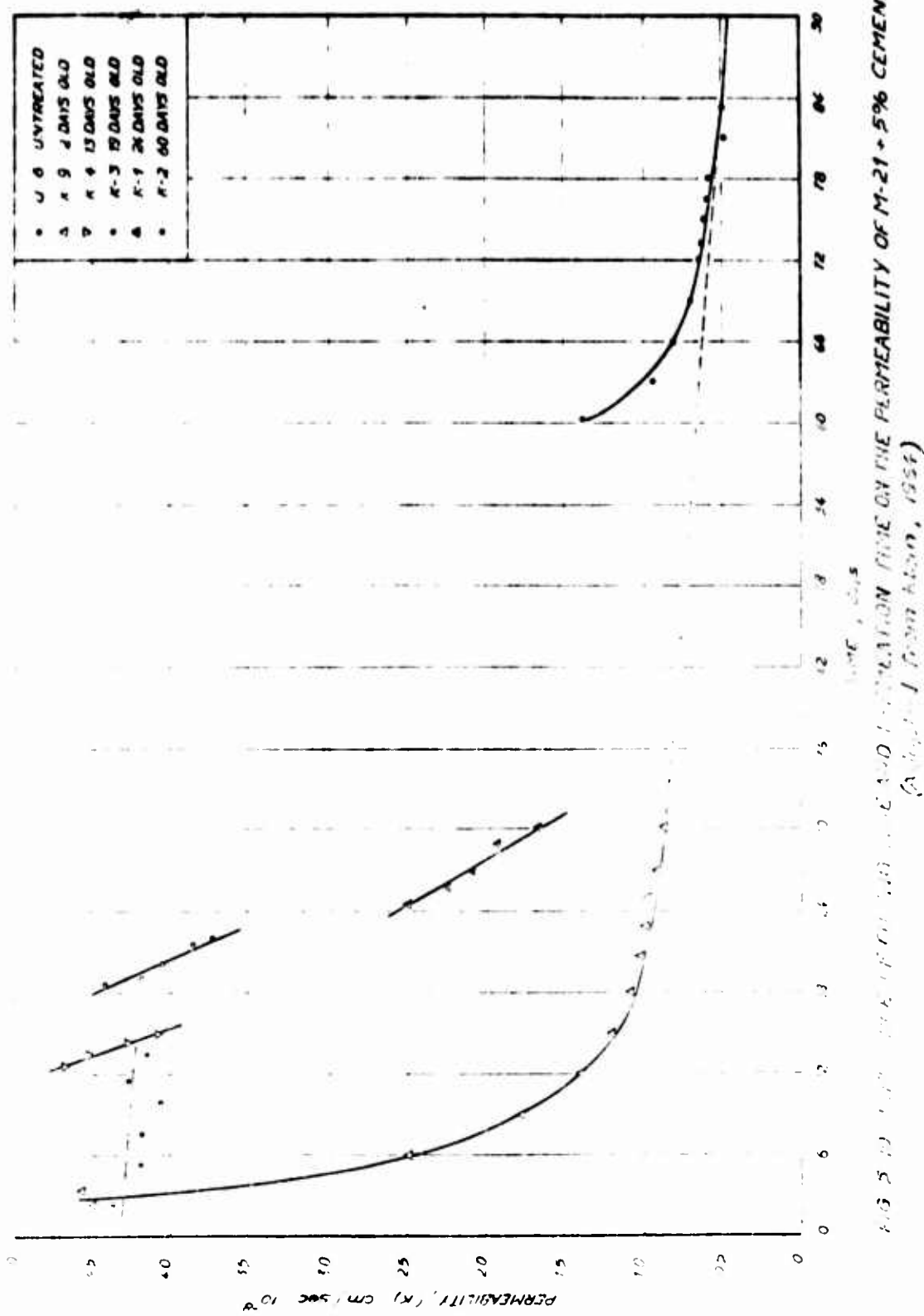


FIG. 5.9. INFLUENCE OF MOLDING CONDITIONS ON THE PERMEABILITY BEHAVIOR OF SEALED SPECIMENS OF M-21+5% CEMENT



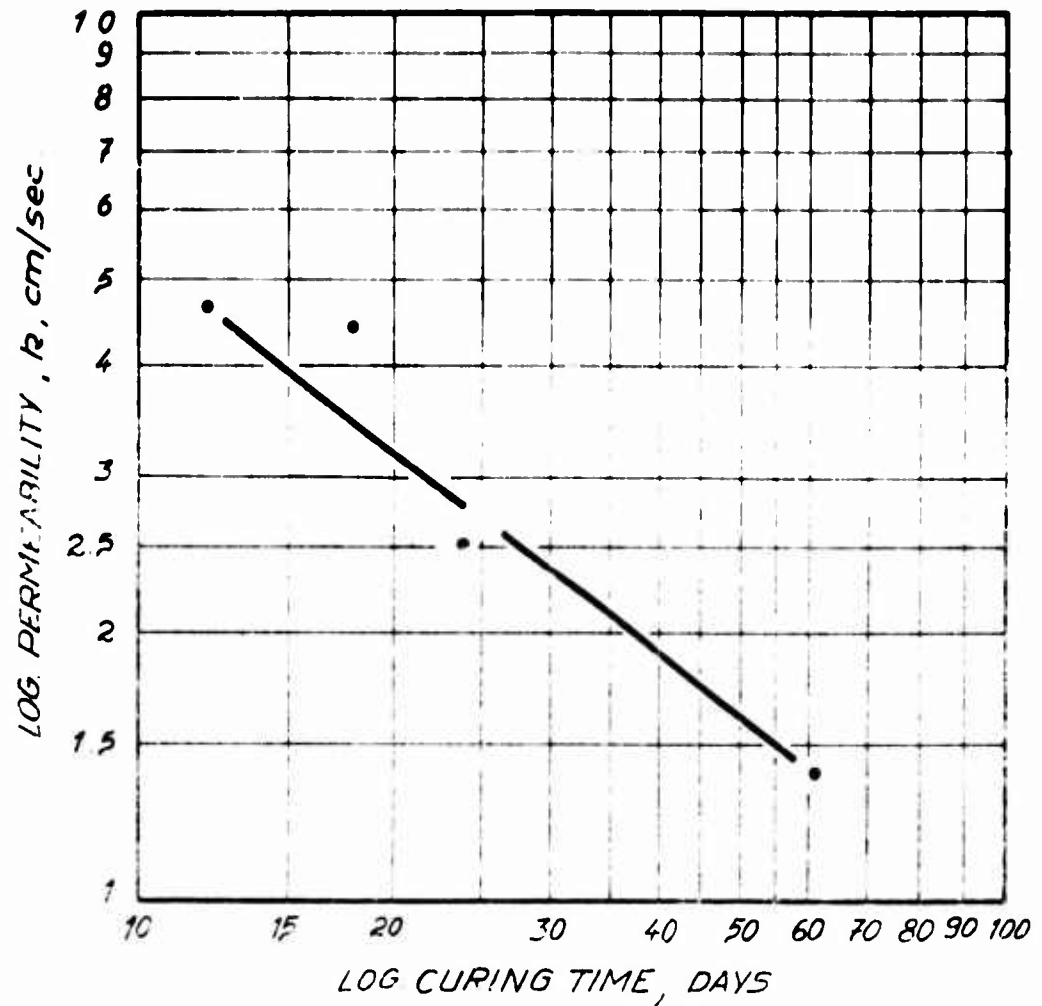
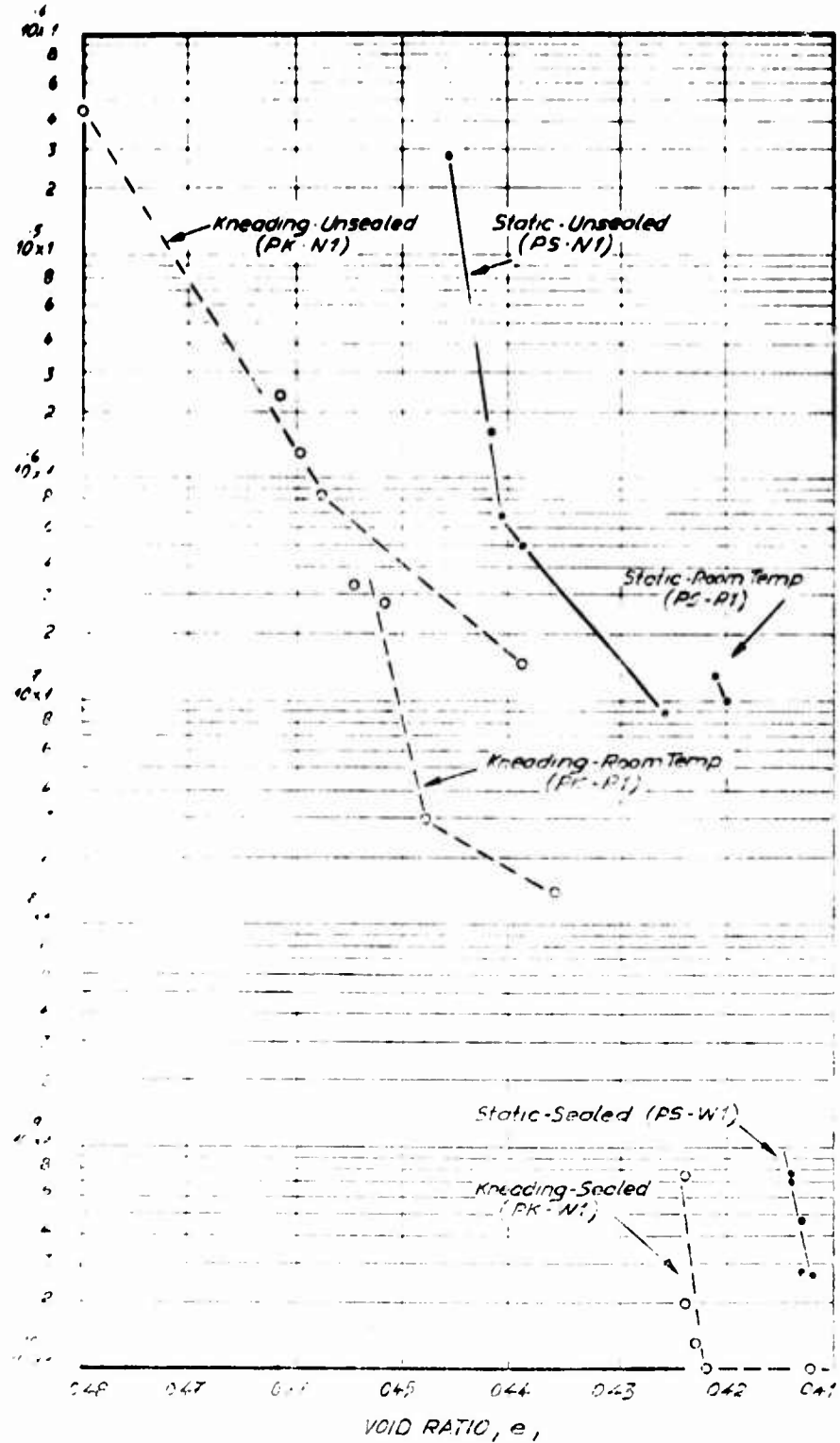


FIG. 5.11 INFLUENCE OF CURING TIME ON
THE INITIAL PERMEABILITY OF
M-21 STABILIZED WITH 5%
CEMENT. (Adopted from Klem, 1964)



-G 5 12 INFLUENCE OF CURING CONDITIONS ON M-21+5% CEMENT COMPACTED NEAR OPTIMUM.

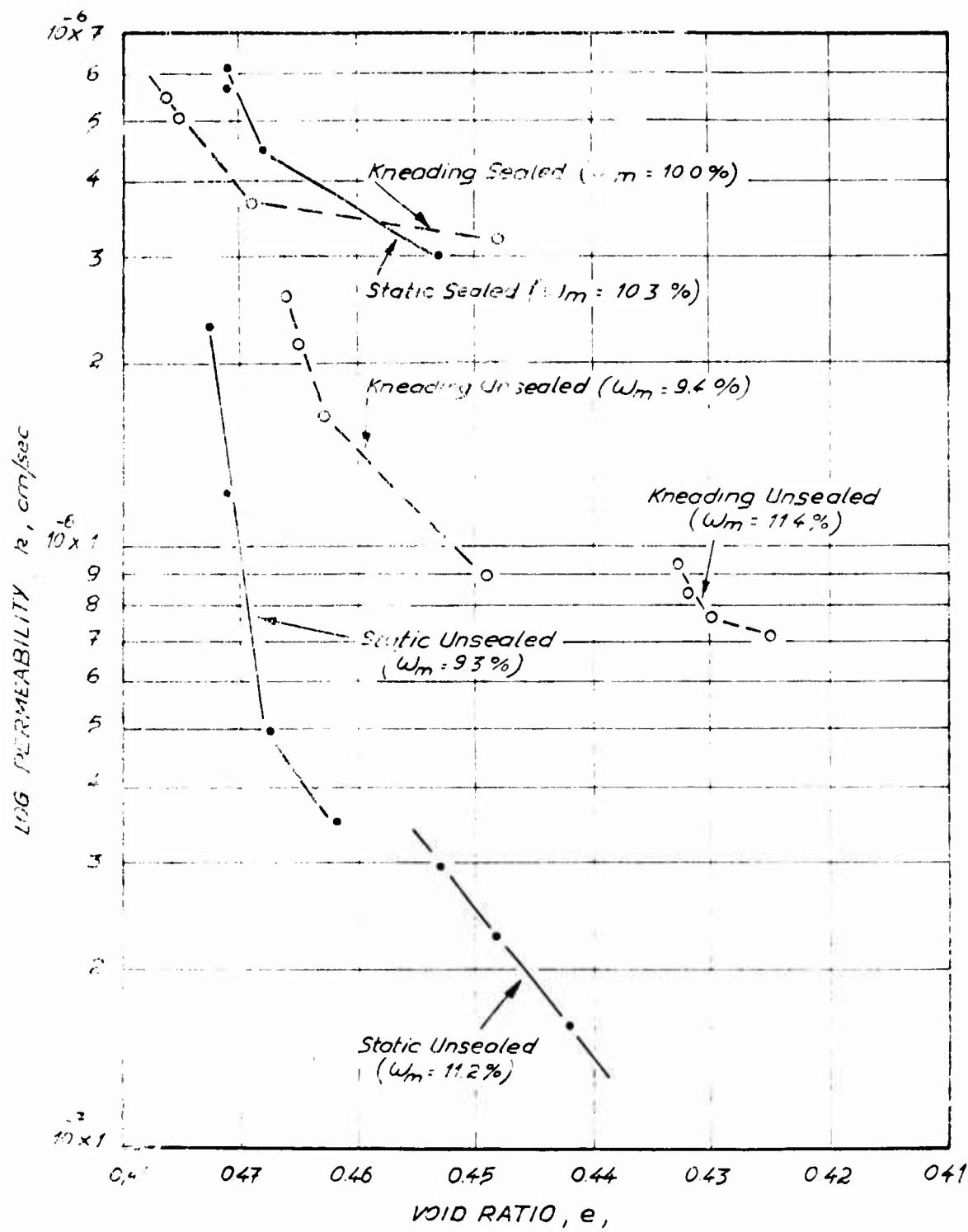


FIG. 5. 15. INFLUENCE OF SEALING DURING HOT CURE ON
PERMEABILITY BEHAVIOR OF M-21 + 5 %
CEMENT COMPACTED DRY OF OPTIMUM

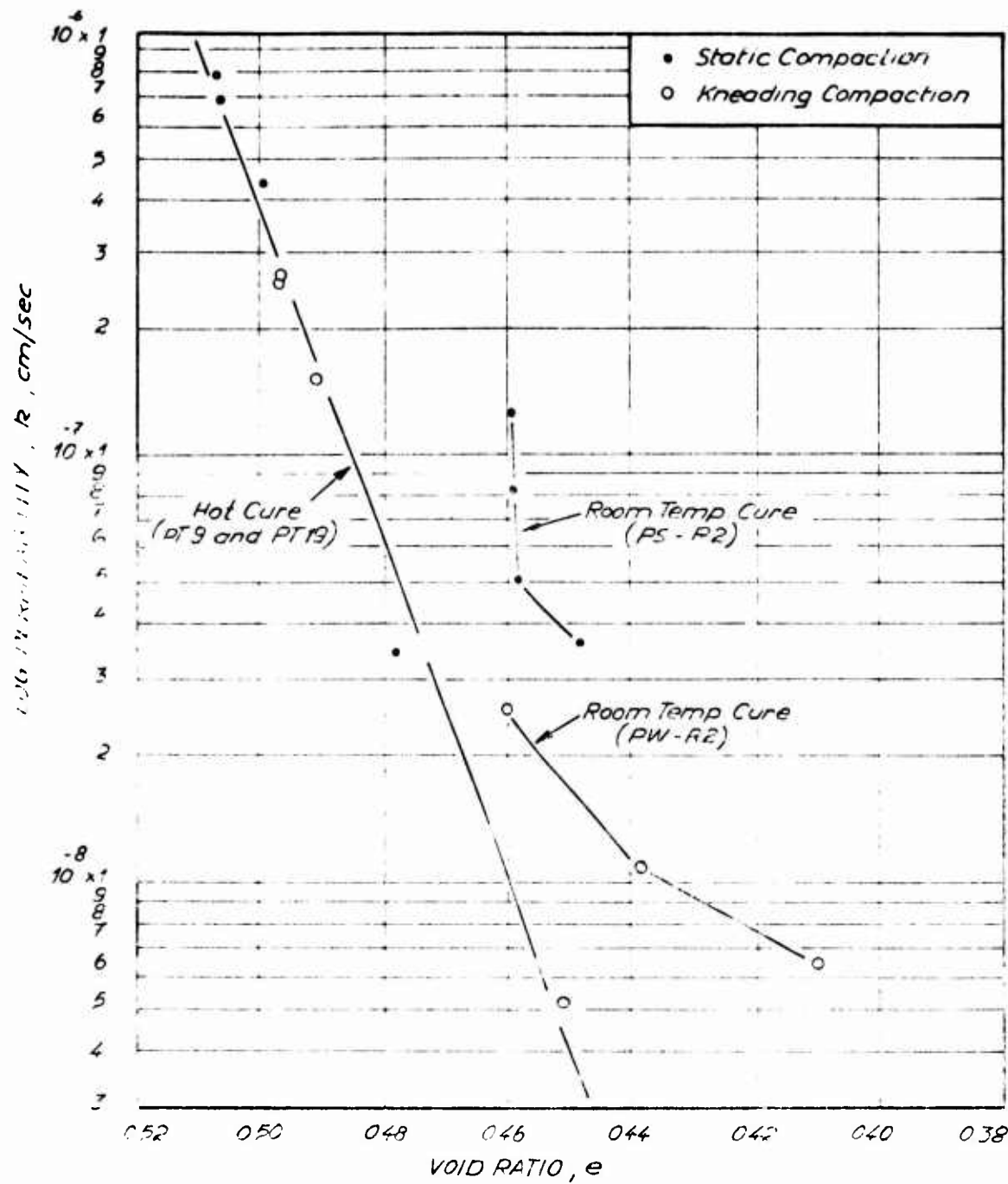


FIG. 5.14 INFLUENCE OF CURING TEMPERATURE ON THE PERMEABILITY BEHAVIOR OF UNSEALED M-21 + 5% CEMENT SPECIMENS COMPACTED WET OF OPTIMUM.

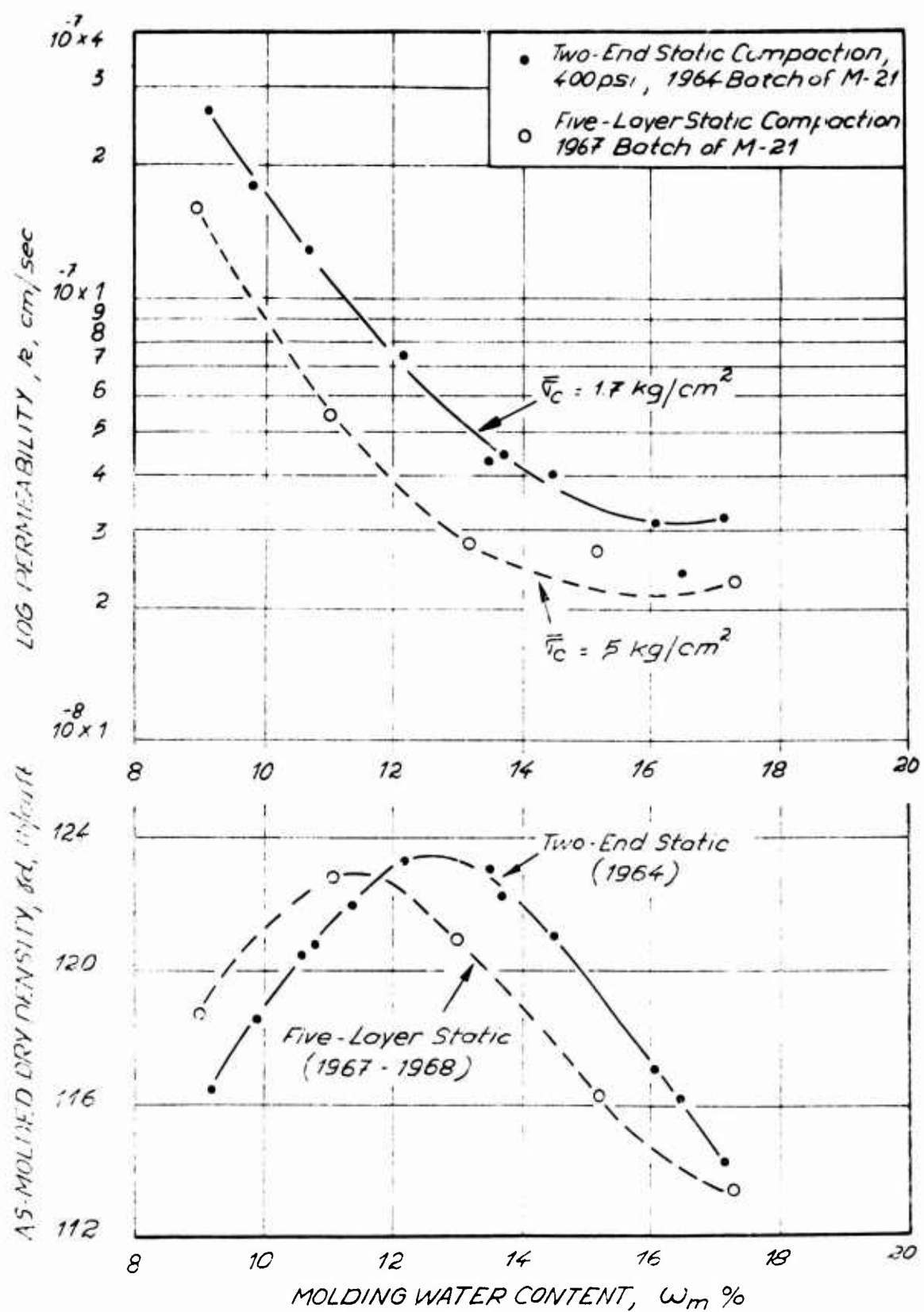
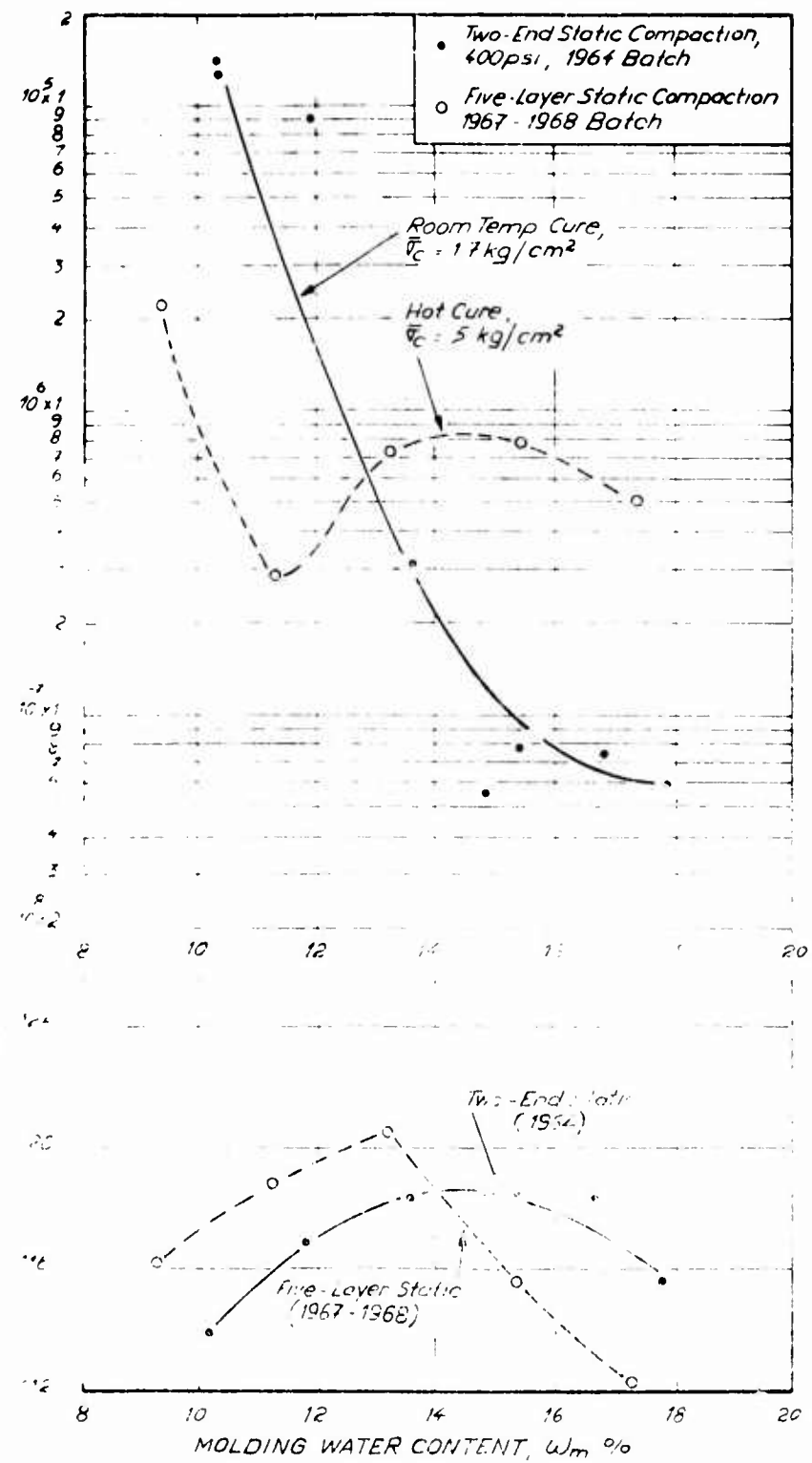


FIG. 5.15 MOISTURE-DENSITY-PERMEABILITY BEHAVIOR OF UNTREATED M-21 USED IN 1964 AND 1967-1968.



G 5 16 MOISTURE-DENSITY-PERMEABILITY BEHAVIOR
OF M-21+5% CEMENT USING UNSEALED
CURING AT ROOM TEMPERATURE AND AT 70°C

Chapter VI

SUMMARY AND CONCLUSIONS

6.1 Objectives of the Investigation

Since 1961 stabilization research at M.I.T. has concentrated on determining the influence of artificial cementation on the engineering properties of soils. While previous reports studied the shear strength behavior of stabilized soils, the present report covers the influence of artificial cementation on the compressibility and permeability properties of soils. A high pressure triaxial-permeability setup was constructed for this investigation. With this equipment five specimens could be tested simultaneously over a wide range of confining pressures (0 to 70 kg/cm²) under a back pressure of up to 15 kg/cm². Using a constant hydraulic gradient of 250 (2 kg/cm² pressure difference across a specimen 8 cm long) and a sample having a cross-sectional area of 10 cm², permeabilities down to 5×10^{-10} cm/sec could be measured accurately with this equipment. To measure lower permeabilities, higher hydraulic gradients can be applied or the length of the test specimen must be reduced and its cross-sectional area increased. Alternatively, the sensitivity of the volume change measuring

burettes can be increased from ± 0.01 cc to ± 0.001 cc by reducing their capacity from 5 cc to 0.5 cc. Since most of the test specimens used in this investigation had permeabilities greater than 5×10^{-10} cm/sec, it was not necessary to improve the sensitivity of the equipment.

6.2 Compressibility Behavior

6.2.1 Untreated M-21

The influence of molding water content on the compressibility of kneadingly and statically compacted untreated M-21 was determined over a consolidation pressure range from 5 kg/cm² to 50 kg/cm². The results showed that:

(1) At low consolidation pressures (from 5 to 10 kg/cm²) the compressibility is highest for compacted soil having the least flocculated fabric, i.e., kneading compaction, wet of optimum. However, at high consolidation pressures (from 25 to 50 kg/cm²), the highest compressibility may occur when the as-molded fabric of the soil is most flocculated, i.e., static compaction dry of optimum. This can be explained by a collapse of the flocculated fabric at high consolidation pressures. (see Figure 6.1 and Figure 4.2).

(2) The swelling when rebounding the test specimens from a consolidation pressure of 50 kg/cm² to about 1.5

kg/cm^2 was greatest for the samples having the most flocculated as-molded fabric, i.e., static compaction dry of optimum. This strongly suggests that a portion of the compressibility of the soil at high consolidation pressures is due to recoverable elastic deformation of the soil particles.

6.2.2 M-21 + 5% Cement

For the major testing program, unsealed hot curing caused cracking of the stabilized test specimens. Even at high consolidation pressures (25 to 50 kg/cm^2), this cracking controlled the compressibility of the stabilized soil.

The cracking was most severe for samples compacted slightly wet of optimum using kneading compaction. The samples showing the most severe cracking were also the most compressible (see Figure 4.3).

When cracking was prevented by sealing the test specimens during the hot-cure period, the compressibility of the stabilized soil was primarily dependent on the as-molded dry density, i.e., the higher the as-molded dry density, the lower the compressibility (see Figure 5.6). The decrease in compressibility with increasing as-molded dry density is in part due to a decrease in the as-molded

void ratio and in part due to an increase in the cementation between the strongly cemented soil aggregates, (see Wissa and Ladd, 1965).

For unsealed samples, curing at room temperature caused less cracking than curing at 70°C since the room-temperature-cured samples were less compressible than the hot-cured samples (see Figure 5.7).

6.3 Permeability Behavior

6.3.1 Untreated M-21

A linear relation exists between void ratio and log permeability, provided the compacted soil has the same as-molded fabric. This can be seen from Figure 3.16a where the kneading and static compaction samples dry of optimum have about the same flocculated fabric and therefore share the same linear relation between void ratio and log permeability. Further, very wet of optimum, kneading and static compaction apparently have the same as-molded fabric since both samples have the same linear relation. At optimum and slightly wet of optimum, the linear relations between void ratio and log permeability are not the same for kneading and static compaction (Figure 3.16b). The static compaction samples have a more flocculated fabric

and therefore have higher permeabilities than the corresponding kneading samples at the same void ratio.

Figures 3.12, 3.13, and 5.15 showed the influence of molding water content on the permeability of untreated M-21. At a given consolidation pressure, the permeability decreases with increasing molding water content and reaches a minimum wet of optimum. This is due to the soil fabric becoming less flocculated with increasing water content.

Figure 4.4 showed the influence of molding water content and type of compaction on the permeability of untreated M-21 at a constant void ratio. While the influence of molding water content is not as pronounced at constant void ratio as at constant consolidation pressure, the same trends exist, i.e. permeability decreases with increasing molding water content and it is lower for kneading compaction than for static compaction at molding water contents close to optimum.

6.3.2 M-21 + 5% Cement

Molding water content and type of compaction had a marked influence on cracking of the stabilized samples during unsealed hot curing. Cracking was most severe at optimum water content and wet of optimum, and kneading compaction caused more cracking than static compaction. The

effect of molding water content on the permeability of M-21 + 5% cement shown in Figures 3.19 and 3.20 reflects the influence of cracking during curing. Like untreated M-21, at a constant void ratio the permeability of the unsealed hot-cured samples of M-21 + 5% cement decreased with increasing molding water content (Figure 4.6). However, the decrease in permeability was much greater than for the untreated soil. At the same molding water content and void ratio, the static compaction samples were less pervious than the kneading compaction samples. This is opposite to the behavior of the untreated soil and is due to the kneading samples cracking more during curing.

For room-temperature unsealed curing, the permeability of M-21 stabilized with 5% cement decreased rapidly with increasing molding water content (Figure 5.16). Sealed hot curing, which presumably prevented cracking during curing, resulted in the kneading compaction samples being less pervious than the static compaction samples. While the difference in permeability was not very large, it agrees with the effect type of compaction had on the untreated soil.

Figures 6.2 and 6.3 compare the influence of molding

water content on the permeability behavior of untreated and cement-stabilized M-21 using static and kneading compaction, respectively. It is apparent from these figures that the permeability of the stabilized soil can be decreased by at least four orders of magnitude by increasing the molding water content whereas the permeability of untreated M-21 can be only decreased by a little over one order of magnitude. Further, at optimum water content, the permeability of the stabilized soil is about one and a half orders of magnitude lower than that of the untreated soil even though it is at a higher void ratio. This decrease in permeability of the cement-stabilized soil is due to the clogging of pores by the cement gel.

Finally, the permeability of cement-stabilized M-21 decreases with increasing curing time and time of permeation, and this is probably the reason why a linear relation does not always exist between void ratio and log permeability. The observed relatively large decreases in permeability due to small decreases in void ratio caused by consolidation are probably due to time effects rather than the very small void ratio decreases.

6.4 Conclusions

This investigation has shown the severe effect unsealed hot curing has on the permeability and compressibility behavior of M-21 stabilized with 5% cement. The cracking during unsealed hot curing is probably also the cause for the scatter in triaxial test results obtained recently when elevated temperatures were used to accelerate curing of the test specimens.

The large decrease in permeability of soil-cement with increasing molding water content makes it suitable to use plastic soil-cement (soil-cement at high molding water contents) for canal linings; however, such a material is more vulnerable to cracking during curing and therefore must be prevented from losing moisture during the curing period.

Finally, the effects of curing time and time of permeation on the permeability of soil-cement should be investigated in further detail. In addition, the influence of molding water content on the permeability of room-temperature-cured and sealed-cured soil-cement should be determined over a wider range of moisture condition than those used in this investigation.

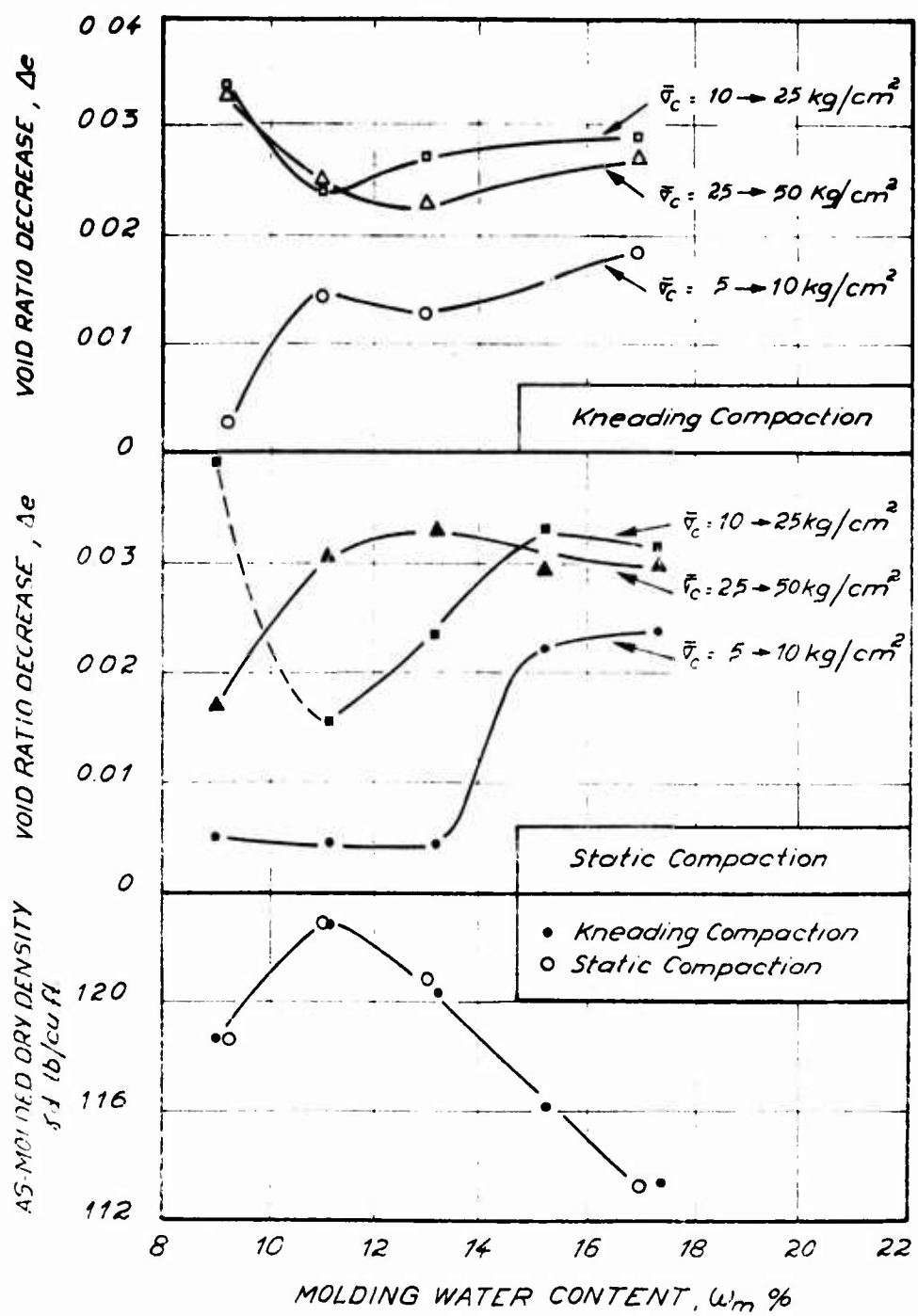


FIG. 6.1. COMPRESSIBILITY BEHAVIOR OF
UNTREATED M-21 AS A FUNCTION OF
MOLDING WATER CONTENT AND
TYPE OF COMPACTION.

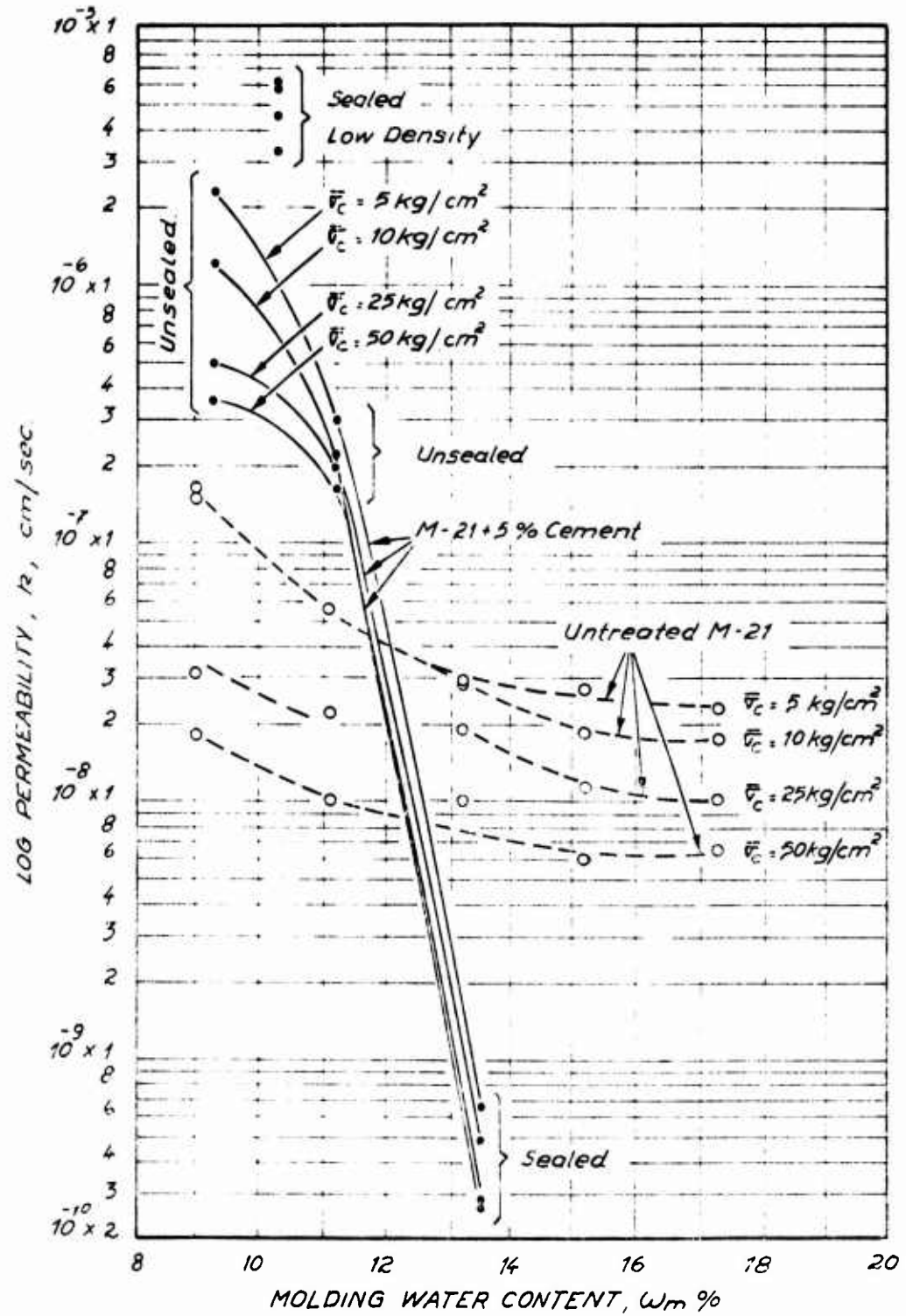


FIG. 6.2. INFLUENCE OF CEMENT STABILIZATION ON THE PERMEABILITY OF STATIC COMPACTED M-21

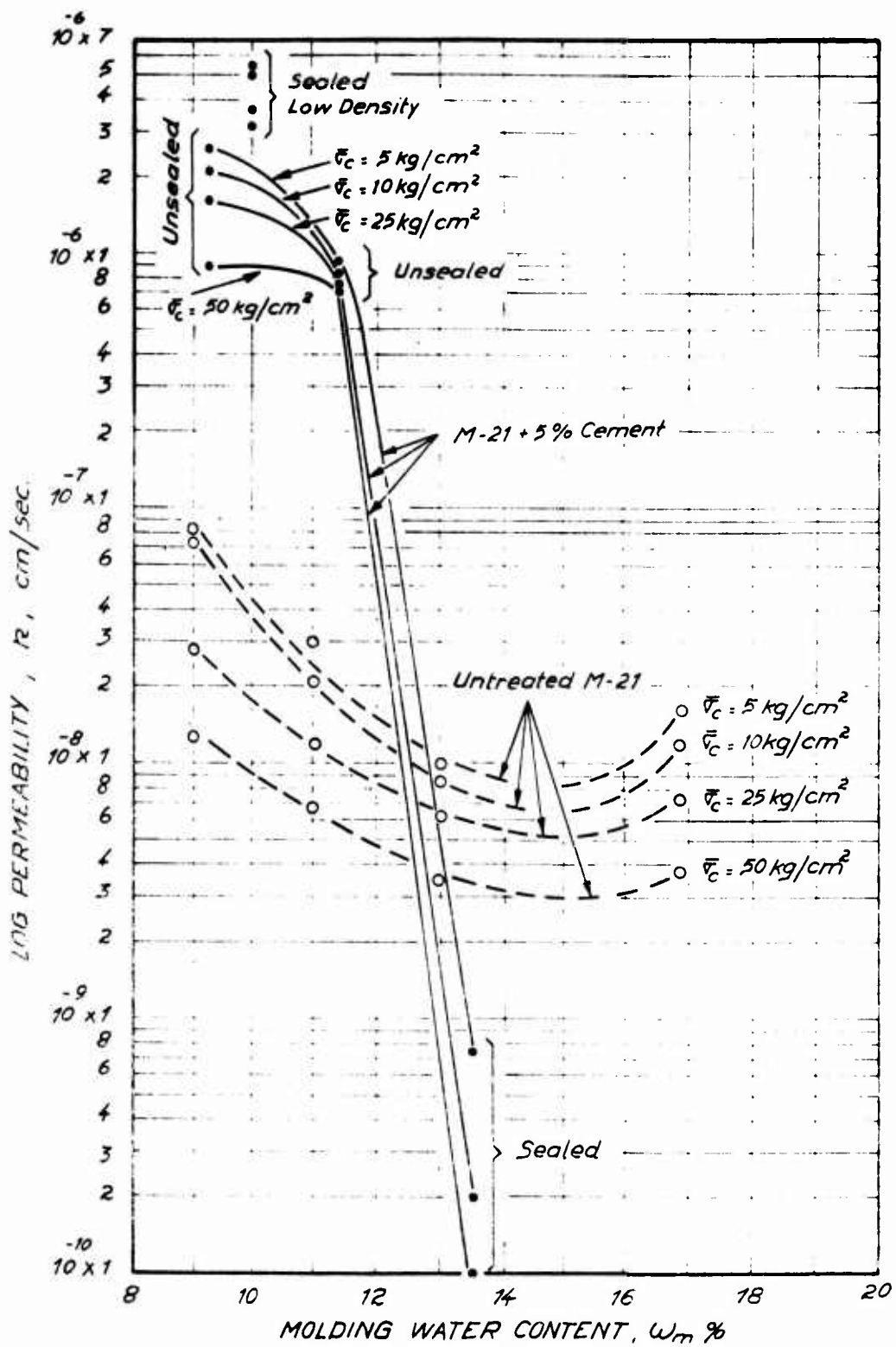


FIG. 6.3. INFLUENCE OF CEMENT STABILIZATION ON THE PERMEABILITY OF KNEADING COMPACTED M-21

LIST OF REFERENCES

- Bishop, Alan W. and Henkel, D.J. The Measurement of Soil Properties in the Triaxial Test, Second edition. Edward Arnold [Publishers] Ltd., London, 1962.
- Clare, K.E. and Pollard, A.E., "The Effect of Curing Temperature on the Compressive Strength of Soil-Cement Mixtures" Geotechnique, Vol. IV, No. 3, 1954.
- Feferbaum-Zyto, Samuel. "Influence of Molding Conditions on the Effective Stress-Strength Behavior of Stabilized Soils," S.M. thesis, Department of Civil Engineering, M.I.T., June 1966.
- George, K.P., "Shrinkage Characteristics of Soil Cement Mixtures," Paper Presented at the 47th Annual Meeting of the Highway Research Board, Washington, D.C., January, 1968.
- Klem, Johannes H. "Permeability of a Cement-Stabilized Soil," S.B. thesis, Department of Civil Engineering, M.I.T., May, 1964.
- Lambe, T. William, "Improvement of Soil Properties With Dispersants," Journal of the Society of Civil Engineers, Vol. 41, No. 2, 1954.
- Lambe, T. William, "The Permeability of Fine-Grained Soils," American Society for Testing Materials, June, 1954.
- Lambe, T. William, "The Permeability of Fine Grain Soils," American Society for Testing Materials, Special Technical Publication No. 163, 1955.
- Lambe, T. William, "The Engineering Behavior of Compacted Clay," ASCE Proceedings No. 1655, May, 1958.
- Michaels, A.S. and Lin, C.A., "The Permeability of Kaolinite," Industrial and Engineering Chemistry vol. 46, June, 1954.
- M.I.T., "Triaxial Equipment and Computer Program for Measuring the Strength Behavior of Stabilized Soil," Department of Civil Engineering, M.I.T. Soil Stabilization Phase Report No. 2. September, 1963.
- Mitchell, James K., Hooper, Don R., and Campenella, Richard G., "Permeability of Compacted Clay," Journal of the Soil Mechanics and Foundations Division, ASCE, vol. 91, No. SM4 Proc. Paper 4392, July, 1965.

Seed, H.B., Mitchell, J.K., Chan, C.K., "The Strength of Compacted Cohesive Soils," ASCE Research Conference on Shear Strength of Cohesive Soils, Boulder, Colorado, June, 1960.

Wissa, Anwar E.Z. and Ladd, Charles C., "Effective Stress-Strength Behavior of Compacted Stabilized Soils," Department of Civil Engineering, M.I.T., Soil Stabilization Phase Report No. 3, July, 1964.

Wissa, Anwar E.Z. and Ladd, Charles C., "Shear Strength Generation in Stabilized Soils," Department of Civil Engineering, M.I.T., Soil Stabilization Phase Report No. 5, June, 1965.

APPENDIX A

DISCUSSION OF TEST COMPUTATIONS

A.1 Compaction Data

The initial sample volume was calculated using the sample length as measured to 0.0001 inches with a dial guage, as shown in Figure A.1, and the inner diameter of the sample mold (1.405 inches). It was the volume determined from these measurements that was used in the computation of initial dry density. The average of two initial water contents was used to compute the dry density and weight of soil in the samples.

A.2 Computation of Void Ratio

A.2.1 Void Ratio and Volume During Curing

To compute the volume change occurring during cure, only a length change was measured. In addition to this length change, and from a single circumference measured immediately before the samples were mounted into the cells, it was necessary to make some assumption concerning the magnitude of lateral dimension change in order to calculate the volume change during cure. The diameter measurements were taken as very approximate, since the sample sides do not remain plane during cure and since

only a single measurement was taken for each sample. Even a small difference in diameter is reflected as a relatively large change in volume, and a single measure over a nonuniform surface is capable of being more than slightly in error.

In order that the volume computation would not be endowed with any more surficial precision than the data justified, an admittedly rough volume calculation based on proportionally equal width-to-length change was employed. The solid line in Figure A.2 is a plot of axial length change versus volume based on the above mentioned assumptions. From this plot, the volumes were determined for use in the data involving void ratio change during cure.

While the actual lateral-to-axial expansion ratio for a given sample undoubtedly varies from the simple assumption made in Figure A.2, the diameter measurements made after curing would suggest that the assumption is at least generally correct. Table A.1 shows approximate width and length changes, as well as initial dimensions of the samples that had significant volume change (W_m of 13, 15 and 17%) during hot cure. As can be seen, the calculated relationship between lateral and axial

length change is pretty close to the assumption of Figure A.2, i.e. $(\Delta d/d_0)/(\Delta L/L) = 1$. Since the accuracy of the diameter measurements are no better than ± 0.02 inches, the assumption of proportionally equal axial and lateral strains was considered to be more accurate and was used to compute sample volumes during cure.

The void ratio during cure was computed using the sample volume computed using the procedure described above and the dry weight of the test specimen. It should be noted, however, that the void ratios reported during cure are applicable only to the sample as a whole; that is, the cracking which took place during curing caused large voids to exist within the soil sample. It should therefore be remembered that it was these overall void ratios which were used to plot void ratio versus curing time in this report, and these are not the true void ratios of the soil skeleton excluding cracks.

A.2.2 Void Ratio During Consolidation

The void ratio of the rebounded sample was computed by using the relationship $G_w = S_e$. Saturation was assumed to be equal to 100%, and the final water content was determined by weighing the entire sample after the test. With

this information, the soil weight, and the volume change for each increment of consolidation pressure, the void ratios of the test specimens could be computed at each consolidation pressure.

A.3 Permeability Computations

As a general rule, permeability was computed from only those portions of the flow in which quantity of flow had reached a steady state condition. Where the hydraulic gradient had changed during a period of permeation, an average value was used for the computation, unless the distribution of head with time was known.

Generally, the flow into the samples did not exactly equal the flow out of the specimens. The differences were nearly always small, and when (rarely) flow into the sample was greater than flow out, the difference was not figured into the volume change-void ratio calculations. When the flow out of the sample was greater than the flow in (the large majority of cases), the change was generally considered to be due to additional consolidation and therefore was included in the void ratio calculations.

A.3.1 Area and Length of Samples for Permeability Calculations

Permeability values were computed using initial length and area data throughout the complete stress range. This procedure was followed since the actual length and area changes induced by consolidation were relatively small, and the proportioning of the volume change between them for each increment of consolidation pressure would have been only approximate. In addition the length changes and cross-sectional area changes tend to be self-cancelling with respect to flow since increasing length is accompanied by decreasing area and the former will tend to decrease flow and the latter tends to increase flow. The net effect on permeability calculation is therefore small.

Final sample measurements taken after testing indicated that this procedure induced no measurable error in the stabilized samples and very small error in even the wettest (most compressible) untreated samples.

A.3.2 Temperature and Permeability

The room temperature under which the tests were run was recorded periodically during the test and varied generally between 21 and 24°C. No corrections to the computed permeability values were made for these temperature variations.

TABLE A.1 JUSTIFICATION FOR FIGURE A.1

Sample	Before Cure Initial Width (d ₀)	During Cure Approx. Max. Width Change (ΔL / d)	Max. Length Change (ΔL)	Δd/d ₀	ΔL/L ₀	(Δd/d ₀) / (ΔL/L ₀) *
<u>Kneading</u>						
PT 6	INSIGNIFICANT AL IN CURING					
PT 7	INSIGNIFICANT AL IN CURING					
PT 8	1.405	3.151	+0.038	+0.081	0.0270	0.0257
PT 9	1.405	3.137	+0.045	+0.114	0.0320	0.0363
PT 10	1.405	3.126	+0.020	+0.048	0.0142	0.0159
<u>Static</u>						
PT 16	INSIGNIFICANT AL IN CURING					
PT 17	INSIGNIFICANT AL IN CURING					
PT 18	1.405	3.152	+0.027	+0.07	0.0192	0.0149
PT 19	1.405	3.152	+0.021	+0.041	0.0149	0.0131
PT 20	1.405	3.122	+0.020	+0.048	0.0142	0.0154

*For proportionally equal lateral & axial length changes, $(\Delta d/d_0) / (\Delta L/L_0) = 1.0$

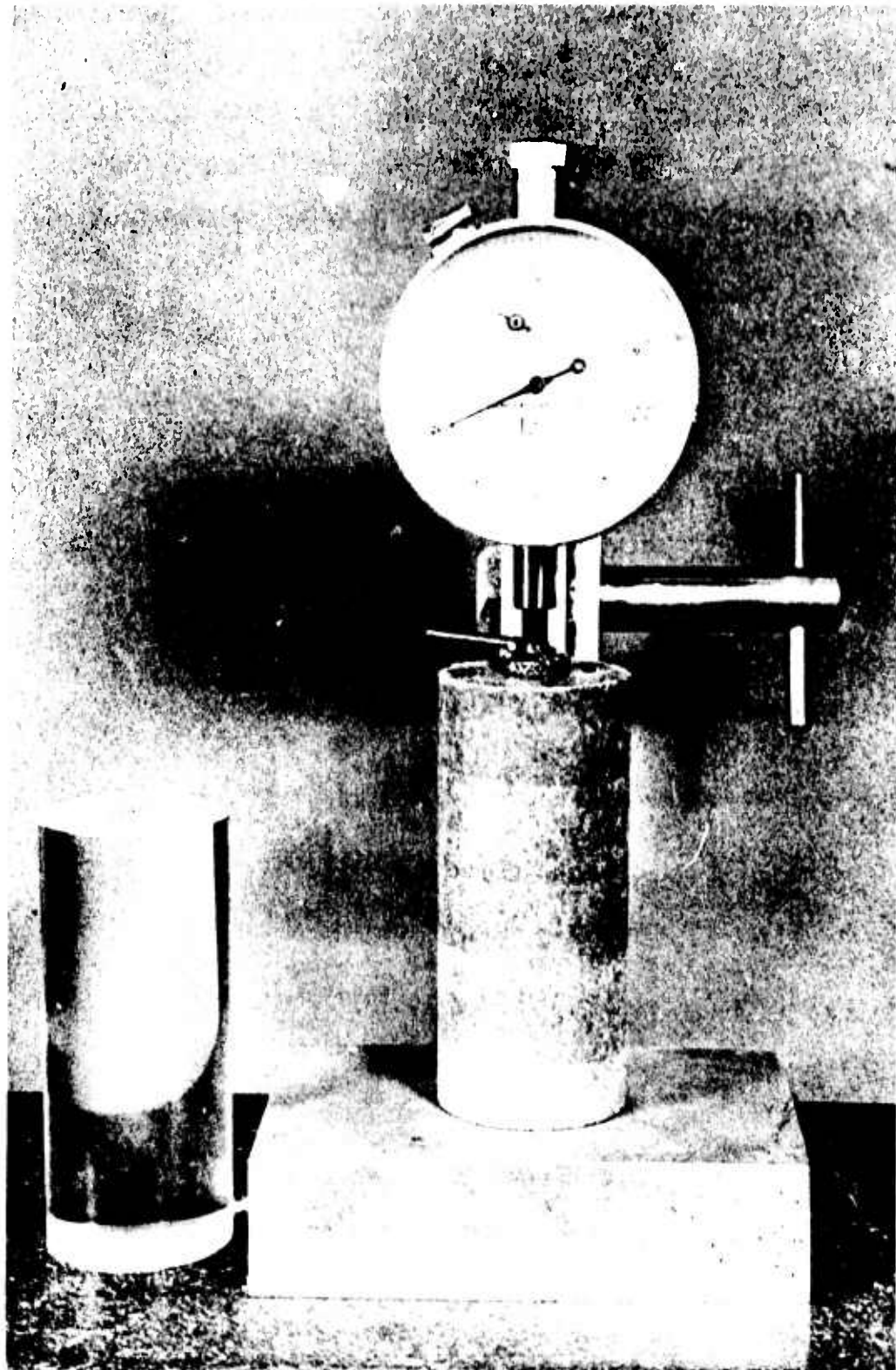


FIG. A.1 DIAL GAGE USED TO MEASURE LENGTH
OF TEST SPECIMENS

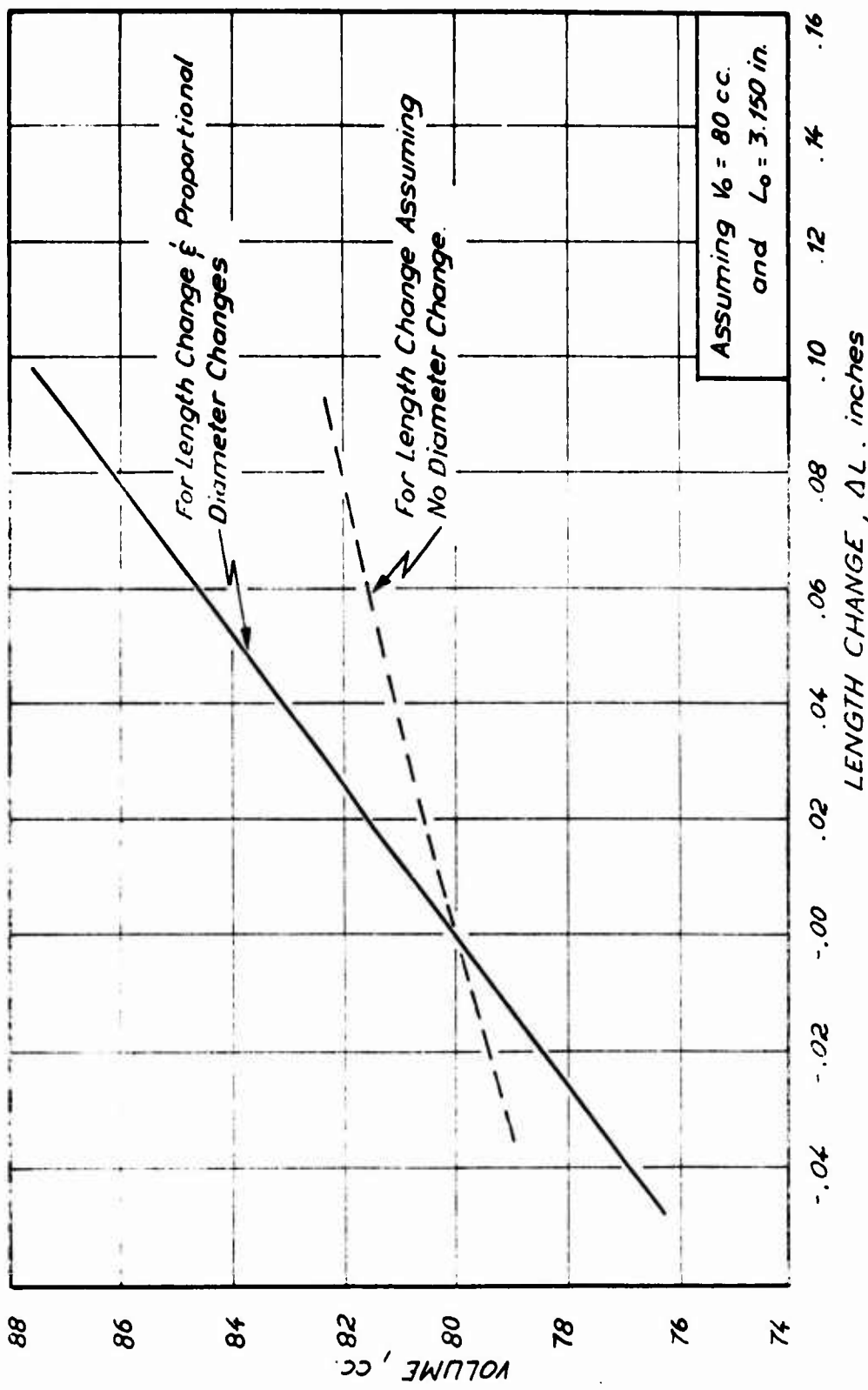


FIG. A.2. ASSUMED VOLUME VERSUS LENGTH CHANGE DURING HOT CURING OF UNSEALED STABILIZED SAMPLES.

Unclassified

Security Classification

DOCUMENT CONTROL DATA - R & D

(Security classification of title, body of abstract and indexing annotation must be entered when the overall report is classified)

1. ORIGINATING ACTIVITY (Corporate author) Soil Mechanics Division, Department of Civil Engineering, Massachusetts Institute of Technology, Cambridge, Massachusetts		2a. REPORT SECURITY CLASSIFICATION Unclassified
2b. GROUP		
3. REPORT TITLE SOIL STABILIZATION; COMPRESSIBILITY-PERMEABILITY BEHAVIOR OF UNTREATED AND CEMENT STABILIZED CLAYEY SILT		
4. DESCRIPTIVE NOTES (Type of report and Inclusive dates) Phase Report No. 6		
5. AUTHOR(S) (First name, middle initial, last name) Anwar E. Z. Wissa Randolph P. Monti		
6. REPORT DATE December 1968	7a. TOTAL NO. OF PAGES 156	7b. NO. OF REFS 15
8a. CONTRACT OR GRANT NO. DA-22-070-eng-465	8b. ORIGINATOR'S REPORT NUMBER(S) Soils Publication No. 227 Research Report R68-94	
8c. PROJECT NO. I-T-0-1451-R-52-A30	9b. OTHER REPORT NO(S) (Any other numbers that may be assigned this report) U. S. Army Engineer Waterways Ex- periment Station Contract Report No. 3-13, Phase Report No. 6	
e.	d.	
10. DISTRIBUTION STATEMENT This document has been approved for public release and sale; its distribution is unlimited.		
11. SUPPLEMENTARY NOTES 1. Consideration for U. S. Army Engineer Water- ways Experiment Station, CE, Vicksburg, Mississippi.		12. SPONSORING MILITARY ACTIVITY U. S. Army Materiel Command Washington, D. C.
13. ABSTRACT A high pressure triaxial-permeability equipment has been developed to study the compressibility and permeability behavior of compacted untreated and stabilized soils at confining pressures up to 70 kg/cm ² under back pressures up to 15 kg/cm ² . Permea- bility down to 10 ⁻⁹ cm/sec can be measured using cylindrical test specimens 8 cm long and 1.6 cm ² cross-sectional area. This equipment has been used to study the in- fluence of cement stabilization, molding water content, and type of compaction on the compressibility and permeability behavior of Massachusetts clayey silt (X-21). The results of this investigation show: (1) Both molding water content and type of com- paction influence the degree of cracking that occurs during unsealed hot curing of 1% cement; (2) Sealing during curing eliminates cracking; (3) Cracking causes an increase in the permeability and compressibility of the stabilized soil at confining pressures up to 10 kg/cm ² ; (4) Provided cracking during curing is pre- vented, the stabilized soil shows a much larger decrease in permeability with in- creasing molding water content than does the untreated soil. Further, kneading com- paction results in a lower permeability than static compaction at molding water con- tent which is optimum for the stabilized soil; (5) The permeability of the stabilized soil increases with increasing curing time and increasing time of reconsolidation.		

DD FORM 1473

REPLACES DD FORM 1473, 1 JAN 64, WHICH IS
OBSOLETE FOR ARMY USE.

Unclassified

Security Classification

Unclassified

Security Classification

14. KEY WORDS	LINK A		LINK B		LINK C	
	ROLE	WT	ROLE	WT	ROLE	WT
Cement soil stabilization Clay soils Silts Soil stabilization Soil tests						

Unclassified

Security Classification